Controls on present-day and future rainfall over southern Africa in coupled climate models

CALLUM MUNDAY

St Edmund Hall

A thesis submitted for the degree of Doctor of Philosophy

University of Oxford

Trinity Term 2018

Abstract

Global climate change will likely alter rainfall at a regional scale. This is a particular concern in southern Africa, where rainfall is central to socioeconomic wellbeing and where we do not understand the full complexity of the climate system. Climate models are the only tools available to estimate future rainfall change, but in the southern African summer rainfall season the latest generation of general circulation models disagree on the sign and magnitude of this change. Some models project small increases in rainfall (~20 mm.season^{-1}) while other simulate large decreases (~100 mm.season^{-1}), and this diversity occurs in the context of large positive rainfall biases (up to 300%) in the present day. Regional policymakers are thus left with the task of designing strategies for climate change adaptation across a wide range of possible futures. With a view to assessing model reliability, this thesis addresses this problem by investigating the physical processes which underlie present day rainfall biases over southern Africa, and which explain the range in future rainfall projections. In tropical and eastern regions of southern Africa, present day intermodel variability in the strength of an important regional circulation feature, the Angola Low, accounts for 40 to 60% of intermodel rainfall variability. Meanwhile, in the subtropical region, intermodel variability in the strength of anomalous northeasterlies across the high topography of Tanzania and Malawi explains 72% of the intermodel spread in rainfall. These findings suggest that improving the representation of the Angola Low, topography and the northeasterly flow should be targets for model development. In the future projections, the model diversity in rainfall response is associated with differences in the large scale adjustment of the tropical atmosphere to warming. In models projecting the highest magnitude drying, the northern tropical oceans warm at a faster rate than the tropical mean (+0.5 K), and this is associated with enhanced subsidence and greater atmospheric stability over southern Africa. However, the most severe projections of drying (>60 mm.season^{-1}) only occur in models with large biases in the present day circulation, tropical sea-surface temperatures, topography and rainfall. The thesis therefore suggests that extreme drying is an unlikely scenario.

Table of Contents

Abstract i
Author's Note v
Preface vi
Acknowledgements ix
List of Tables xii
List of Figures xiii
List of Abbreviations and Acronyms xxi
1. Introduction 1
1.1. Background 2
1.2 Aims and Objectives 5
1.3 The Southern African climate system and rainfall 8
2. Climate Model Evaluation 18
2.1 Background 19
2.2 Performance based model evaluation and its application in southern Africa 19
2.3 Process-orientated approaches 25
2.3.1 The value of process-based analysis 25
2.3.2 Review of process-based analysis in southern Africa 31
3. Data and Methods 40
3.1 Background 41
3.2 The CMIP5 dataset 41
3.3 Reference data sets 43
3.4 Composite and Correlation analysis 46
4. Circulation controls on southern African precipitation in coupled models: the role of the Angola Low 50
Authorship declaration 50
Abstract 51
4.1. Introduction 52
4.2 Background: The Angola Low 57
4.2.1 Variability of the Angola Low and southern African rainfall 58
4.2.2 Climate model representation of the Angola Low 60
4.3 Data 61
4.4 Characterizing the Angola Low 63
4.4.1 The mean state and seasonal cycle of the Angola Low 63

4.4.2 Defining the Angola Low for intermodel comparison 67
4.5 The Angola Low in CMIP5 models 68
4.5.1 The near-surface Angola Low 68
4.5.2 Vertical structure of the Angola Low 70
4.6 The Angola Low and rainfall 73
4.7 Moisture circulation and the Angola Low 77
4.8 Discussion and Conclusion 81
4.8.1 Discussion 81
4.8.2 Conclusion 85
Acknowledgments 87
5. Systematic climate model rainfall biases over southern Africa: links to moisture circulation and topography 89
Authorship declaration 89
Abstract 90
5.1 Introduction 91
5.2 Data 93
5.3 Background 96
5.3.1 The observed rainfall climatology 96
5.3.2 The relationship between Madagascan and southern African rainfall 99
5.4 CMIP5 circulation 100
5.4.1 Zonal overturning circulation 100
5.4.2 Moisture circulation in wet and dry models 105
5.4.3 Upstream circulation, topography and CMIP5 rainfall 107
5.5 Summary and discussion 117
5.5.1 Summary of the processes associated with intermodel rainfall variability 117
5.5.2 Foci for model development 118
5.6 Conclusions 120
Acknowledgements 122
Supplementary Material for Chapter 5 123
6. Controls on the diversity in climate model projections of early summer drying over Southern Africa 125
Authorship declaration 125
Abstract 126
6.1 Introduction 127
6.2 Background: Potential mechanisms of change 129
6.3 Data 132
6.4 Local diagnosis of southern African rainfall projections 135
6.4.1 Changes to the vertical atmospheric structure 135

6.4.2 Changes in moisture circulation 139
6.4.3 The relationship among projections of rainfall, surface temperature and evaporation 141
6.5 Connections with tropics-wide projections 144
6.5.1 Spatial changes in southern African and tropical rainfall 144
6.5.2 Changes in tropical SSTs and southern African rainfall 146
6.6 Potential connections with present day rainfall biases 152
6.7 Discussion and Conclusions 156
6.7.1 Summary and Discussion 156
6.7.2 Conclusion 159
Acknowledgements 160
7. Conclusions 161
7.1 Introduction 162
7.2 The climate processes underlying the simulation of present day rainfall over southern Africa 163
7.2.1. The role of the Angola Low 164
7.2.2 Moisture circulation and topography 166
7.2.3 Implications of present day process biases for model reliability 168
7. 3 Mechanisms of rainfall future change in CMIP5 171
7.4 Controls on intermodel diversity in rainfall projections 172
7.5 Links between present day model simulations and their future rainfall change 174
7.6 Targets for model improvement 177
7.6.1 The Angola Low 177
7.6.2 Northeasterly moisture transport 178
7.6.3 Topography 179
7.7 CMIP5 based insights into the southern African climate system 180
7.8 Future outlook for modelling southern African rainfall 184
Bibliography 189

Author's Note

The thesis takes an article-based format, with three scientific papers accompanied by a framing introduction, literature review and conclusion. Two of the scientific articles in this thesis, Chapters 4 and 5, are published in the *Journal of Geophysical Research: Atmospheres* and *Journal of Climate* respectively. Chapter 6 is in review at *Journal of Climate*. Various parts of the thesis have also been presented at a number of conferences, including at the UK Met Office, at the Working Group for Numerical Experiments (WGNE) workshop in Montreal and at the International Association of Meteorology and Atmospheric Sciences (IAMAS) conference in Cape Town. Authorship statements for the scientific papers that comprise Chapters 4 to 6 are included at the start of each chapter.

The thesis contributes to the Future Climate for Africa (FCFA), Uncertainty Reduction in Models for Understanding Development Applications (UMFULA) project, which is funded by the Natural Environmental Research Council (NERC) and Department for International Development (DfID). The funding of the FCFA programmes reflects a growing recognition that we need to do more to advance our understanding of African climate systems and their response to global warming. I hope that this thesis contributes in a small way to this goal.

Preface

Climate models are remarkable tools which simulate the emergent properties of Earth's climate system based on a series of fundamental physical equations. They have been successfully employed in support of a wide range of scientific questions, including in the prediction of global temperature rise over the past 30 years, in the detection of the human imprint on observed climate changes and in accounting for the gross features of atmospheric General Circulation. Buoyed by these successes and driven by the need to understand the implications of unprecedented human forcing of the climate system, scientists have used climate models to address increasingly difficult questions.

Of these questions, one of the most challenging concerns how regional rainfall might respond to greenhouse gas forcing into the 21st century. To simulate regional rainfall change, models must be able to capture the complicated interaction between dynamics, thermodynamics, local and remote forcing which influences the production of rainfall, and how that interaction responds to continued human interference. This is a stringent test for climate models, especially given the computational limits on model resolution. It is incumbent upon scientists, therefore, to demonstrate the adequacy of climate models for projecting regional rainfall change, or to suggest how models might be improved to this end.

One way to rigorously test the adequacy of models for projecting rainfall change is to evaluate their performance in regions of considerable climatological complexity. Southern Africa is one such region. Extending through the tropics and subtropics, the

mean climate of southern Africa is maintained by both tropical and mid-latitude climate processes as well as by their interaction through continental-scale tropical-temperate cloud bands. These atmospheric influences are modified in turn by the variability in sea surface temperatures, upper ocean heat content and sub-surface processes in global ocean basins, and through local forcing by the complex regional topography and the proximity of the warm Agulhas current and the cold Benguela upwelling system. The relative importance of these factors in sustaining the mean rainfall climatology is not fully known, and yet models must simulate their delicate balance in order to reliably project rainfall change. The purpose of this thesis is to assess the reliability of the latest generation of climate models for projecting rainfall change in this complex setting.

In support of this broad objective, this research evaluates climate models by investigating the physical processes which govern their simulations of southern African rainfall. A physical understanding of model simulations is a fundamental step in building confidence in projections of rainfall change, and helps identify essential areas for model development. Detailed investigation of model simulations also has the potential to lend important insights into the operation of the climate system in the real world. This may be particularly beneficial over southern Africa, where a number of factors, including the limited observational base, have frustrated efforts to fully understand the controls on rainfall and its variability.

The thesis starts with a discussion of the scientific and social importance of climate model evaluation in southern Africa along with our aims and objectives of the thesis. Chapter 1 also presents a brief overview of the southern African climate system. This is

followed by a critical appraisal of current approaches to climate model evaluation in Southern Africa and elsewhere in Chapter 2. Chapter 3 presents an overview of the datasets used in the thesis and the methods of analysis. The original analysis begins in Chapter 4, with an evaluation of model simulation of an understudied, yet important, regional circulation feature: the Angola Low. Chapter 5, goes on to investigate the drivers of a key rainfall bias present in a range of climate models; namely that they tend to simulate too much rainfall over southern Africa yet too little over Madagascar. Following the evaluation of model rainfall simulation in the present day, attention turns to their projections of future rainfall change in Chapter 6. In this chapter, the mechanisms of rainfall change among climate models are assessed, and the relationship between present day model rainfall biases and their projections of change is interrogated. Chapter 7 draws together the findings, considers their implications and suggests important avenues for future research.

Acknowledgements

The DPhil is funded by the Natural Environmental Research Council (NERC) Environmental Research Doctoral Training Programme (DTP), and through a Met Office CASE studentship. I am extremely grateful for this funding, without which this thesis would not exist. I am additionally thankful to Teddy Hall, Keble College and the School of Geography who have provided me with various opportunities to teach on the undergraduate Geography programme over the last three years.

The path to writing this thesis started at the Perse School, where I was lucky to have a series of excellent geography, maths and science teachers who inspired me to take geography at undergraduate and, as it turns out, beyond. Duncan King and Bob Smith deserve a mention here. At Teddy Hall, I had the good fortune to be tutored in geography by Rob Whittaker and Lorraine Wild, who introduced me to academic geography and who have been a source of support and guidance throughout my seven years in Oxford. I look forward to working with them more closely next year.

The scientific content of this thesis is much enriched by countless conversations with a number of excellent scientists. I have enjoyed discussing the puzzle that is the southern African climate system with Neil Hart, Rachel James, Emma Howard and Richard Jones. It has also been fun and intellectually challenging working on the UMFULA project. Hours in Oxford, Brighton, Cape Town and on Skype with Martin Todd, Chris Reason, Rondro Barimalala, Ross Blamey, Melissa Lazenby, Seshu Kosulu, Wilfred

Pokam and Fabien Desbiolles have given me much food for thought. My thanks also go to Chris Reason and Cath Senior who took the time to examine the thesis.

In the Geography department, I owe thanks to many people who made the practical side of doing the DPhil easy and working with climate model datasets as straightforward as possible. Special thanks in this regard must go to Sebastian Engelstaeder, David Ford, Alex Black and Joe Milkovic. On the subject of climate model datasets, I am also grateful for the toils of the many modelling centres around the world who provided the unique set of coordinated experiments on which the thesis is based.

The DPhil would have been an entirely different experience without a number of good friends. Amy Creese deserves first mention here, as a true friend, as a scientific advisor, as an editor and because I would have largely failed to do anything on time without her. Cheers also to Matt for moving to Oxford to help me finish the PhD, to Yossi for saying yes to many beers, to Beth and Tim for taking the brave decision to live with me and to many others who made the last four years fun: Bags, Anna, Moley, Z, Miller, Toby, Hobby, Nick, Ewing, Robyn, Ian, James, Mel, Dave, Ollie, Dicko, Muz, Louis, Winnie, and Gigi.

My family: Clare, Rory, Soph, Mum and Dad, have supported and encouraged me throughout the DPhil and, of course, for the 22 years or so before. I am very grateful to them -- they have listened patiently to me talking about the Angola Low for probably too long.

Finally, I would like to thank my supervisor, Richard Washington. Richard was a deciding factor in encouraging me to undertake the DPhil, and his guidance and clear scientific vision have contributed immeasurably to this thesis. It is fun working with him.

List of Tables

Table 3.1 Reference Datasets 44

Table 4.1 CMIP5 models used in this study. Models are ordered from dry to wet according to mean December-February (DJF) precipitation 54

Table 5.1 CMIP5 models. Models are ordered from dry to wet according to mean January-February precipitation (20-30°E; 20-30°S). 95

Table 6.1 CMIP5 models used in this study, their future OND rainfall change over southern Africa (15-40°E; 15-30°S) and their precipitation bias relative to the CMAP dataset. Models are ordered by precipitation change (ΔP) under RCP8.5 (2073-2099 minus 1979-2005), models in bold are those included in the low magnitude (LM) and high magnitude (HM) change composites. Stars indicate the 10 models with highest present day bias, crosses indicate models with lowest present day bias. 134

List of Figures

Figure 1.1 Political map of southern Africa.....8

Figure 1.2 The annual cycle of rainfall over Africa in four season: April to June (top left), July to August (top right), October to December (bottom left) and January to March (bottom right). Data is from the CMAP satellite/rain-gauge dataset 9

Figure 1.3 Key features of the summer circulation over southern Africa. Topography (shaded) is from the USGS GTOPO30 dataset.....11

Figure 1.4 Longitudinal (left) and latitudinal (right) cross sections of surface height across southern Africa. The longitudinal (latitudinal) cross-section is averaged over 15 to 30°S (20-30°E). Topography data is from USGS GTOPO30 digital elevation model. 16

Figure 2.1 Station data contributing to the (CRU, version 2.23) rainfall (black) and Integrated Global Radiosonde Archive (IGRA) u wind at 1200 UTC (pink). (top) Coverage map for 1979–2013. Black squares indicate the location of 0.5° × 0.5° grid boxes that have at least one contributing station during at least 50% of the months; pink circles indicate stations with at least 10 records per month in at least 50% of the months. (bottom) Time series showing the number of stations contributing in each month (40°S–40°N, 30°W–60°E). *Source: James et al. (2018) BAMS.*.....24

Figure 2.2 The CMIP (top left) and AMIP (top right) MMM climatological rainfall biases (1979-2005) for January. The bottom left plot shows CMIP MMM minus AMIP MMM rainfall, with non-significant differences among the 25 model ensembles masked. Significance is assessed via the Students t-test ($p<0.05$).....35

Figure 4.1 Mean (1979-2005) annual cycle of southern African rainfall (averaged over 10-52E,10-35S) in CMIP5 models (boxplots) compared to CMAP (dashed line) and

GPCP (solid line). The red lines show the median model for each month, the box encompasses the interquartile range of models and the tails represent the full range. 53

Figure 4.2 Mean rainfall (1979-2005) in CMIP5 models minus satellite-rain gauge estimates. Satellite rain gauge estimates are a mean of GPCP and CMAP climatology. Reanalyses datasets are in bold. 55

Figure 4.3 Topography (shaded) and key features of southern African climate during December-February. Black arrows denote key moisture transport pathways. Red dashed circles represent low-level cyclonic circulation; Angolan Low (AL), Kalahari heat low (KHL) and Mozambique Channel trough (MCT). Topography data is from USGS GTOPO30 global digital elevation model. 58

Figure 4.4 Mean DJF 850 hPa geopotential height in reanalysis data (1979-2005).....63

Figure 4.5 Austral summer (October to March) monthly progression of the Angola Low and southern African heat low in an ensemble mean of reanalyses. Shaded areas are mean 850 hPa geopotential heights (1979-2005), contours are of 850 hPa potential temperature. First contour is at 296K, the contour interval is 0.5K.....65

Figure 4.6 Austral summer (October to March) mean monthly latitude-height cross sections of equivalent potential temperature ($\theta_{e;}$ shaded) and potential temperature (θ; contours) in an ensemble mean of reanalyses. Longitudes are averaged over 18-24°E. The black rectangle represents the minimum in 850hPa geopotential height associated with the Angola Low and the red rectangle represents the maximum in potential temperature associated with the subcontinental heat low. Note in March, the presence of the Angola Low in the mean climatology is unclear so no rectangle is plotted.....66

Figure 4.7 Mean DJF Angolan Low in CMIP5 models and reanalyses. Models and reanalyses are ordered from driest model (top left) to wettest model (bottom right). The Angolan Low is defined by lowest 5% of 850 hPa geopotential height. Model rainfall is

expressed as an index between 0 and 1 based on mean DJF rainfall (Table 4.1) and is shown above each composite.....70

Figure 4.8 Mean DJF latitude-height cross sections of vertical velocity (Pa s^{-1}; shaded) and geopotential height anomaly (contours; interval 5m) for CMIP5 models and reanalyses. Models are ordered as in Figure 4.7. Longitudes are averaged over 18-24°E. The black rectangle in each composite represents the latitude of minimum 850 hPa geopotential height associated with the Angolan Low in each model or reanalyses.....71

Figure 4.9 Relationship between DJF mean Angolan Low Index (see Section 4.4.2 for details) and southern African rainfall (10-35°S;10E-52°E). Models are indicated by dots, reanalyses by crosses. Note that the linear regression and Pearson's test do not include reanalyses.....74

Figure 4.10 The percentage of inter-model variance in grid-box precipitation associated with the models' Angolan Low Index (see Section 4.4.2 for details). Relationship is for mean DJF and variance predicted is calculated based on r^2. Values below 20% are not significant at $p<0.05$ and are masked. 76

Figure 4.11 Mean DJF moisture flux and divergence at 850 hPa in (a) seven models with strongest Angolan Low, (b) seven models with weakest Angolan Low and (c) strongest Angolan Low models minus weakest Angolan Low models. In (c) we have only plotted moisture flux vectors where either meridional or zonal moisture flux values were significantly different between the two sets of models. Significance was calculated using Students t-test. 78

Figure 4.12 The percentage of inter-model variance in grid-box meridional moisture flux predicted by the models' Angolan Low Index (see Section 4.4.2 for details). Relationship is for mean DJF and variance explained is calculated based on r^2. Values below 20% are not significant at $p<0.05$ and are masked. 79

Figure 5.1 a) January-February (JF) climatological rainfall bias (1979-2005) in CMIP5 models relative to CMAP satellite-rain gauge product in subtropical southern Africa (20-30°E; 20-30°S: blue bars) and in Madagascar (44-56°E,12-28°S) b) JF multi-model mean precipitation bias (1979-2005) relative to CMAP. 92

Figure 5.2 a) CMAP climatological precipitation (shaded) and ERA-Interim reanalysis 850 hPa moisture flux climatology for JF (1979-2005) b) Grey contours show topography above 800m (contour interval is 200m) and moisture divergence (g kg s^{-1} x 10^6) is shaded. The supposed positions of the Congo Air Boundary (CAB) and Intertropical Convergence Zone (ITCZ) are drawn following van Heerden and Taljaard (1998). 97

Figure 5.3 Longitude-height cross sections of streamlines (u; w x10^2) averaged over 23-29°S in NCEP2 (top left) and CMIP5 models ordered dry to wet (Table 5.1). Shading is vertical velocity (Pa s^{-1}x10^2), with purples as negative (upward) vertical velocity and oranges as positive (downward) vertical velocity. ERA-Interim is not included here but is qualitatively similar to NCEP2. HadGEM2-CC, MIROC4h and CNRM-CM5 did not have vertical velocity data available and are not included. 101

Figure 5.4 January-February climatological vertical profiles of a) moist static energy, b) dry static energy, c) specific humidity and d) dew point depression at Upington (28°S, 21°E). The red and blue dashed lines are average of 2pm and 2am local time radiosonde data, respectively. The solid lines are estimates of the daily mean vertical profile from CMIP5 models , the green (black) dotted lines is ERA-Interim (NCEP2) reanalysis. For reanalyses and models we have used data from the gridbox closest to the Upington station. 103

Figure 5.5 January-February climatological mean 850 hPa moisture flux (vectors) for an average of a) the set of six driest models b) set of six wettest models and c) the difference between wet and dry model sets. Shading in a) and b) is observed topography (USGS GTOPO30 dataset) above 1000m. Shading in c) is the 850 hPa moist static energy difference (kJ kg^{-1}) between wet and dry models. 106

Figure 5.6 The relationship between JF climatological (1979-2005) model Froude number (details in text) and mean subtropical southern Africa precipitation (20-30°E, 20-30°S). Diamonds represent reanalyses and satellite-rain gauge estimates. 109

Figure 5.7 Pearson's correlation coefficients for the relationship between JF climatological (1979-2005) model Froude number (details in text) and gridbox rainfall over southern Africa. We control for the false discovery rate (FDR) of significant correlation following Wilks (2016), with a conservative control FDR value of α_{FDR}=0.10 yielding a threshold level of significance as p_{FDR}=0.026. Non-significant values are masked. The purple box shows the Tanzanian Escarpment region. 110

Figure 5.8 Wind speed (m s^{-1}) upstream of Tanzania at 36-42°E; 3-11°S in reanalyses (first two bars) and CMIP5 models (ordered dry to wet; see Table 5.1). 113

Figure 5.9 Longitudinal cross-section of surface height across southern Africa at 10°S for CMIP5 models (dotted lines) and NASA GTOPO30 (green solid line). 114

Figure 5.10 The relationship between the Tanzanian Escarpment topography (5-13°S,30-36°E) and a) Kalahari Basin precipitation (20-30°E,20-30°S) , and b) total downstream wind speed (850hPa) in a northeasterly direction (20-42°E,20-30°S). To compute total downstream northeasterly flow we mask grid boxes with westerly and southerly flow, compute wind speed at remaining grid boxes and sum the wind speed across these grid boxes. 115

Figure 5.11 The difference in climatological January-February rainfall between the six models with the lowest average topography and the six models with the highest average topography over the Tanzanian Escarpment (purple box). Stipples indicate gridboxes where at least 5 out of 6 models with low topography over the Tanzanian escarpment are wetter (blues) or drier (reds) than all of the models with relatively high topography. ..116

Figure 6.1 CMIP5 future rainfall change (mm.season^{-1}) over southern Africa (15-40°E; 15-30°S) (black bars) for OND (2073-2099 minus 1979-2005) and the present day bias (red bars) in mm.season^{-1} relative to the CMAP dataset. 128

Figure 6.2 Longitude-height (in hPa) cross section (averaged between 15 and 30°S) of future change in moist static energy (kJ.kg^{-1}) in high magnitude drying (left) and low magnitude drying (right) sets of models. 136

Figure 6.3 Longitude-height (in hPa) cross section (averaged between 15 and 30°S) of future change in vertical velocity (10^2 Pa.s^{-1}) (shading) in high magnitude drying (left) and low magnitude drying (middle) models, and their difference (right). The contemporary climatology (1979-2005) in HM and LM models is shown by grey contours.....138

Figure 6.4 Low-level (850 hPa) moisture divergence (shading; 10^8kg.kg^{-1}.s^{-1}) and moisture flux (vectors; barb in lower right corner of plots shows scale). The first row is the present day climatology (1979-2005) in a) high magnitude drying models and b) low magnitude drying models. The second row is the future change for c) high magnitude drying models and d) low magnitude drying models. The last plot, e), is the difference in future change between high and low magnitude drying models.....140

Figure 6.5 The intermodel relationship between future rainfall change over southern Africa (15-40°E; 15-30°S) and a) future surface temperature change (K) over southern Africa relative to the tropical mean temperature change (180°W-180°E; 20°N-20°S), and b) future latent heat flux change (W.m^{-2}) over southern Africa. The blue (red) dots represent models which are part of the LM (HM) composites 143

Figure 6.6 Future tropical rainfall change in mm.season^{-1} (shading) averaged over the set of a) HM models, b) LM models and c) the difference in future rainfall change between HM and LM models. Black contours in a) and b) show the present day rainfall climatology in HM and LM models respectively, contours start at 180 mm.season^{-1} and the contour interval is 90 mm.season^{-1}. The stippling in c) is a metric of model

agreement, a stipple indicates that all models in the→ HM composite simulate lower or higher magnitude changes relative to all models in the LM composite (e.g. over southern Africa, all models in HM composite project greater drying than those in LM composite). 145

Figure 6.7 Future SST change (K) at each grid point minus the tropical mean (180°W-180°E; 20°N-20°S) SST warming averaged over the set of a) HM models, b) LM models and c) the difference in relative future SST change between HM and LM models. Stipples are applied in same way as in Figure 6.6. 148

Figure 6.8 The intermodel relationship between a) warming of northern tropical SSTs (10-25°N;180°W-180°E) minus tropical mean warming (20°N-20°S; 180°W-180°E) in K and rainfall change (mm.season^{-1}) over southern Africa (15-40°E; 15-30°S) and b) tropical mean warming (20°N-20°S; 180°W-180°E) and rainfall change over southern Africa. Blue (red) dots indicate models which are part of the LM (HM) composites. The cross marks the outlying FIO-ESM model, note that the linear regression in a) (green line) excludes this model. 149

Figure 6.9 As in Figure 6.8, but for future rainfall change (mm.season^{-1}) in South America (60-40°W; 10-25°S). 151

Figure 6.10 Climatological (1979-2005) precipitation bias (mm.season^{-1}) relative to the CMAP dataset averaged across a) HM models, b) LM models and c) their difference. The stipples in c) indicate where all HM models are either wetter or drier compared to LM models (e.g. the green areas with stipples show that all HM models are wetter than all LM models in the present day) 153

Figure 6.11 As in Figure 6.10, but for climatological (1979-2005) SST biases (K) relative to ERSSTv5 155

Figure 7.1 Schematic of austral summer circulation in wet models (top) and dry models/reanalysis (bottom).....170

Figure 7.2 Schematic of the present day and future climatologies of OND rainfall, evaporation and upper-level uplift. Models are grouped according to the magnitude of future change (black arrows). 176

List of Abbreviations and Acronyms

AEJ-S	Southern component of the African Easterly Jet
AL	Angola Low
AMIP	Atmospheric Model Intercomparison Project
AR4	Fourth Assessment Report (of IPCC)
AR5	Fifth Assessment Report (of IPCC)
BH	Botswana High
CCAM	Conformal-Cubic Atmospheric Model
CMAP	Climate Prediction Center Merged Analysis of Precipitation
CMIP	Coupled Model Intercomparison Project
CMIP3	phase 3 of the Coupled Model Intercomparison Project
CMIP5	phase 5 of the Coupled Model Intercomparison Project
CORDEX	Coordinated Downscaling Model Experiments
CRU	Climate Research Unit
DFID	Department for International Development
DJF	December to February
DMSP	Defence Meteorological Satellite Program
DRC	Democratic Republic of Congo
DSE	Dry Static Energy
ENSO	El Niño Southern Oscillation
EOF	Empirical Orthogonal Function
ERSSTv5	Extended Reconstructed Sea Surface Temperature version 5
ESGF	Earth System Grid Federation
ESM	Earth System Model
FDR	False-discovery rate
FEWS-NET	Famine Early Warning Systems Network
Fn	Froude Number
GCM	General Circulation Model
GEWEX	Global Energy and Water Cycle Experiment

GFDL	Geophysical Fluid Dynamics Laboratory
GoG	Gulf of Guinea
GPCC	Global Precipitation Climatology Center
GPCP	Global Precipitation Climatology Project
GPI	Global Precipitation Index
GTOPO30	Global 30 Arc-Second Elevation (USGS global digital elevation model)
HL	Heat Low
HM	High Magnitude
IGRA	Integrated Global Radiosonde Archive
IPCC	Intergovernmental Panel on Climate Change
IR	Infrared
ITCZ	Intertropical Convergence Zone
JF	January-Feburary
JFM	January to March
KHL	Kalahari Heat Low
LM	Low Magnitude
MCT	Mozambique Channel Trough
MDTF	Model Diagnostics Task Force
MMM	Multi-model mean
MSE	Moist Static Energy
MSLP	Mean Sea-level Pressure
MW	Microwave
NASA	National Aeronautics and Space Administration
NCEP	National Center for Environmental Prediction
NERC	Natural Environmental Research Council
NOAA	National Oceanic and Atmospheric Administration
OLR	Outgoing Longwave Radiation
ON	October-November
OND	October to December
PCMDI	Program for Climate Model Diagnosis and Intercomparison
RCM	Regional Climate Model

RCP	Representative Concentration Pathway
RMSE	Root Mean Squared-error
SAFARI	Southern African Fire-Atmosphere Research Initiative
SAH	South Atlantic High
SCTR	Seychelles-Chagos Thermocline Ridge
SHL	Sahara Heat Low
SICZ	South Indian Convergence Zone
SIOCZ	South Indian Ocean Convergence Zone
SIOD	South Indian Ocean Dipole
SIOH	South Indian Ocean High
SON	September to November
SRES	Special Report on Emissions Scenarios
SSM/I	Special Sensor Microwave Imager
SST	Sea-surface temperature
SWIOD	South-west Indian Ocean Dipole
TIROS	Television and Infrared Observation Satellite
TOA	Top of Atmosphere
TOVS	Operational Vertical Sounder
TRMM	Tropical Rainfall Measurement Mission
TTCB	Tropical-temperate cloud bands
TTT	Tropical-temperate Trough
USGS	United States Geological Survey
WGNE	Working Group on Numerical Experiments
WRCP	World Climate Research Programme

1. Introduction

1.1. Background

Rainfall is central to socioeconomic wellbeing in southern Africa. Agriculture supports a large proportion of the regional economy (40% in Malawi), electricity generated via hydropower accounts for almost all the power produced in some countries (96% in Zambia) and water supply to large cities (including Cape Town and Maputo) relies on the seasonal recharge of reservoirs. Despite its importance, annual rainfall totals across much of southern Africa are less than 700 mm, leaving the population base vulnerable to perturbations to the mean climatic state. Low rainfall when coupled with the high average regional temperature and a propensity to heat waves can lead to severe climate-related hazards. Unusually dry and hot conditions associated with the 2015/2016 El Niño, for example, resulted in acute water shortages, widespread reduction in crop yields and mass migration (Hirons and Klingaman 2016; Archer et al. 2017; Siderius et al. 2018). At the other extreme, floods associated with the 2010-2011 La Niña displaced close to 315000 people and lead to over 450 deaths (OCHA 2011).

Climate change, associated with the emission of greenhouse gases at an unprecedented rate, has the potential to alter the mean hydrological balance and exacerbate climatic extremes in the future (Meehl et al. 2000). With this possibility in mind, hundreds of climate change impact studies have highlighted the various ways in which climate change could affect the physical and social environment in southern Africa. These include the potential for large scale remobilisation of dune systems in the Kalahari Desert (Thomas et al. 2005), increased likelihood of droughts or more severe floods (Pohl et al. 2017; Lehner et al. 2017), reductions in crop yields (Schlenker and Lobell 2010), loss of biodiversity (Midgley and Thuiller 2011) and reduced capacity for

electricity generation via hydropower (Conway et al. 2015). The potential impacts of climate change are ethically troublesome since the African continent is the least responsible for climate change as measured by their historical emissions of greenhouse gases (Fields 2005).

Climate models, and especially general circulation models (GCMs), are the only tools available to assess the response of regional rainfall to continued anthropogenic forcing. Particularly important are publicly available simulations from GCMs which contribute towards the Coupled Model Intercomparison Projects (CMIPs). Projections from CMIP models inform the Intergovernmental Panel on Climate Change (IPCC) reports and are the basis of many climate impact studies. Typically, the impact studies and IPCC assessments operate under an assumption that each model projection represents an equally likely possible future. This 'one-model-one-vote' approach (Knutti 2010) leads to assessments of future change which are based on the average projection of a range of CMIP models, along with metrics for model agreement ("robustness"). This approach may be problematic in Africa, where model capability is generally low and where improvements from one model generation to another are modest at best. Moreover, in southern Africa, there is a wide range of future rainfall projections, with climate models disagreeing on both the sign and magnitude of future change (Meehl et al. 2007; Shongwe et al. 2009; Collins et al. 2013). In the absence of any guiding information which supports the reliability of one model projection over another, policymakers are left with the problem of designing and financing strategies for climate change adaptation across a wide range of possible futures.

One way to constrain the range of possible futures is to interrogate the physical processes which underlie model simulations of present day and future rainfall. Climate models which simulate features of the climate system that are important for rainfall in a manner which is at odds with reality can be considered less reliable than those which simulate key aspects of the climate system faithfully (Notz 2015). If the poor model simulation of a feature in the present day has a direct bearing on its simulation future rainfall change, this is grounds for questioning the credibility of the model projection. This process-based approach to model assessment has been applied in a wide variety of contexts (e.g. Guilyardi et al. 2009; Niznik and Lintner 2013; Jiang et al. 2012), and in some cases has yielded important constraints on the range of future climate projections (e.g. Hall and Qu 2006; Kidston and Gerber 2010). Over southern Africa, however, there has been limited evaluation of climate models and their ability to simulate the climate processes associated with regional rainfall. As a result, we do not yet know whether it is possible to constrain the range of future rainfall projections. This thesis addresses this shortcoming by identifying key physical processes which are associated with model simulations of rainfall in the present day and in the future.

1.2 Aims and Objectives

A broad objective in the thesis is to assess the reliability of climate model projections of future rainfall change over southern Africa. As the most widely used set of models for climate projection, this thesis focuses on the climate models from the latest iteration of the Coupled Model Intercomparison Project (CMIP5). The CMIP5 dataset consists of a common set of experiments run by a range of over thirty different GCMs from different modelling centres around the world (Taylor et al. 2012). The commonality of the experiments enables for straightforward intercomparison between different climate models. Intercomparison between models can help to identify the processes and features which influence the simulation of rainfall across the ensemble. These processes can then be compared with observations and theoretical expectation to provide insights into the reliability of models. Our central aim, therefore, is to understand the key drivers of intermodel spread in the simulation of southern African rainfall. We can split this central aim into four main components:

i) To understand the climate processes associated with the intermodel spread in rainfall in the present day
ii) To assess the mechanism(s) of future rainfall change in the CMIP5 ensemble
iii) To understand the controls on the diversity of future rainfall projections
iv) To evaluate whether models' simulation of the present day climate system influences their projections of rainfall change.

In addition to yielding insights into the reliability of models, process-based evaluation can help to provide tractable information to guide model improvement. Rather than focusing on the broad goal of improving rainfall in southern Africa, model developers can focus on a more specific problem, for example, in improving the representation of a key feature which is known to be important for the simulation of rainfall. This constitutes a fifth aim:

v) To identify specific processes or features within models which, if improved, could enhance the simulation of southern African rainfall

Finally, the analysis of intermodel differences may prove to be valuable for guiding further observations and experiments. If we consider the CMIP5 ensemble to be a range of different possible representations of the climate system, or as individual theories of climate (Schmidt and Sherwood 2015), sensitivity across the ensemble to the representation of a particular process or feature might imply that the same feature/process is important for sustaining conditions as they are in the real world. This heuristic value of coordinated model ensembles is not well appreciated in the climate science community, and may be particularly valuable in areas, such as southern Africa, where there are sparse observations and where a strong grasp on some of the critical climate influences remains elusive. A final aim of the thesis therefore is:

vi) To explore how process-based approaches to evaluation can be used to generate hypotheses regarding the operation of the southern African climate system.

Before reviewing the state of the literature on climate model evaluation in southern Africa (and elsewhere), it is useful to ground the discussion with an overview of the working the southern African climate system.

1.3 The Southern African climate system and rainfall

This section provides a brief overview of the southern African climate system as it relates to the rainfall climatology. In this thesis, southern Africa is defined as Africa south of the Congo Basin (10°S) and from the western coast of Angola, Nambia and South Africa at ~10°E to the eastern coast of Madagascar at ~52°E (see Figure 1.1). On account of the extensive body of literature addressing the controls on the southern African climate system, prominence in the discussion is given to the features of the climate system which are considered later on in the thesis. For a more detailed treatment, the reader is referred to excellent reviews of the southern African climate by Reason (2017) and Tyson and Preston-Whyte (2000).

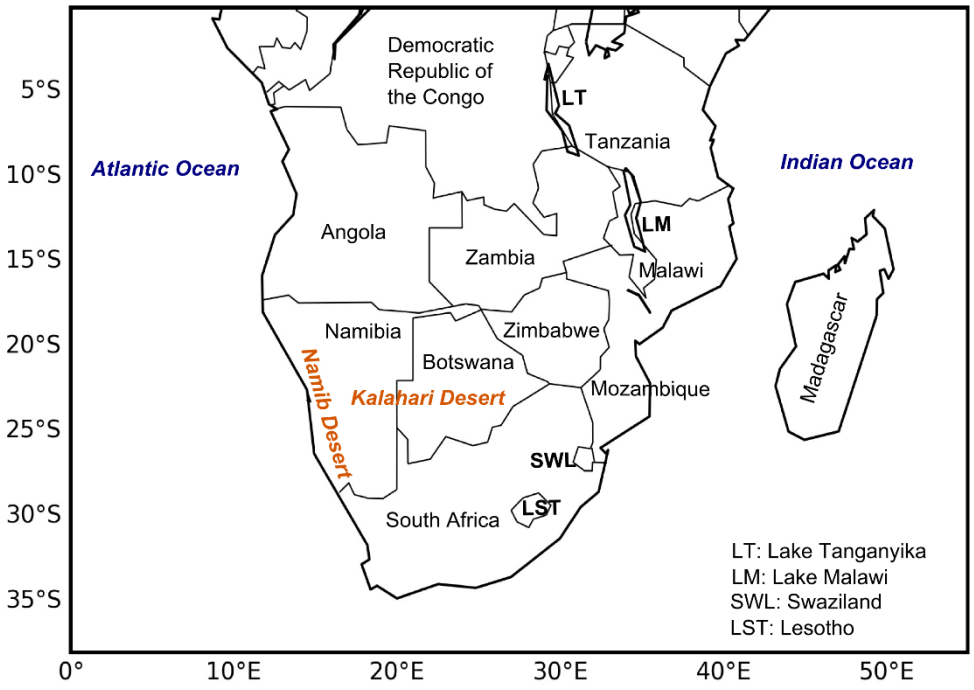


Figure 1.1 Political map of southern Africa

The latitude of maximum African convective activity lags the solar zenith throughout the year by approximately one month (Figure 1.2). With the exception of the southwestern and southern Cape region of South Africa, which is affected by frontal rainfall in the winter and transition seasons respectively, this seasonal cycle results in a rainfall maximum over southern Africa in the southern hemisphere summer (October to March). In the summer, the major rain band over southern Africa is tilted diagonally from the northwest to south east, along South Indian Ocean Convergence Zone (SIOCZ) (Streten 1973; Cook 2000), and there is a strong zonal gradient in rainfall between the wet north-eastern regions and the dry Kalahari Basin and Namib deserts. The extended summer season contributes an average of ~80%[1] of the annual rainfall across the area from 0- 52°E and 10-34°S, and is the focus of this thesis.

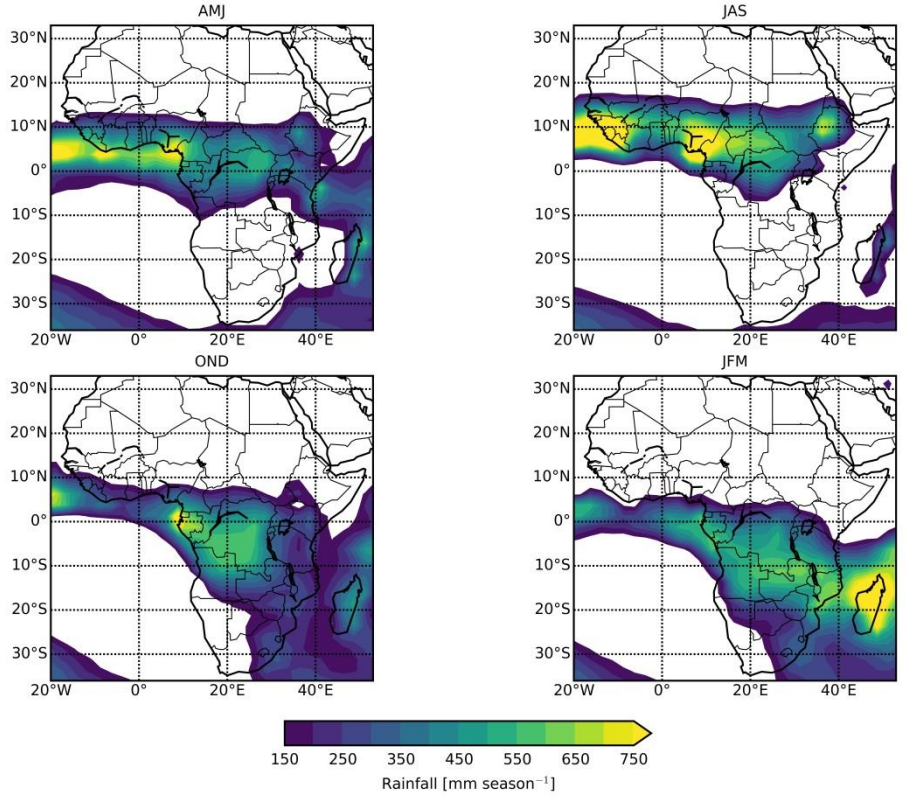


Figure 1.2 The annual cycle of rainfall over Africa in four season: April to June (top left), July to August (top right), October to December (bottom left) and January to March (bottom right). Data is from the CMAP satellite/rain-gauge dataset

[1] Based on the 1979-2005 climatology from the CMAP satellite/rain-gauge dataset

The summer rainfall climatology is maintained by a number of important features, which are summarised in Figure 1.3. Starting in the tropics, the low-level circulation is dominated by the presence of a cyclonic feature, the Angola Low, which is centred near the Bie Plateau in Angola at ~17°S and extends into Namibia, Botswana and Zambia. The Angola Low, together with the South Indian Ocean High (SIOH) and South Atlantic High (SAH), helps to set up a strong zonal pressure gradient between the subcontinent and the adjacent South Atlantic and South Indian Oceans. It is thus an important component in the northeasterly, southeasterly and northwesterly moisture transport pathways over the subcontinent (Rouault et al. 2003; Cook et al. 2004; Hermes and Reason 2009a; Hart et al. 2010). Hart et al. (2010) also point to the potential importance of the Angola Low in the development and intensification of tropical-temperate cloud bands (TTCBs) over southern Africa. TTCBs are the synoptic expression of SIOCZ, forming through the interaction of tropical convection and midlatitude transient eddies, and contribute between 40 and 60% of the regional rainfall (Harrison 1984; Hart et al. 2013).

Despite its significance for the climate system, the Angola Low is poorly understood and has been described variously in the literature as a shallow, thermal low and a deep convective low[2]. Prior to the reanalyses era, the Angola Low was sampled occasionally when tropical lows forming within the Congo Air Boundary were identified in Zambia and sometimes to the south in Botswana. As a consequence, pioneers of southern African climate science tended to refer to the Angola Low as the Botswana Low (van Heerden and Taljaard 1998; Tyson and Preston-Whyte 2000), the Botswana Trough

[2] The dynamics of the Angola Low are now much better understood owing to the excellent analysis by Emma Howard and Richard Washington in the last year. We describe these new results in the context of our own findings (cf. Chapter 4) in the concluding chapter.

(Taljaard 1972, 1986) or Zambian Low (Leroux 1983). To the author's knowledge, the first published reference to the Angola Low is by Zunckel et al. (1996), following an investigation of radiosonde data from northern Namibia as part of the Southern African Fire-Atmosphere Research Initiative (SAFARI) observational campaign in 1992. With the support of newly available reanalysis datasets, Henry Mulenga provided the first detailed account of the meteorology of the Angola Low in his 1998 PhD thesis (Mulenga 1998). Since then, our understanding of the circulation around the Angola Low has been based on fewer than six reanalyses products, none of which is well constrained by observations in southern Angola and which differ substantially from one another in their estimates of the circulation (Zhang et al. 2013). Our knowledge of the Angola Low is therefore predominantly based on numerical models, but to date no attempt has been made to assess how it is simulated across range of different model structures.

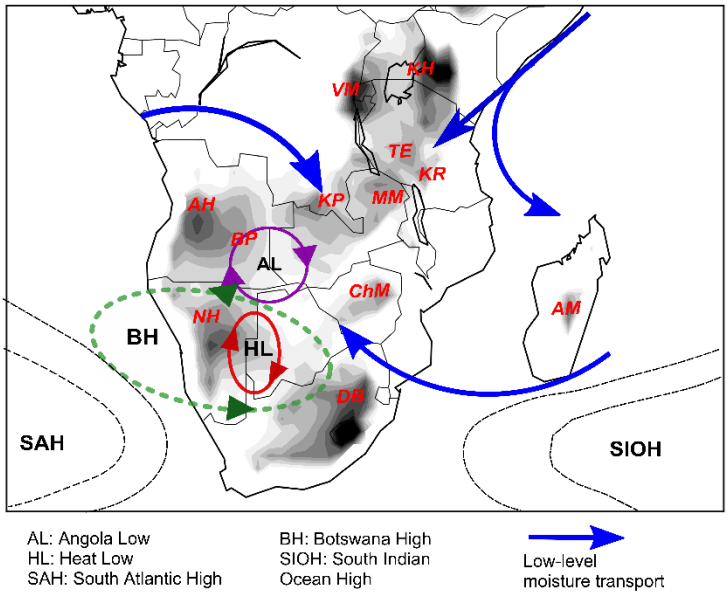


Figure 1.3 Key features of the summer circulation over southern Africa. Topography above 1000m (shaded) is from the USGS GTOPO30 dataset, with key features labelled. AH: Angola Highlands; BP: Bie Plateau; NH: Namibian Highlands; DB: Drakensburg Mountains; ChM:

Chimanimani Mountains; AM: Ankaratra Massif; MM: Muchinga Mountains; KP: Katanga Plateau; KR: Kipengere Range; TE: Tanzanian Escarpment; VM : Virunga Mountains; KH: Kenyan Highlands.

Alterations to the tropical moisture pathways are associated with coherent rainfall anomalies across southern Africa at all timescales, from the daily to the multi-decadal, and are especially important in the core of the summer season from December onwards (e.g. D'Abreton and Tyson 1995; Fauchereau et al. 2009). In their influential paper in 1993, D'Abreton and Lindesay show that wet Januaries are associated with an enhancement of the northwesterly moisture transport over the central subcontinent and an increase in northeasterly moisture supply from the tropical Indian Ocean. Subsequent studies have confirmed the associations between enhanced moisture flux and rainfall (e.g. Cook et al. 2004; Washington and Preston 2006), with a later study also suggesting a role for the southern component of the mid-level African Easterly Jet (AEJ-S) in transporting moisture from the African tropics poleward (Vigaud et al. 2007).

At the interannual timescale, the modulation of moisture supply and convergence is predominately understood as an atmospheric response to sea surface temperatures (SST) by teleconnection with prominent modes of SST variability. Among these are the El Niño Southern Oscillation (ENSO; Lindesay 1988; Nicholson and Kim 1997; Richard et al. 2001), which typically leads to dry (wet) conditions during the El Niño (La Niña) phase; and the Subtropical Indian Ocean Dipole (SIOD; Behera and Yamagata 2001; Reason 2001; Fauchereau et al. 2003; Hermes and Reason 2005). In positive phases of the SIOD, SSTs are anomalously high (low) in the southwestern (central and south eastern) Indian ocean and this is associated with above average rainfall. The opposite occurs during negative phases. Based on a set of targeted model experiments, Reason

(2001) argues that the warm pole south (and west) of Madagascar is particularly important in driving the above average rainfall. This is consistent with observational and modelling studies showing that above average rainfall in central and eastern southern Africa occurs when there are unusually high SSTs in the greater Agulhas current region (Walker 1990; Mason 1995; Reason and Mulenga 1999). Through its influence on tropical easterly moisture supply, a stronger ocean high pressure system to the east and north of Madagascar, associated with anomalously cold SSTs, has also been linked with summers of high rainfall (Washington and Preston 2006).

In the subtropics, the mid- to upper-level Botswana High plays an important role in the southern African summer rainfall climatology and variability. The high likely forms in response the tropical heating in the Congo Basin convective region (Reason 2016), and is similar in that regard to the Bolivian High which forms in response to diabatic heating in the Amazon (Lenters and Cook 1997). A strengthened Botswana High over southern Africa is associated with reduced rainfall over Zimbabwe (Matarira 1990; Unganai and Mason 2002) and over southern Africa as a whole (Reason 2016; Driver and Reason 2017). While the high is known to strengthen during El Niño years (e.g. Dieppois et al. 2015), Reason (2016) describes a second mode of variability, independent of ENSO, in which the strength of the Botswana High varies contemporaneously with the mid-level highs over Bolivia and northwestern Australia.

The clear skies associated with upper level subsidence, coupled with the high top of atmosphere (TOA) incoming solar radiation favour the formation of a thermal low in early summer over the western Kalahari Basin. The contribution of the thermal low to

the circulation over southern Africa has not received significant attention. Taljaard (1986) suggests that the position of the thermal low plays a role in determining the western boundary to which low-level moist air can circulate. The thermal low may therefore be an important component in determining the location of the SIOCZ (Cook 2000). It also strengthens the meridional temperature gradient, with Adebiyi and Zuidema (2016) showing that the strong surface temperature gradient between subtropical and tropical Africa gives rise to the mid-level AEJ-S. The AEJ-S in turn influences the transport of mineral aerosols off the coast of southwest Africa.

Southern Africa is bounded to the west by the cold Benguela upwelling zone and to the east by the warm SSTs (20-24°C) associated with Agulhas current. The Benguela upwelling system is a band of upwelled cold SST, orientated along the western southern Africa coastline, which is driven by the surface southerly wind-stress associated with the eastern edge of the South Atlantic High pressure system. The cold SST (~14-16°C) stabilises the overlying atmosphere, and together with the climatological subtropical subsidence helps to account for the aridity of the Namib Desert and the northwest coast of South Africa (Reason 2017). The Agulhas current region has the opposite effect in the east. Large latent heat losses, averaging ~200 $W.m^{-2}$ in summer (Walker and Mey 1988), occur as the Agulhas current meets the midlatitude westerlies and retroflects into the southern Indian Ocean. Together with the anomalously warm SSTs, there is evidence that this process acts to intensify storms especially over southern parts of southern Africa (Rouault et al. 2002; Singleton and Reason 2007; Blamey et al. 2017), thus contributing to the east-west rainfall gradient (Figure 1.2).

An additional influence on the distribution of summer rainfall over southern Africa is the complex topography. Most of the southern Africa landmass consists of a plateau which is over 1000m high, with sharp gradients in topography present at the eastern and western coasts, and at the northern terminus of the plateau as it descends into the Congo Basin at ~10°S (Figure 1.4). Model experiments which assess the role of the southern African topography are rare and inconclusive regarding the potential effects. Potter et al. (2017) find a reduction in rainfall across the subcontinent when they set the southern African topography to 3m high in GFDL's CM2M model, with part of the reduction likely owing to the decreased relative humidity associated with hotter temperatures. In an atmosphere-only GCM (HadAM3) experiment, which removed the East African Highlands down to 15°S, Slingo et al. (2005) find that the northeasterly monsoon flow weakens over southern Africa and that there are slight reductions in rainfall. Reason (2017), meanwhile, posits that the presence of Madagascar contributes to the aridity over the subtropical southern Africa by blocking the moisture inflow from the Indian Ocean. Moore's (2013) results concur with this assessment and, based on reanalysis data, he suggests that the Madagascan landmass helps to account for the southeasterly orientation of moisture inflow across the Mozambique coast by contributing to the formation of the Mozambique Channel Trough. Most recently, Barimalala et al. (2018) showed that continental Southern Africa is wetter when Madagascan topography is reduced or removed in climate model simulations.

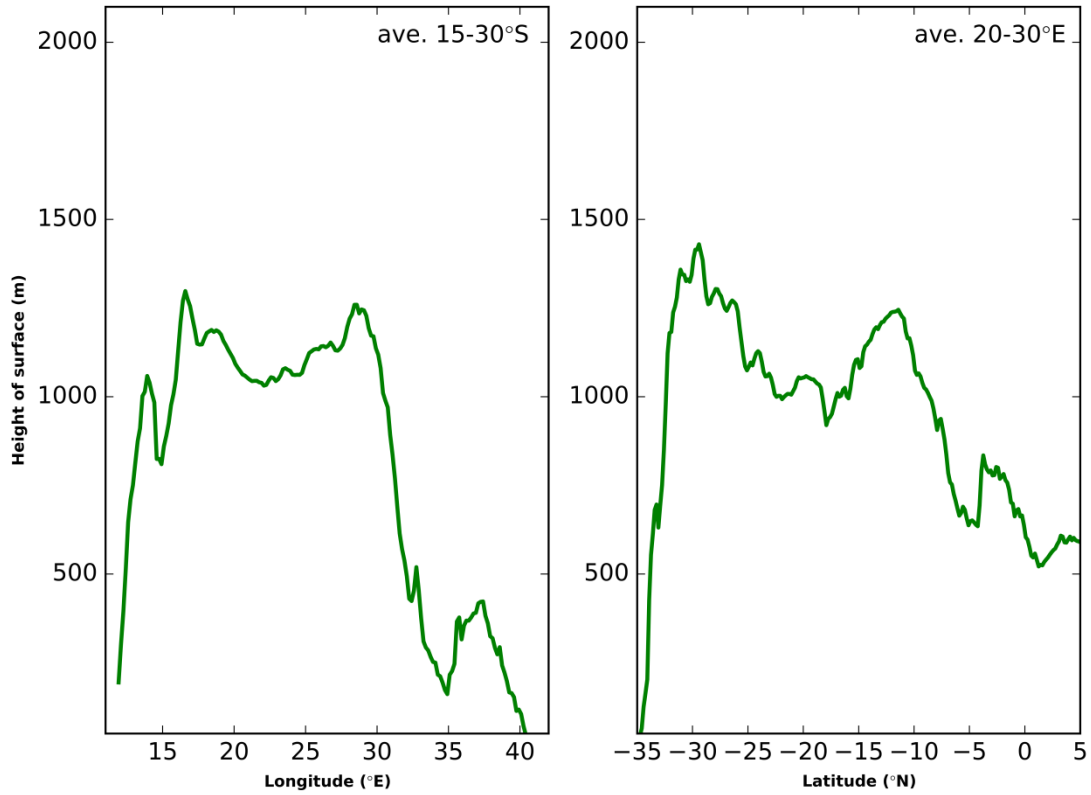


Figure 1.4 Longitudinal (left) and latitudinal (right) cross sections of surface height across southern Africa. The longitudinal (latitudinal) cross-section is averaged over 15 to 30°S (20-30°E). Topography data is from USGS GTOPO30 digital elevation model.

The southern African climate system thus consists of a complicated web of influences, with much of the complexity not yet fully understood. This complexity, together with a historical lack of attention to African climate in general (Washington et al. 2006), has ensured that southern Africa is a challenging environment for climate models. These models must therefore be thoroughly evaluated ahead of their use for climate change prediction in this vulnerable region

2. Climate Model Evaluation

2.1 Background

Climate model evaluation is an assessment of the extent to which a climate model resembles the climate system (Räisänen 2007). Approaches to model evaluation are varied, but can be split into two broad categories; quantification of performance and process-based analysis (James et al. 2018). The present section critically reviews these two approaches and outlines the current state of knowledge of the performance of climate models in southern Africa. It then goes on to discuss previous research into the mechanisms of future rainfall change over southern Africa, before outlining the current gaps in our understanding of model simulations of climate change.

2.2 Performance based model evaluation and its application in southern Africa

The quantification of model performance relative to observations is the dominant mode of model evaluation (Baumberger et al. 2017), and forms the basis of IPCC assessment of model reliability (Flato et al. 2013). Systematic analysis of model performance starting in the 1990s has identified persistent problems in coupled models at a global scale. These include the simulation of a 'double Intertropical Convergence Zone (ITCZ)' over the Pacific Ocean (Mechoso et al. 1995; Dai 2006), the displacement of the extratropical storm tracks equatorward (Bracegirdle et al. 2013; Kidston and Gerber 2010) and the warm sea surface temperature (SST) biases in eastern subtropical ocean basins (Wang et al. 2014). Simple metrics, such as root mean squared errors (RMSE), or more complex multivariate 'skill scores' (e.g. Watterson et al. 2014) have been used to summarise the performance of models in simulating features of the climate system, to 'validate' climate models for particular purposes, to rank different models based on their

relative skill and to track model improvements through time (Reichler and Kim 2008; Gleckler et al. 2008; Schaller et al. 2011).

Over southern Africa, successive generations of climate models have struggled to represent the observed rainfall climatology (Joubert 1995; Mason and Joubert 1997; Cook 2001; Moise and Hudson 2008; Mueller and Seneviratne 2014; Dieppois et al. 2015; Lazenby et al. 2016). While most models successfully simulate the phase of the annual cycle, including the onset and cessation of seasonal rainfall (Dunning et al. 2017), the amplitude of the annual cycle is generally too low, and there is a systematic tendency to simulate too much rainfall throughout the year (Dieppois et al. 2015). Dieppois et al. (2015) show that while the range of mean southern African (36°–20°S, 10°–36°E) rainfall in CMIP5 models is generally less than 30 mm month^{-1} in the drier winter months, in January it is close to 100 mm month^{-1}. For comparison the average observed rainfall in January, estimated by the Climate Research Unit (CRU; Harris et al. 2014), is 70 mm month^{-1} (Dieppois et al. 2015). The rainfall excess over southern Africa is accompanied by a deficit over Madagascar and the southwest Indian Ocean across most coupled models (Lazenby et al. 2016), with the anomalous diabatic heating associated with the enhanced precipitation likely to influence regional overturning circulations.

Similar errors in the simulation of southern African rainfall are a feature of atmosphere-only climate models within the Atmospheric Model Intercomparison Project (AMIP) (Lazenby et al. 2016) and in some regional climate models (RCMs) which form part of the Coordinated Downscaling Model Experiments (CORDEX) (Kalognomou et al.

2013). In CMIP, AMIP and CORDEX ensembles, the wet biases present in individual models do not cancel in the multi-model mean (MMM). This suggests that model rainfall biases relative to observations are not caused by random errors alone, but rather are a consequence of common structural deficiencies in models (Sanderson and Knutti 2012), for example in grid resolution or in the representation of convection (Kalognomou et al. 2013).

Finding the source of these rainfall biases and assessing their implications for model reliability is clearly important, but is difficult with purely performance-based approaches. This is for a few key reasons. First, the observational baseline against which we compare models is uncertain. While there is a high density of observation stations in South Africa, most of the region and especially tropical areas north of 15°S have very poor coverage (Figure 2.1). Rainfall estimates here are uncertain, but also important given the high contribution to the regional precipitation. In the case of rainfall estimates over Okavango Basin, Wilk et al. (2006) compare rainfall estimates from the Nicholson African monthly rainfall database (Nicholson et al. 1997) with estimates from an extended data set with 56 additional rainfall stations from the national meteorological services of Angola, Botswana and Namibia. They find that the addition of a single rainfall station in the Okavango Catchment results in an estimate of median wet season (November to April) rainfall totals which are 20-60% higher in the extended dataset compared to the Nicholson dataset. The sensitivity of observational datasets to the addition of a single station suggests that we do not have a firm grasp on the true rainfall climatology, especially as the scale of analysis contracts. It also implies that our quantitative understanding of model biases is not robust.

The problem of sparse station coverage has been eased in part by the development of satellite-based estimates of rainfall, available from 1979 onwards (e.g. Xie and Arkin 1997). While the latest products generally agree on the spatial pattern of rainfall for the mean climatology (e.g. Novella and Thiaw 2013), there remain large quantitative differences between rainfall estimates (Sylla et al. 2013; Kalognomou et al. 2013; Awange et al. 2015). In Central Southern Africa, Sylla et al. (2013) note that there is a 23% difference in rainfall between the Famine Early Warning Systems Network (FEWS-NET) dataset and the Global Precipitation Climatology Project (GPCP) dataset, while Tropical Rainfall Measurement Mission (TRMM) rainfall differs by up to 50% compared GPCP in tropical Africa (Nikulin et al. 2012). The causes of rainfall differences between observational datasets are complex, with the technique of interpolation; the algorithms used to convert radiative signatures to precipitation; and quality control, all playing a part. These factors in turn are dependent in some way on the density of rain gauge stations (Wilk et al. 2006; Awange et al. 2015) which is unlikely to increase rapidly over Africa in the near future (Washington et al. 2006; James et al. 2018).

The observational uncertainty undermines attempts to evaluate the reliability of models based on quantitative approaches alone. This is well illustrated by a debate in the Journal of Climate over the mechanism by which ENSO influences southern African rainfall (Cook 2000; Nicholson 2003; Cook 2003). Based on idealised experiments in a version of the Geophysical Fluid Dynamics Laboratory (GFDL) GCM model and in a more realistic GCM validated against the global precipitation index (GPI) satellite product

(Arkin and Meisner 1987), Cook (2000) argues that the El Niño teleconnection to southern African rainfall can occur via a purely atmospheric mechanism; Rossby wave generation in response to Pacific SST anomalies. Nicholson (2003) disagrees with this interpretation, predominantly on the basis that she considers the GFDL model to be inadequate for purpose, as judged by comparison of its rainfall climatology with the Nicholson African monthly rainfall database (Nicholson et al. 1997). Cook (2003) responds by highlighting the uncertainty among satellite and rain gauge products in their estimation of southern African rainfall; suggesting that, in terms of model performance, 'beauty is in the eye of the beholder!' (pp 565). This implies that model evaluation at the process-level is imperative.

Even in a counterfactual scenario where we have a 'perfect' set of observations, there would be fundamental limits of performance-based approaches to model evaluation. In southern Africa, despite knowledge of model rainfall biases for nearly three decades there has been no compelling diagnosis of why the biases arise. The lack of diagnosis leaves model developers in the dark over which elements of models they should target in order to improve the simulation of rainfall. Moreover, it remains unclear how different a model must be from observations to be deemed 'unreliable'. An arbitrary difference in rainfall climatology between a model and a 'perfect' set of observations of, say, 0.5 mm day^{-1} might be inconsequential if the simulated climate system is able to respond to external forcing in a manner consistent with reality (Notz 2015). By contrast, if the difference of 0.5 mm day^{-1} is caused by a fundamental misrepresentation of a process which is important for the simulation of future change, then it is clear that the model is not adequate for the purpose. These issues would be the same even if no rainfall bias detected in models. This is a fundamental limit of quantification relative to observations

which the IPCC chapter on model evaluation acknowledges, but does not fully discuss

(Flato et al. 2013; p756):

'This [approach] does not, however, provide an answer to the much more difficult question of determining how well a model must agree with observations before projections made with it can be deemed reliable'.

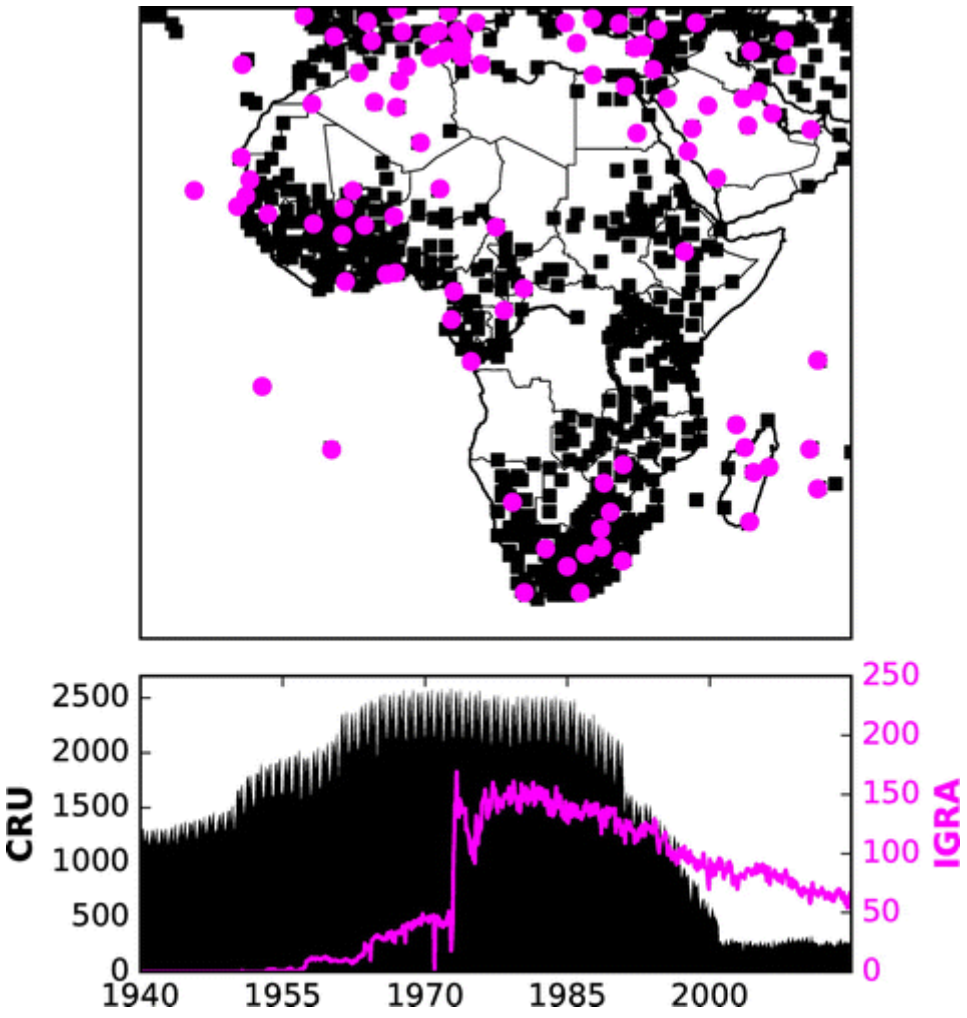


Figure 2.1 Station data contributing to the (CRU, version 2.23) rainfall (black) and Integrated Global Radiosonde Archive (IGRA) u wind at 1200 UTC (pink). (top) Coverage map for 1979–2013. Black squares indicate the location of 0.5° × 0.5° grid boxes that have at least one contributing station during at least 50% of the months; pink circles indicate stations with at least 10 records per month in at least 50% of the months. (bottom) Time series showing the number of stations contributing in each month (40°S–40°N, 30°W–60°E). *Source: James et al. (2018) BAMS.*

2.3 Process-orientated approaches

Partially in response to the issues outlined in the preceding section, there has been increasing recognition over the last decade that understanding model simulations at a process level is the key to assessing model reliability. This is reflected in the creation of number of international projects, working groups and special collections in prominent journals aimed at advancing process-orientated approaches to model evaluation[3]. This section discusses the value of a process-based approach to model evaluation, focussing on model ensembles, and considers existing process-based diagnosis of model simulations of the southern African climate system.

2.3.1 The value of process-based analysis

Process-orientated approaches examine the model simulation of processes which are thought to be, or are demonstrated to be, important for the model simulation of a key variable, such as rainfall. In the context of intercomparison projects, such as CMIP or AMIP, process-based evaluation often proceeds by examining the differences in the representation of key dynamics, or features, amongst models and compared to some observational reference, commonly reanalysis estimates of circulation. Such an approach to evaluation contains a number of key benefits, including: a more meaningful assessment of model reliability (as opposed to performance-based approaches); demonstration of essential areas for model improvement; and the potential to guide

[3] For example, the NOAA Modeling, Analysis, Predictions and Projections program has a dedicated project - The Model Diagnostics Task Force (MDTF) – which aims to advance on process-based evaluation of models, while Journal of Climate have an open special collection on process-orientated model diagnostics (https://journals.ametsoc.org/topic/process_oriented_model_diagnostics).

observations and generate hypotheses concerning the functioning of the real climate system. In practice, the first two of these benefits are widely acknowledged, while the heuristic value of coordinated model ensembles is less well appreciated. This section discusses the justifications for process-based approaches in more detail.

2.3.1.1 Assessment of model reliability

Process-orientated approaches to evaluation can provide physically-based insights into a model's adequacy for projecting future change. If the physical processes which are known to be important for the simulation of the climate system are poorly represented, this could be a basis for excluding models; especially if that physical process is demonstrated to be important for the simulation of future change (Knutti 2010; Overland et al. 2011; McSweeney et al. 2012; Thibeault and Seth 2014; Schmidt and Sherwood 2015). One example of this approach is a study by Hall and Qu (2006) which shows that projected snow-albedo feedbacks in CMIP3 models are closely tied with their contemporary seasonal cycle. Most models underestimate the amplitude of the seasonal cycle, and thus are also likely to underestimate the snow-albedo feedback. Physically, this is logical, because models with high albedo in the present day simulate a sharper contrast between snow-covered areas and snow-free areas, and thus simulate a stronger feedback in response to external forcing, whether it is driven by the seasonal cycle in insolation or emissions forcing. The high confidence in this constraint on future projections, therefore, rests on a strong physical understanding of the processes linking present day performance and future change.

In many other examples, however, the relationship between present day bias and future projections is less clear. The exclusion of models with largest biases, when evaluated against a range of physical metrics of interest, has commonly failed to constrain the range of future projections (Sanderson and Knutti 2012; Rowell et al. 2016; McSweeney et al. 2012). For instance, Rowell et al. (2016) attempt to constrain the future projection uncertainty in the CMIP5 ensemble over the Sahel and East Africa by excluding models on the basis of their contemporary performance against a range of 23 process-orientated metrics thought to be relevant for projecting rainfall change. They find no considerable reduction in future projection uncertainty, with projections from poorly performing models distributed throughout the intermodel range. Part of the reason behind this lack of coherence between past performance and future change could be that the processes underlying future change may be different from those which control the contemporary climatology (Sanderson and Knutti 2012).

An alternative possibility is that the metrics chosen to assess the present day performance of models are not critical for the model simulation of the variable of interest. In Rowell et al. (2016), the 23 metrics are chosen for their relevance for rainfall in East Africa, including the representation of key observed teleconnections with global oceans and the simulation of the annual cycle. However, there is no indication of the relative importance of these metrics, or whether they are in fact important in distinguishing between model performances in the present day. For the East African 'short rains' (OND), for example, a recent study has found that in the CMIP5 ensemble, overestimation of rainfall is closely associated with erroneous simulation of mean low-level winds in the equatorial Indian Ocean (Hirons and Turner 2018). In the wettest CMIP5 models, the climatological winds are easterly, whereas they are westerly in dry

models and observations. Low-level winds are not considered as a relevant metric in Rowell et al. (2016), but could help constrain future projections. Indeed, Giannini et al. (2018) find that in the ensemble mean CMIP5 model, future rainfall increases over East Africa are closely tied to an alteration of the low-level easterlies. It could therefore be the case that the East African response to climate forcing builds on an error in the model simulation of important climate processes in the present day. This demonstrates the value of developing bespoke, regionally-specific metrics for model simulations based on a detailed analysis of their present day climatology.

The above example also highlights that, in contrast to performance-based approaches, process-based analysis is not limited to analysis of the contemporary period. Insight into the reliability of models can be gleaned from a direct assessment of the mechanisms of projected change (Giannini 2010; Seth et al. 2013; James et al. 2015). For example, James et al. (2015) investigate future drying in West Africa in a suite of models at differing resolutions. They find that the climate models' simulation of future drying is associated with anomalous subsidence in the upper troposphere, with the same vertical structure as in model simulations of drought in the contemporary period. Crucially, the circulation associated with the historical simulation of drought has no observational counterpart, thus calling into question the credibility of the model projection. Such mechanisms of change could also be evaluated against theoretical expectation of the response of rainfall to warming and by comparison with simpler models to provide further insights into the physical plausibility of the model response.

2.3.1.2 Guidance for model improvement

Identification of model deficiencies can help to guide areas for model improvement. This is particularly valuable in cases where a model deficiency can be firmly linked to the simulation of a variable of interest. Previous work has shown, for example, that global scale biases in rainfall can be linked to the inadequate representation of orographic drag in models (Berckmans et al. 2013; Pithan et al. 2016; van Niekerk et al. 2016), to cloud biases in the Southern Hemisphere (Hwang and Frierson 2013) and to biases in the representation of Antarctic sea ice extent (Bracegirdle et al. 2018). Such global scale evaluations can set the priorities for model development and have led to the formation of specific task forces, such as the Working Group on Numerical Experiments (WGNE) orographic drag intercomparison project[4].

The causes of model errors at a regional scale may be different from those at a global scale, and in specific regions may be dominated by a particular climatic influences, for example SSTs (Creese and Washington 2018), topography (Martin and Thorncroft 2015) and soil moisture (Taylor et al. 2013). In a process-based evaluation of the model simulation of Congo Basin rainfall in the boreal autumn (September-November;SON), Creese and Washington (2018) find that some models simulate spuriously high rainfall in the west of the Basin which is connected to an anomalously high SST bias in the Gulf of Guinea (GoG). For these models to improve their simulation of contemporary Congo Basin climate, this SST bias must be addressed. Addressing process biases at a regional

[4] http://collaboration.cmc.ec.gc.ca/science/rpn/drag_project/

scale could also lead to improvements in the basic physics of models, and thus enhance the performance of models at coarser scales.

2.3.1.3 Heuristic value of model ensembles

A third value of process-based evaluation is in guiding observations and experiment. This heuristic value of process-based analysis is often overlooked, especially in the context of model intercomparison projects where the stated aims are most often to assess the relative performance and reliability of models, or to guide model improvements (Räisänen 2007). Nonetheless, the identification of important processes which distinguish between models can generate or support hypotheses about how the climate system functions in the real world (Schmidt and Sherwood 2015), and may also be a useful guide for observations (Massonnet et al. 2016; Creese and Washington 2016).

The heuristic value of model intercomparison can be elucidated through an example of process-based assessment of CMIP3 simulations of rainfall change in the Sahel, and its relation with the Sahara Heat Low (SHL; Biasutti et al. 2009). Biasutti et al. (2009) find that the strength of the SHL in all models correlates with Sahelian rainfall in all models at the timescales of interannual and interdecadal historical variability. They also show that models projecting the strongest deepening of the SHL in the future tend to simulate largest increases in rainfall. This result is attractive in its simplicity, and recasts the SHL as an important driver of Sahelian rainfall, independent of SST variability. This helped to motivate a number of lines of scientific investigation, including: observational campaigns which probed the structure of the SHL (Engelstaedter et al. 2015; Marsham

et al. 2015); analyses of the relationship between SHL and rainfall in observations (Hurley and Boos 2013; Tseng et al. 2016; Peyrille et al. 2016; Shekhar and Boos 2017; Dyer et al. 2017); and evaluations of the representation of the SHL in the latest generation of CMIP5 climate models (Vizy et al. 2013; Gaetani et al. 2017; Dixon et al. 2017, 2018). The net result of this work is that the original conclusions of Biasutti et al. (2009) have been questioned (e.g. Shekhar and Boos 2017; Dyer et al. 2017), but our scientific understanding of West African climate system has advanced. In southern Africa, where we do not yet fully understand some of the critical climate influences, process-based analysis could fulfil a similar, generative role and help to advance the scientific agenda.

2.3.2 Review of process-based analysis in southern Africa

In comparison to other global regions, and to East and West Africa, analysis of climate models at the process level is lacking in southern Africa. This section discusses the literature which investigates the processes underling model simulation of southern African rainfall in the contemporary period, before evaluating research into the potential mechanisms of future rainfall change. The focus of discussion is the simulation of austral summer climate, as this is the focus of the thesis.

2.3.2.1 Contemporary climatology

In the 1990s, several studies started to consider the processes associated with the overestimation of summer rainfall in climate models (Joubert and Hewitson 1997;

Mason and Joubert 1997; Tennant 2003; Joubert 1995). In a comparison of seven atmosphere-only models as part of the AMIP ensemble (Gates 1992), Joubert and Hewitson (1997) found that the positive rainfall bias over southern Africa in models was associated with strengthened continental low pressure, and slight overestimations in the strength of the South Indian Ocean High (SIOH). For all models, the mean sea level pressure (MSLP) lay below one standard deviation of the observed mean estimate over the continent. Biases at the surface were accompanied by underestimations of geopotential height in mid-levels in the atmosphere (Joubert 1995; Joubert and Hewitson 1997). South of the southern Africa landmass, the subtropical (barotropic) jet was additionally displaced equatorward in all model versions (Mullan and McAvaney 1995; Joubert and Hewitson 1997), which Tennant (2003) suggested could encourage more frequent or intense tropical-temperate interactions in models.

The circulation and rainfall biases in atmosphere-only models with very coarse resolution have largely been inherited by higher resolution atmosphere-only and coupled climate models (Moufouma-Okia and Jones 2014; Dieppois et al. 2015; Lazenby et al. 2016). Across a suite of models with differing resolutions (from 150km to 12km), Moufouma-Okia and Jones (2014) show that errors in the simulation of southern African rainfall are positively correlated with biases in vertically integrated moisture transport in DJF. This finding is consistent with circulation biases in CMIP5 (Lazenby et al. 2016) and CORDEX (Kalognomou et al. 2013) simulations, which exhibit enhanced moisture circulation, particularly around the Angola Low, associated with a positive precipitation bias. The latest generation of AMIP and CMIP models also tend to place the southern hemisphere subtropical jet too far northward (e.g. Bracegirdle et al. 2013), consistent

with assessments of early global model versions (Joubert 1995; Joubert and Hewitson 1997; Mullan and McAvaney (1995); Tennant 2003).

There are a number of potential sources of the rainfall and circulation biases, including model representation of the complex southern African topography (Mason and Joubert 1997; Pinto et al. 2016), SST biases (Dieppois et al. 2015), convective parameterisations (Kalognomou et al. 2013; Tozuka et al. 2014), and the representation of land surface characteristics; including soil moisture (New et al. 2003; Cook et al. 2006) and vegetation (Williams and Kniveton 2012). In the case of model representation of topography, the coarse scale of GCM grids (~100-200km) relative to the fine scale topographic gradients in southern Africa, could lead to problems in the simulation of orographic rainfall. Indeed, various authors have noted that the model rainfall bias appears to worsen in the vicinity of the complex and high topography of the eastern escarpment (Mason and Joubert 1997; Pinto et al. 2016; Dedekind et al. 2016). The effect of coarse resolution on modelled circulation is less clear, although a few experimental studies which remove and smooth the topography over parts of southern Africa have shown the potential for significant alterations to climatology of low-level winds (Slingo et al. 2005; Potter et al. 2017; Barimalala et al. 2018). The resolution required to adequately represent the Southern African topography is not known.

Through their influence on the vertical profile of diabatic heating, model convection schemes can affect the large scale circulation, and are a known source of error in GCMs globally (e.g. Maher et al. 2018). Over southern Africa a few studies have attempted to test the effect of different convective parameterisations on the rainfall and circulation

bias (Crétat et al. 2012; Tozuka et al. 2014; Ratna et al. 2014). These studies have all shown some differences between the simulations of southern African rainfall in climate models related to the choice of convection schemes, particularly in the simulation of synoptic weather events. However, interpretation of these results is complicated by the fact that the development of the dynamical core in climate models rarely occurs in isolation from the choice and implementation of parameterisations schemes, and thus some of the differences may not be directly linked to the convective parameterisation scheme. Moreover, in all three studies the wet bias across southern Africa remains regardless of the choice of convective parameterisation scheme (Tozuka et al. 2014). This suggests that there are common features of convective parameterisations which might contribute to the rainfall biases. Indeed recent work which has investigated the performance of a convective permitting model over southern African (Hart et al. 2018) has shown some significant reduction in the rainfall bias related to improved local overturning circulation.

Similarly, attempts to attribute rainfall errors to the large SST biases in the vicinity of southern Africa (Wang et al. 2014) have not been conclusive. For instance, Weber et al. (2017) investigate the effect of replacing the simulated SSTs from the MPI-ESM-LR model in the Indian and Atlantic Oceans with observed SSTs from ERA-Interim reanalysis. They find some modest improvements in rainfall simulation over the western tropical regions of southern Africa and over Angola when the large SST biases in the Atlantic Ocean (particularly in the Benguela upwelling region) are removed. However, there is little improvement over the rest of the subcontinent, and the correction of Indian Ocean SSTs appears to have little effect on the rainfall climatology. These findings are consistent with comparisons between AMIP and CMIP model ensembles; while the wet

bias near the Angola Coast is reduced in AMIP models, rainfall and moisture circulation biases in central and eastern southern Africa are remarkably similar in both model sets (Figure 2.2 and Lazenby et al. 2016). This implies there is some atmospheric origin of the rainfall bias, which is the line of enquiry that this thesis follows.

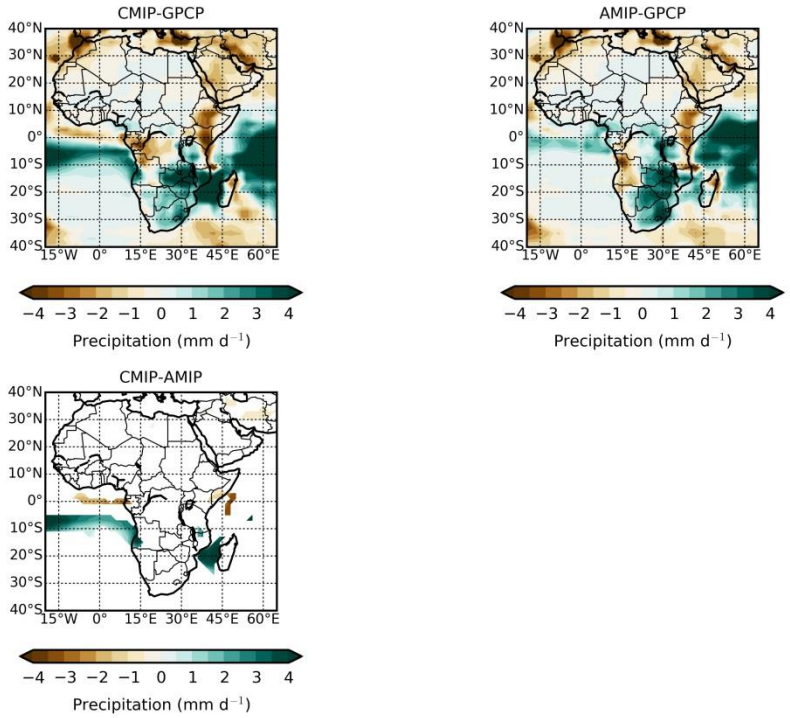


Figure 2.2 The CMIP (top left) and AMIP (top right) MMM climatological rainfall biases (1979-2005) for January. The bottom left plot shows CMIP MMM minus AMIP MMM rainfall, with non-significant differences among the 25 model ensembles masked. Significance is assessed via the Students t-test ($p<0.05$).

2.3.2.2 Mechanisms and uncertainty in future rainfall change

Potential future rainfall changes over southern Africa have received a great deal of attention from a climate impacts point of view. In the early summer there is general consensus among models that rainfall will decline (e.g. Meehl et al. 2007; Shongwe et al. 2009; Collins et al. 2013; He and Soden 2016), while in the late summer (JFM), the

signal is mixed (Shongwe et al. 2009); roughly half of models project increases in future rainfall and while the other half project decreases (Figure 2.3). Some of the rainfall projections, if realised, could have deleterious social consequence, with Cook and Vizy (2013), for example, showing that projected rainfall declines in austral spring could lead to a 40-80% reduction in the number of growing season days in tropical regions of southern Africa. In light of the potential impact, recent work has considered the mechanisms of future rainfall change as a first step to assessing their plausibility.

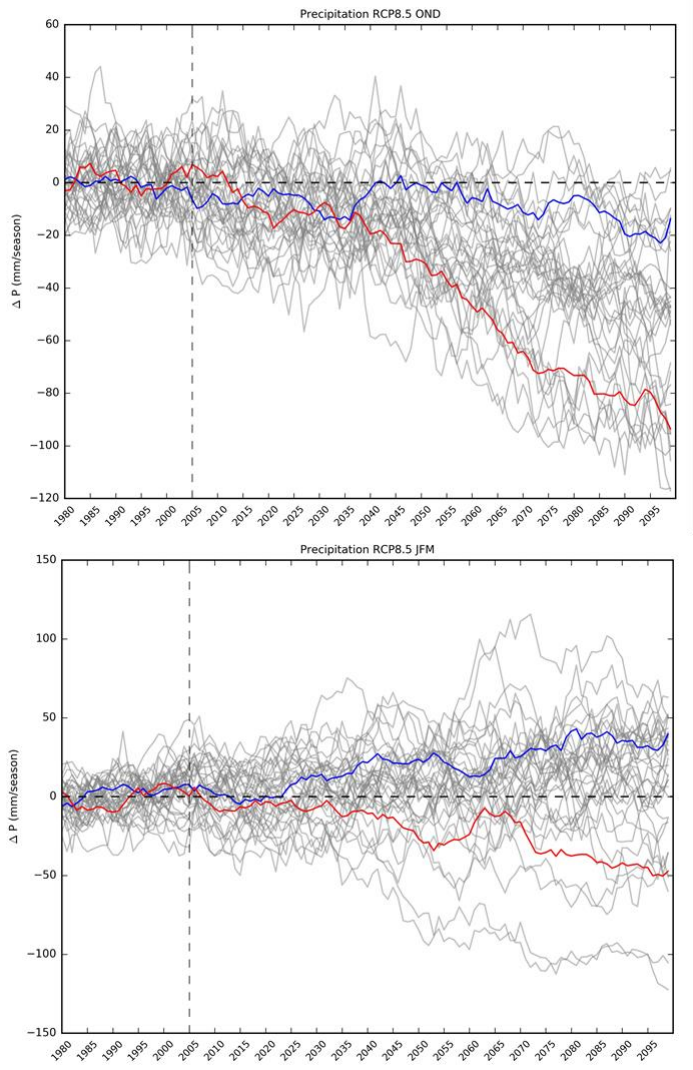


Figure 2.3 Evolution of rainfall change over southern Africa under RCP8.5 from 1980 to 2100 in CMIP5 models (grey lines). The time series is smoothed by a 10-yr rolling mean. The top plot is for OND and the bottom plot is for JFM, with the red (blue) lines showing the average change in the eight models projecting strongest drying (greatest wetting or lowest magnitude drying).

For the early summer, a number of studies have characterised the rainfall decline as a northeastward shift of the main summer rainfall band, the SIOCZ (Shongwe et al. 2009; Cook and Vizy 2013; Lazenby et al. 2018). Both Cook and Vizy (2013) and Lazenby et al. (2018), in a regional model and CMIP5 models respectively, suggest that the northeastward shift is associated with a strengthening of the continental heat low and a weakening of the South Indian Ocean High. Shongwe et al. (2009), in an investigation of future change in CMIP3 models, also note that the southeasterly moisture feed increases in strength and is diverted northeastward in association with the shift of the SIOCZ.

Seth et al. (2013) examine the rainfall decline in a moist static energy framework. Following the work of Giannini (2010) in a Sahelian context, they suggest that the rainfall decline in the ensemble mean model is driven by large increases in upper level dry static energy (DSE) caused by mean oceanic warming. The increases in DSE at upper levels stabilises the vertical profile in the CMIP5 ensemble mean, with reduced moisture supply following a drier dry season contributing to enhanced column moisture divergence and reduced evaporation. The increase in dry static energy aloft reported by Seth et al., (2013) is consistent with Engelbrecht et al. (2009) who find that the decline in OND rainfall in the variable resolution Conformal-Cubic Atmospheric Model (CCAM) is linked with a strengthening of mid- to upper-level high pressure.

In the late summer, the enhanced moisture supply may be sufficient to overcome the effects of increased subsidence aloft, resulting in reduced moist stability and slight

rainfall increases in the MMM of CMIP3 and CMIP5 (Seth et al. 2011, 2013). The slight increase in rainfall in late summer has also been attributed to a potential increase in the number or intensity of TTCB events (Shongwe et al. 2009; Engelbrecht et al. 2013), although the mechanism by which this occurs is unclear. More generally projections indicate an increase in intensity of extreme rainfall events (Pohl et al. 2017). This is consistent with a large body of literature which suggests extreme rainfall increases should scale with increases in atmospheric water vapour content due to warming (Allen and Ingram 2002). The delay and amplification of the seasonal cycle projected over southern Africa is also a feature of other subtropical regions in Australia, South America and West Africa, and could relate tropics-wide mechanism in which the margins of convective regions dry as more moisture is advected towards the convective core (Neelin et al. 2003; Chou and Neelin 2004).

Projected changes in the rainfall over southern Africa are accompanied by projections of rapidly increasing surface temperatures (Engelbrecht et al. 2015; Meehl et al. 2007). In a small sample of CMIP3 models in addition to the CCAM model, Engelbrecht et al. (2015) show temperature rises which are 1.5 to 3 times the global mean by the end of the 21st century, with attendant increases in the intensity and frequency of heat waves. The reduction in rainfall, through its influence on evaporation and reduced cloud cover (enhanced net solar radiation) could be linked with the amplification of temperature change over southern Africa, as it is in other semi-arid regions (Giannini 2010; Brown et al. 2016), although this has not been demonstrated.

In contrast to the mechanisms of change, the causes of large intermodel uncertainty in future projections (Figure 2.3) have received almost no attention. In a paper examining rainfall change across a few regional climate models, Tadross et al. (2006) suggest that the choice of cumulus convection scheme may lead to some divergence in projections. More recently, Lazenby et al. (2018) examine the contributions of dynamic and thermodynamic mechanisms of rainfall change to the intermodel spread in rainfall change in OND and DJF. They find that while the overall rainfall decline is driven equally by the thermodynamic and dynamic terms, the intermodel uncertainty is dominated by the dynamic term. By investigating composites of the differences between models with significant shifts in the location of convection as against models with modest shifts, they make the argument that the intermodel differences could be caused by uncertainty in meridional SST gradient changes in the Indian Ocean. The significant role played by dynamics in driving intermodel uncertainty is consistent with assessment of the intermodel spread in tropics wide (e.g. Chadwick et al. 2013; Kent et al. 2015) and African (e.g. Park et al. 2015; Rowell et al. 2018) rainfall projections.

3. Data and Methods

3.1 Background

This thesis relies on data from the Coupled Model Intercomparison Project phase 5 (CMIP5), alongside a number of observational reference datasets including reanalysis products and satellite/rain-gauge datasets. The particular models and observational datasets used in each chapter reflect various context-specific factors including the aims of the chapter and the availability of data at the time of analysis. The reasoning behind the choice of models and observational references is made clear in each individual chapter, along with the detailed descriptions of the methods used. Rather than rehearsing these details, the aim of this brief chapter is to provide an overview of the CMIP5 dataset (Section 3.2) and the observational references (Section 3.3) used, in addition to a discussion of the key methods used (composite and correlation analysis) throughout this thesis.

3.2 The CMIP5 dataset

The CMIP5 project is the most recent of the coordinated model experiments organised by the World Climate Research Programme (WRCP), and was prepared in advance of the IPCC AR5 report (Taylor et al. 2012). Data from the project is freely available to download via the Program for Climate Model Diagnosis and Intercomparison (PCMDI) Earth System Grid Federation (ESGF) portal. The ~40 models which form part of CMIP5 are the latest generation of state-of-the-art coupled models contributed by over 20 modelling centres around the world. Each modelling centre runs a common set of experiments with standardised forcings to provide a unique and comparable dataset. The CMIP5 models generally have improved resolution compared to previous model

versions (e.g. CMIP3 models) and some models (Earth System Models; ESMs) incorporate dynamic feedbacks from the carbon cycle, biosphere and atmospheric chemistry.

The aim of the thesis is to examine CMIP5 performance over southern Africa both in the historical period (Chapters 4 and 5) and in the future (Chapter 6). Historical experiments in CMIP5 are forced with twentieth century estimates of known forcing agents including; greenhouse gases, sulphate aerosols, and in some models solar variability and volcanic eruptions. The future change experiments in CMIP5 use the representative concentration pathways (RCPs) developed by van Vuuren et al. (2011). These represent emissions pathways that lead to a certain level of forcing by the end of the century; for example, in RCP4.5 the global net radiative forcing by 2100 is 4.5 W m^{-2}. This thesis uses the most extreme of these scenarios, RCP8.5, which is comparable to the previous CMIP3 Special Report on Emission Scenarios (SRES) A2 scenario based on a 'business as usual' approach to climate change mitigation. We choose the most extreme pathway in part because it is easier to investigate the mechanisms and uncertainty in projections of change when the signal-to-noise ratio is larger, and in part because there is currently little evidence to suggest our emission of carbon dioxide and other greenhouse gases is slowing in the early 21st Century. For both historical and future experiments the data is interpolated to a common grid to allow for comparison across models, and only the first ensemble member (r1i1p1) is used for each model.

In evaluating the CMIP5 ensemble, we should be cognisant of the nature of the model sample. Models are not islands, and several models share significant portions of code,

owing in part to the development of models at the same institution, and in part to model developers working at multiple modelling centres through their career (Masson and Knutti 2011; Knutti et al. 2013). As a consequence, models cannot be considered as fully independent from one another, and thus the effective degrees of freedom may be truncated (e.g. Knutti and Sedláček 2013). In recognising that the CMIP5 ensemble is an 'ensemble of opportunity', we adopt few mitigating strategies. First, within data limits, as many models as possible are selected to increase the effective sample size. Second, a high threshold of significance is adopted for evaluating the probability of a true null hypothesis ($p<0.01$) when undertaking statistical tests for differences and relationships between models. Third, and most importantly, we ensure that there is a strong physical explanation which underlies and justifies the use of statistical tests.

3.3 Reference data sets

Table 1 shows the reference datasets which will be used in various parts of the thesis. As Chapter 2 explains, estimating the precipitation climatology in southern Africa is not straightforward due to the dearth of station data, especially in tropical parts of the subcontinent (e.g. Washington et al. 2006). In this thesis two satellite-rain gauge products are used; The Climate Prediction Center (CPC) Merged Analysis of Precipitation (CMAP; Xie and Arkin 1997) and Global Precipitation Climatology Project (GPCP) version 2 (Adler et al. 2003) datasets, to sample some of this uncertainty.

Table 3.1 Reference Datasets

Product	**Type**	**Resolution**	**Coverage**	**Period Available**
GPCP	Satellite-rain gauge	1°x1°	Global	1979-2011
CMAP	Satellite-rain gauge	2.5°x2.5°	Global	1979-2005
NCEP	Reanalysis	2.5°x2.5°	Global	1948-2017
NCEP2	Reanalysis	2.5°x2.5°	Global	1979-2017
ERA-Interim	Reanalysis	0.7°x0.7°	Global	1979-2017
20CRv2	Reanalysis	2.0°x 2.0°	Global	1871-2012

The CMAP product merges rain-gauge measurements from the Global Precipitation Climatology Center (GPCC; Rudolf and Schneider 2005) with a variety of satellite estimates including those derived from infrared (IR) and microwave (MW) radiance. In light of scarcity of rain gauge estimates in tropical southern Africa, this thesis uses a version (V605) that includes some infilling of values, particularly over oceans, from National Center for Environmental Prediction (NCEP) reanalysis. The GPCP product was developed as part of the Global Energy and Water Cycle Experiment (GEWEX) project devoted to improving analyses of global precipitation. Similarly to the CMAP dataset, the GPCP dataset merges rain-gauge data from a variety of sources with satellite-based microwave and infrared data including those from Special Sensor Microwave Imager (SSM/I), the Defence Meteorological Satellite Program (DMSP), Television and Infrared Observation Satellite (TIROS) Operational Vertical Sounder (TOVS) and outgoing longwave radiation (OLR) measurements. Both GPCP and CMAP products are bias-corrected during their production, as detailed in Adler et al.

(2003) and Xie and Arkin (1997). The choice to use merged products to estimate rainfall follows the guidance of Awange et al. (2015), who suggest that rainfall biases over Africa are minimised in merged products compared to rain-gauge only or satellite-only estimates of rainfall.

Reanalysis data provide an estimate of the observed circulation. Reanalyses products function by assimilating observations into a numerical model structure, thus providing a physical representation of the climate system which is constrained by observations but with global coverage. Due to the relatively poor observational constraint, especially in tropical parts of the subcontinent, reanalysis cannot be considered to represent the true state of the climate system. Nevertheless, it is interesting to see how they compare with each other and model simulations. Four different reanalysis are used in the thesis; ERA-Interim (Dee et al. 2011), 20th Century Reanalyses version 2 (20CRv2; Compo et al. 2011), National Center for Environmental Prediction (NCEP) reanalysis (Kalnay et al. 1996) and the later reanalysis version from the same center (NCEP2; Kanamitsu et al. 2002). Quantitative differences amongst reanalyses in their estimation of the southern African circulation are relatively large (Zhang et al. 2013), but spatial patterns of circulation are largely coherent. Differences amongst reanalysis reflect the observations used in the assimilation phase and the idiosyncratic model structure. In this regard, one might expect 20CRv2 to behave differently from the other reanalyses, as it only assimilates synoptic surface pressure, monthly SST and sea ice distribution (Compo et al. 2011), whereas the other reanalyses include a larger range of variables (Kalnay et al. 1996; Kanamitsu et al. 2002; Dee et al. 2011).

3.4 Composite and Correlation analysis

The primary methods in this thesis are composite and correlation analysis. Composites are simple tools to identify coherent climatic patterns for a given stratified sample, and have been used extensively in climate science, for example, in distinguishing between circulation in wet and dry years. In this thesis, composites are used to distinguish between the circulation and rainfall of models based on an index which describes an attribute of interest. Composite means can be calculated by averaging model variables at each grid box as follows:

$$\frac{x_{1,i,j} + x_{2,i,j} + x_{3,i,j} + \dots x_{n,i,j}}{n} \tag{3.1}$$

Where, x_1 to x_n are models which are selected for a composite based on the rank of an index, and i, j refers to a specific grid box. For example, in Chapter 4, low-level moisture circulation across the southern African domain is evaluated in an average of seven CMIP5 models with strong Angola Lows and seven models with weak Angola Lows. In using composites, the assumption is that they can reveal the presence of coherent features or processes among the subsample of models, since the averaging will retain any signal common to the individual models while removing the noise.

The difference between two composites, the composite anomaly, is calculated by subtracting the composite mean of one model set from another. The significance of difference between the composites is expressed through a two-tailed Students t-test or by metrics of model agreement applied at each grid box; these are detailed in individual chapters.

Correlation assesses whether two series of data co-vary. It is measured by a correlation statistic (r), which is the ratio of shared variance in the two series to the total variance:

$$r = \frac{1}{n-1} \sum_{i=1}^{n} \frac{(x_i - \bar{x})}{S_x} \frac{(y_i - \bar{y})}{S_y} \quad (3.2)$$

In our case we are interested in intermodel correlation, that is, where x_i and y_i are simulated values of two variables from a particular model, and S_x and S_y are the intermodel variance. The phase space associated with the intermodel relationship can be summarised graphically in the form of scatter plots. The computed correlation (r-value) is compared with the p-values from the Students t distribution. A low p-value indicates that the calculated correlation is improbable in two sets of unrelated variables. For example, a p-value of less than 0.01 would suggest that there is less than a 1% chance that the two series are unrelated.

In parts of this thesis, it will be useful to examine intermodel correlations across space; this is achieved by calculating the r statistic at each grid box across the suite of models.

This procedure is commonplace in climate science, and is often used in the context of understanding teleconnections across space, for example between ENSO (captured by the Southern Oscillation Index) and global precipitation (e.g. Dai et al. 1997). However, as Livezey and Chen (1983) note, it is possible to achieve spurious significance at an individual grid box as, in essence, the null hypotheses is tested at every one of thousands of grid boxes concurrently. To guard against overstating the results, we ensure that there is a strong physical basis for understanding the relationship between two variables in a particular location, usually in comparison with composites. Additionally, in Chapter 5, a test to control for field significance is employed, based on sampling of the distribution of p-values across space, as outlined in Wilks (2016).

4. Circulation controls on southern African precipitation in coupled models: the role of the Angola Low

Callum Munday[1] and Richard Washington[1]

[1]School of Geography and the Environment, University of Oxford

Received 02/08/2016, Accepted 06/08/2016, Published Online 23/01/2017

J. Geophys. Res. Atmos.,122, 861–877, **https://doi.org/10.1002/2016JD025736**

Authorship declaration

I conducted all of the analysis and wrote the paper. Richard Washington contributed to the planning of the methodology, interpretation of the findings and helped to edit the manuscript during the preparation and revision stages.

Abstract

In southern Africa, models from the latest Coupled Model Inter-comparison Project (CMIP5) produce a wide variety of rainfall climatologies. Differences between models in rainfall amount reach 70% in the rainy season (December-February; DJF) and the median model overestimates rainfall by between 15 and 40% throughout the annual cycle. This paper investigates the role of an understudied regional circulation feature, the Angola Low, in differentiating between model estimates of precipitation. In austral spring, the Angola Low is a heat low, driven by strong surface heating whereas in DJF it is more similar to a tropical low and is associated with moist instability. In the austral summer, we find that the simulated strength of the Angola Low is associated with between 40-60% of the inter-model variability in model mean rainfall across the subcontinent. The relationship is particularly strong along a north-west, south-east axis aligned from Angola down to the Mozambican Channel. Along this axis, models with stronger Angola Lows simulate enhanced, by up to 50 g kg^{-1} ms^{-1}, north-easterly and north-westerly moisture transport. The enhanced southward moisture flux in models with relatively deep Angola Lows increases the rate of moisture convergence in central areas of the subcontinent, and reduces moisture divergence across the Mozambican coast. The results highlight the need to better understand the links between the Angola Low and southern African rainfall, and suggest that improving the simulation of the Angola Low can help to constrain model estimates of southern African rainfall.

4.1. Introduction

Southern Africa is characterized by a tight coupling between climate and society (Conway et al. 2015). Rain-fed agriculture supports a large proportion of the regional economy and rainfall-sensitive hydroelectric sources sustain energy production in a number of countries including Zambia (World Bank 2014). Understanding how the magnitude and distribution of rainfall will change in response to increasing atmospheric greenhouse gases is therefore important. However, southern Africa's climate system is complex and is driven by a complicated mix of global, local, tropical and temperate climate processes (Reason et al. 2006). This presents a stern test for the coupled climate models which are critical to projections of future change and variability. The reliability of these models must be evaluated if we are to provide useful climate information for adaptation purposes.

Model evaluation studies in southern Africa have uncovered large differences between climate models, especially in their estimates of historical rainfall (Hewitson and Crane 2006; Christensen et al. 2007; Dieppois et al. 2015; Kalognomou et al. 2013; Nikulin et al. 2012). While models reproduce the annual cycle of rainfall well, there is a large spread between ensemble members in rainfall amount (Figure 4.1). The spread is particularly severe in austral summer (December-February; DJF), the main rainy season, when the wettest model simulates 70% more rain than the driest model (difference of 2 mm d^{-1}; Table 4.1). Moreover, the median model simulates between 15 and 40% more rainfall throughout the annual cycle compared to satellite and rain gauge datasets (Figure 4.1), with the largest absolute differences occurring in the summer season (~0.6

mm d^{-1}). The pattern of the rainfall biases is also remarkably consistent amongst models and reanalyses (Figure 4.2). For most models the largest biases, of between 6-12 mm d^{-1}, are concentrated in central and eastern areas with some models exhibiting a dipole structure of increased rainfall over the subcontinent and reduced rainfall over Madagascar. This is worrying given the extensive use of CMIP5 models for projecting future regional climate change, not least because the circulation is partly driven by the diabatic heating associated with the rainfall process.

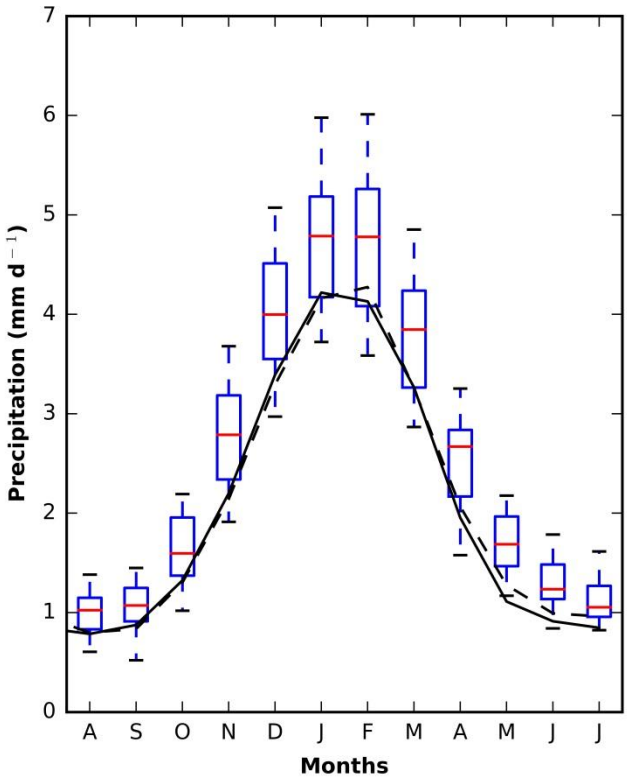


Figure 4.1 Mean (1979-2005) annual cycle of southern African rainfall (averaged over 10-52E,10-35S) in CMIP5 models (boxplots) compared to CMAP (dashed line) and GPCP (solid line). The red lines show the median model for each month, the box encompasses the interquartile range of models and the tails represent the full range.

Model	**Modelling Group**	**Mean DJF Precipitation (mm d^{-1}) (10-52E,10-35S)**
CMCC-CM	*Centro Euro-Mediterraneo sui Cambiamenti Climatici*	3.55
bcc-csm1-m	*Beijing Climate Centre*	3.82
GISS-E2-H	*Goddard Institute for Space Studies*	3.85
CMCC-CESM	*See CMCC-CM*	4.05
FGOALS-g2	*State Key Laboratory of Numerical Modelling for Atmospheric Sciences and Geophysical Fluid Dynamics*	4.16
MRI-ESM1	*Japan Meteorological Agency*	4.19
CanESM2	*Canadian Centre for Modelling and Analysis*	4.27
MIROC-ESM	*National Institute for Environmental Studies (Japan), Atmosphere and Ocean Research Institute (University of Tokyo), Japan Agency for Marine-Earth Science and Technology*	4.37
IPSL-CM5A-MR	*L'Institute Pierre-Simon Laplace*	4.71
IPSL-CM5B-LR	*See IPSL-CM5A-MR*	4.87
MPI-ESM-MR	*Max Planck Institute for Meteorology*	4.91
HadGEM2-ES	*Met Office Hadley Centre*	4.92
CNRM-CM5-2	*Centre National de Recherches Météorologiques*	4.96
CESM1-CAM5	*National Centre for Atmospheric Research*	5.01
CESM1-BGC	*See CESM1-CAM5*	5.17
BNU-ESM	*Beijing Normal University*	5.26
NorESM1-M	*Norwegian Climate Centre*	5.26
GFDL-CM3	*Geophysical Fluid Dynamics Laboratory*	5.39
ACCESS1-3	*The Centre for Australian Weather and Climate Research*	5.45
MIROC5	*See MIROC-ESM*	5.80
GFDL-ESM2G	*Geophysical Fluid Dynamics Laboratory*	5.95

Table 4.1 CMIP5 models used in this study. Models are ordered from dry to wet according to mean December-February (DJF) precipitation

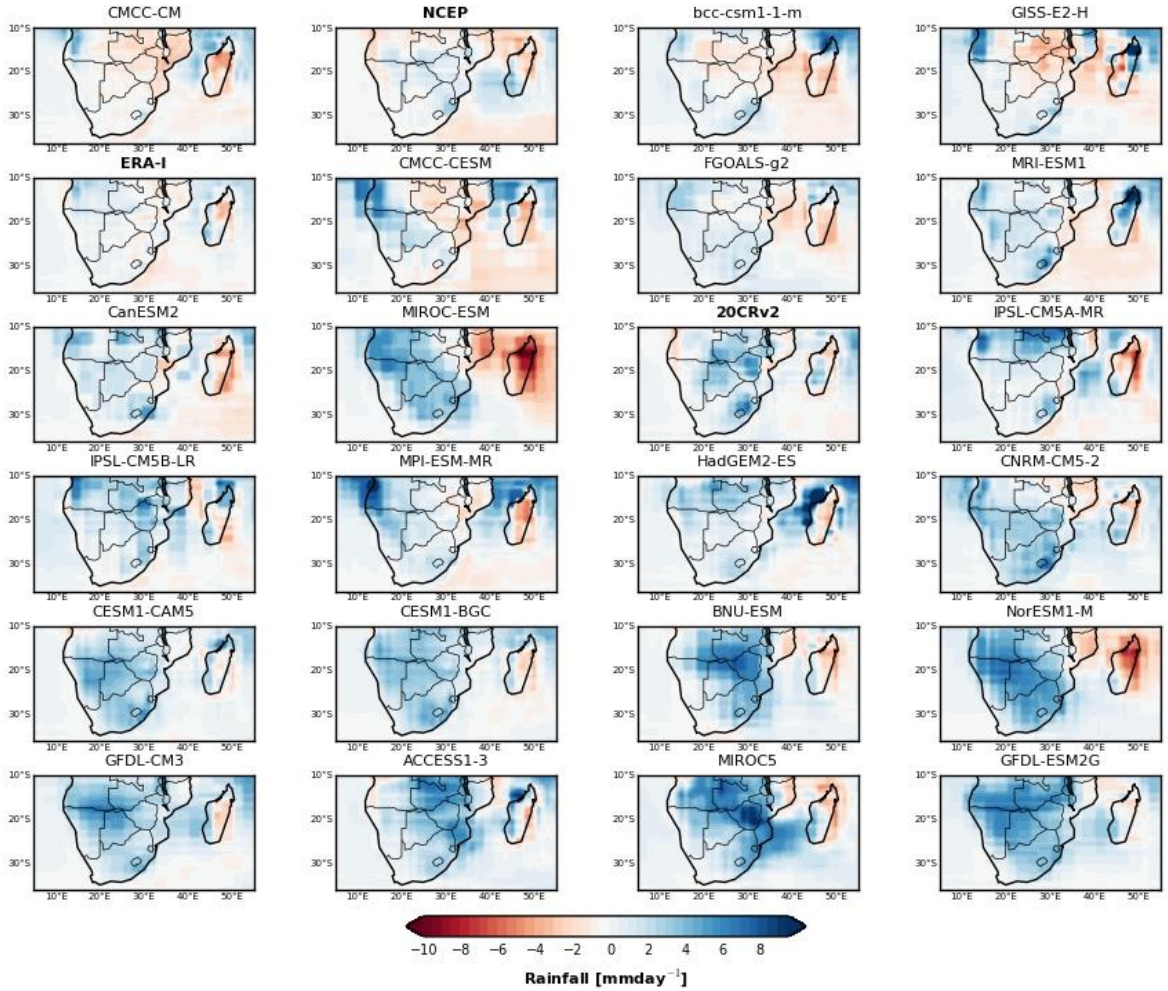


Figure 4.2 Mean rainfall (1979-2005) in CMIP5 models minus satellite-rain gauge estimates. Satellite rain gauge estimates are a mean of GPCP and CMAP climatology. Reanalyses datasets are in bold.

The large variation in model rainfall during austral summer presents an opportunity to explore the regional circulation controls underlying model rainfall climatology. One potential control is the model simulation of the Angola Low (AL); a cyclonic feature which forms during the austral summer. Variation in the strength of the low has been shown to distinguish between wet and dry years in the interannual record (e.g. Cook et al. 2004) and is also important for synoptic weather events (e.g. Hart et al. 2010). In this paper, we aim to evaluate the representation of this feature in the CMIP5 ensemble, to determine whether inter-model differences in its simulation are associated with the spread of rainfall in the CMIP5 ensemble.

Despite its importance, the mean state and seasonal cycle of the Angola Low remains poorly understood. Some studies refer to the Angola Low as a heat low, while others treat it like a tropical low in analysis. The first aim of this paper is therefore to better understand the climatological structure and seasonal cycle of the Angola Low. The rest of the paper focusses more specifically on the CMIP5 ensemble, and will answer the following three questions:

1. What is the climatological structure of the Angola Low during DJF in reanalyses and models?
2. Is the intermodel variability in the strength of the Angola Low related to variation in model rainfall?
3. Are there differences in moisture circulation patterns between models with relatively strong and weak Angola Lows?

The paper is organized as follows: we provide background on the Angola Low and outline the datasets used in the following two sections. Section 4.4 presents a characterization of the mean state and season cycle of Angola Low based on reanalyses data, and Section 4.5 examines the simulation of the Angola Low in CMIP5 models. In Section 4.6 we evaluate the relationship between model simulation of the Angola Low and rainfall before investigating the relationship between the strength of the Angola Low and moisture flux patterns in Section 4.7. We discuss results and conclude in Section 4.8.

4.2 Background: The Angola Low

The Angola Low is a low pressure system which forms in the plateau region to the east of the Angolan and Namibian highlands (Figure 4.3). While a number of studies have looked at the variation of the Angola Low on synoptic and interannual timescales, particularly in reference to rainfall variability (e.g. Cook et al. 2004; Fauchereau et al. 2009; Hart et al. 2010), very little is known about the seasonal cycle of the Angola Low or why it develops. In the present section we briefly review the literature on the Angola Low in relation to rainfall variability in observations and climate models. In the following section we will examine the mean state and seasonal cycle of the Angola Low in reanalyses.

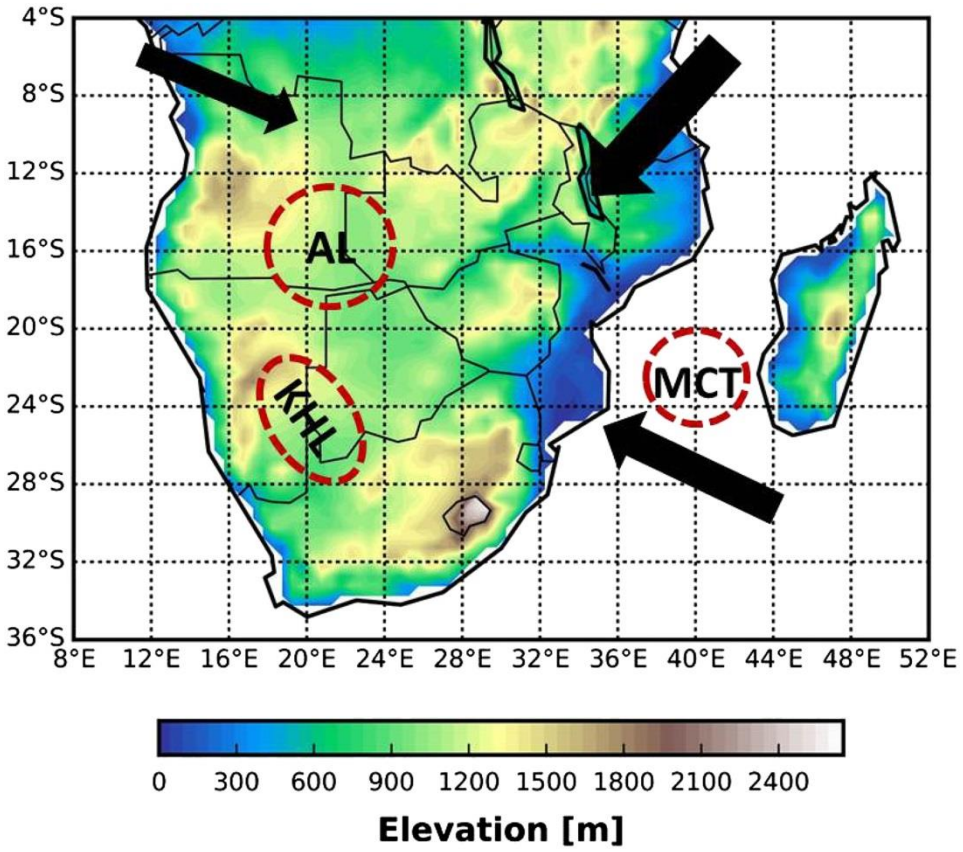


Figure 4.3 Topography (shaded) and key features of southern African climate during December-February. Black arrows denote key moisture transport pathways. Red dashed circles represent low-level cyclonic circulation; Angolan Low (AL), Kalahari heat low (KHL) and Mozambique Channel trough (MCT). Topography data is from USGS GTOPO30 global digital elevation model.

4.2.1 Variability of the Angola Low and southern African rainfall

On a synoptic scale, the intensification of the Angola Low is associated with enhanced local convection (Hermes and Reason 2009a) increased westerly moisture transport from the south-east Atlantic (Rouault et al. 2003; Cook et al. 2004; Hermes and Reason 2009a) and penetration of moisture-bearing north-easterlies deep into the subtropics (Hart et al. 2010). These processes increase the convergence of low-level winds in the

Angola region and in the area to the south-east. When coupled with the passing of a mid-latitude wave, the intensification of the Angola Low can precipitate the formation of northwest-southeast orientated cloud bands (Hart et al. 2010; Macron et al. 2014). These tropical-temperature troughs (TTTs) are important contributors to regional rainfall (Harrison 1984; Macron et al. 2014; Todd and Washington 1998), especially in marginal rainfall areas (Hart et al. 2013) and transfer latent energy and angular momentum poleward (Reason et al. 2006; Todd and Washington 1998).

The interannual variability of the Angola Low is associated with rainfall variability across southern Africa. For a sample of wet and dry years, Cook et al. (2004) show that in wet late summers (January-March; JFM) there is a 10% increase in the strength of the Angola Low, while dry JFMs are associated with a 20% decrease in strength of the Angola Low. The increase in strength of the low during wet years is accompanied by enhanced westerly moisture transport from the south-east Atlantic and stronger north-easterly inflow from the western tropical Indian Ocean (Cook et al. 2004; Vigaud et al. 2009). These two enhanced moisture transport pathways increase the rate of low-level moisture convergence in the subcontinental interior (Cook et al. 2004).

In some years, the variation in strength of the Angola Low is tied to the ENSO – southern Africa teleconnection. By forcing an atmosphere-only climate model with El-Niño type SST patterns, Cook (2000) demonstrates that there tends to be anomalously high geopotential heights over the Angolan-Namibian region during El Niño events. This inhibits the circulation associated with the Angola Low and reduces poleward moisture transport. This result is corroborated by Reason and Jagadheesha (2005), who

show that moisture circulation associated with the Angola Low is suppressed during some El Niño events in the NCEP reanalyses.

4.2.2 Climate model representation of the Angola Low

The ability of climate models to reproduce southern African rainfall climatology may depend in part on the model reproduction of the climatological Angola Low. In comparing an atmosphere-only climate model (HadAM3) with reanalyses data, Reason and Jagadheesha (2005) note that the model underestimates the strength of the Angola Low during the late-summer season (January- March). This could be related to the negative bias in continental rainfall compared to satellite data seen in this model. The authors argue that deficiencies in capturing Angola Low could also affect the modelling of the influence of ENSO over the region. This latter point is consistent with Dieppois et al. (2015) who use Empirical Orthogonal Function (EOF) analysis to evaluate the regional circulation produced in CMIP5 models during model El Niño events. They find that models tend underestimate subcontinental high pressure anomalies both near the surface and at 500 hPa, and suggest that 'this could explain why [El Niño] dry conditions over southern Africa are not correctly reproduced through its influence on the Angola Low' (pp2433).

More recently, Lazenby et al. (2016) found that the wet biases in CMIP5 models (Figures 4.1 and 4.2) are also found in the ensemble of climate models contributing to the Atmospheric Model Intercomparison Project (AMIP) which are driven by observed

SSTs. Both sets of ensembles, AMIP and CMIP, tend to simulate excessive moisture circulation in the Angola Low compared to reanalyses. By extension, Lazenby et al. (2016) argue that the simulation of the Angola Low could be an important control on excessive precipitation throughout the CMIP5 ensemble (Figure 4.1), independently of SST biases. Here, we test this hypothesis by investigating whether the mean simulation of the Angola Low can differentiate between model rainfall climatologies.

4.3 Data

We compare model rainfall with satellite/rain-gauge estimates from the Global Precipitation Climatology Project (GPCP) monthly precipitation dataset (Adler et al. 2003) and Climate Prediction Center Merged Analysis of Precipitation (CMAP; Xie and Arkin, 1997) We interpolate the satellite datasets to 1°x1° grids and evaluate mean rainfall over a 26-yr period from 1979-2005. Both of these datasets reliably reproduce the spatial patterns of precipitation over southern Africa and compare well against station data (Kalognomou et al. 2013; Novella and Thiaw 2013). Novella and Thiaw (2013) provide a detailed discussion of the performance of these datasets over southern Africa.

The focus of the study is historical data (1979-2005) from a sample of 21 models in the CMIP5 ensemble (Taylor et al. 2012). The full list of models used along with their mean December to February (DJF) rainfall in the area 10-52°E, 10-35°S is provided in Table 4.1. Differences between simulations arising from choice of initial conditions used to drive the model runs are negligible when considering the climatology (e.g. Hawkins and

Sutton, 2009) and here we only use one ensemble member (r1i1p1) per model. Models are re-gridded by bilinear interpolation to a common 1°x1° grid for ease of comparison.

We use reanalysis data in Section 4.4 to characterize the Angola Low. We include three reanalyses; NCEP-reanalyses (Kalnay et al. 1996), ERA-Interim (Dee et al. 2011) and 20th Century Reanalyses version 2 (20CRv2; Compo et al. 2011). NCEP and ERA-interim are chosen due to their widespread use in climate research, and because they are frequently used to drive high resolution regional models. We include the 20CRv2 following Zhang et al. (2013), who identify it as one of the best reanalyses for reproducing southern African climate and its variability. Observational data in the Angolan region is scarce: there is no radiosonde data available and very few climate stations with reliable data (Wilk et al. 2006). As a consequence, reanalyses are likely to be relatively unconstrained. As such, we avoid passing judgement on the reliability of models by comparison. Nevertheless, it is interesting to see whether models are reproducing the Angola Low in a similar way to reanalyses and to examine the consistency between reanalyses' estimates of mean climate.

Finally, to identify the minimum atmospheric pressure level for evaluating the near-surface Angola Low, we use surface pressure data from the Grootfontein weather station in Namibia (19.6°S and 18.2°E; 1400m). This data is available on >90% of days between 1991 and 2002.

4.4 Characterizing the Angola Low

4.4.1 The mean state and seasonal cycle of the Angola Low

In the core of the austral summer the Angola Low is identified as the minimum in 850 hPa geopotential height across Africa (Figure 4.4). It forms on the Bie Plateau, at 16-20°S and 18-22°E, and is at the southern limit of a north-east to south-west orientated trough of low pressure extending from the Turkana desert in Ethiopia through central Africa. This trough of low pressure in central Africa is associated with the intertropical convergence zone (ITCZ). The low surface pressure associated with the Angola Low sits to the west of the meridional arm of the ITCZ which extends over Tanzania, and sets up a strong zonal pressure gradient between the southern African landmass and the adjacent subtropical high pressure systems in the South Atlantic and South Indian Oceans.

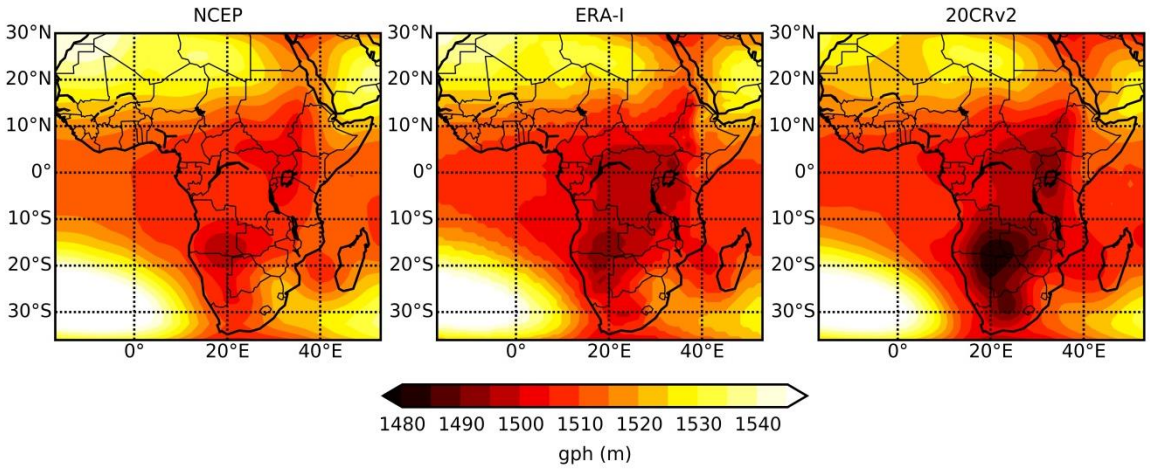


Figure 4.4 Mean DJF 850 hPa geopotential height in reanalysis data (1979-2005)

While all three reanalyses produce a similar location of minimum geopotential height, there are notable differences in the intensity of the Angola Low. 20CRv2, and, to a

lesser extent, ERA-Interim simulate lower 850 hPa geopotential heights than NCEP. 20CRv2 simulates a noticeable southward extension of the low geopotential height in the Kalahari region. This is less pronounced in the other two reanalyses. All reanalyses reproduce a secondary area of relatively low geopotential height in the Mozambican channel. This lee trough forms due to the dynamical adjustment of the easterlies, through conservation of potential vorticity, as they flow over the southern Madagascan topography. The differences between reanalyses are further evidence of the poor observational constraint in the region and there is no clear a priori reason why one reanalyses should be better than another. We will discuss whether this has a bearing on their simulation of rainfall in Section 4.6.

The seasonal cycle of the Angola Low may provide important insights as to its origins (Figure 4.5). The low pressure system first develops over southern Africa in October. At this time it is one of two areas of low geopotential height south of the equator; the other forming between Lake Tanganyika and Lake Victoria in north-western Tanzania. In the austral spring (October-November; ON), the area of low geopotential height over Angola, at 15-16°S, is located slightly to the north of the area of maximum surface heating (Figure 4.5). In this region there are weak negative vertical gradients in equivalent potential temperature ($d\theta_e/dP<0$; Figure 4.6), and steep slopes in potential temperature (θ) contours. This is indicative of the dry convection associated with strong surface heating and the formation of a heat low. Adebiyi and Zuidema (2016) show that the strong meridional temperature gradient between the October-November heat low and convection to the north is important in setting up the southern branch of the African Easterly Jet (AEJ-S).

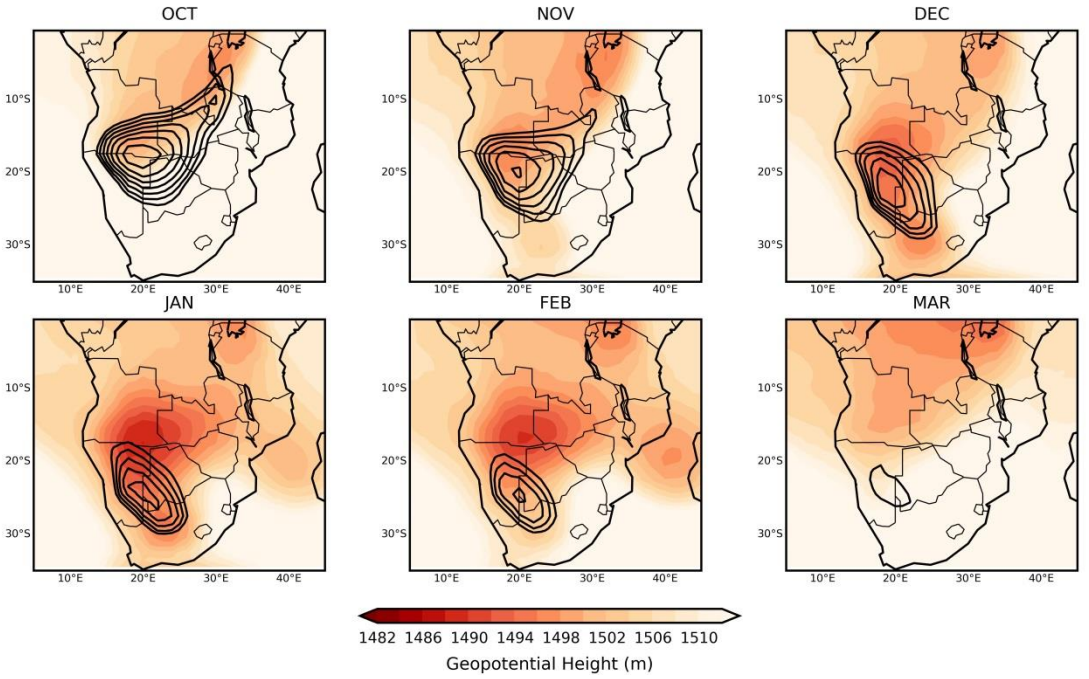


Figure 4.5 Austral summer (October to March) monthly progression of the Angola Low and southern African heat low in an ensemble mean of reanalyses. Shaded areas are mean 850 hPa geopotential heights (1979-2005), contours are of 850 hPa potential temperature. First contour is at 296K, the contour interval is 0.5K.

In December, the minimum in 850 hPa geopotential height remains in the Angola region at c.17°S, while the area of maximum surface heating shifts further south into the Namib and Kalahari Deserts (Figure 4.5). An extension of low geopotential height at 850 hPa forms over the Namib Desert in response to this high surface heating. The latitude-height cross section in December (Figure 4.6) shows two distinct features. The Angola Low, the minimum in 850 hPa geopotential height, now forms in a region of relatively strong vertical θ_e gradients. Such strong gradients in θ_e are indicative of moist instability and tend to be associated with moist convection. To the south, there are only weak vertical gradients in θ_e, due to a lack of moisture availability. Where present, these weak

gradients are driven by intense surface heating associated with subcontinental heat low, which is now situated over the western Kalahari Desert.

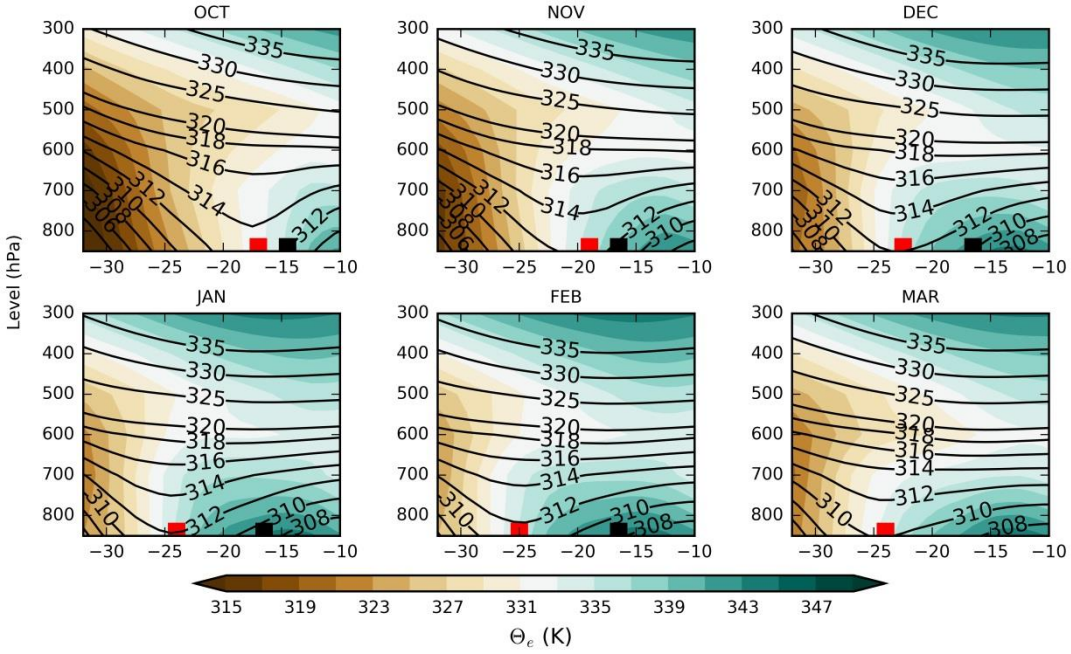


Figure 4.6 Austral summer (October to March) mean monthly latitude-height cross sections of equivalent potential temperature (θ_e; shaded) and potential temperature (θ; contours) in an ensemble mean of reanalyses. Longitudes are averaged over 18-24°E. The black rectangle represents the minimum in 850hPa geopotential height associated with the Angola Low and the red rectangle represents the maximum in potential temperature associated with the subcontinental heat low. Note in March, the presence of the Angola Low in the mean climatology is unclear so no rectangle is plotted.

As the summer season progresses into January and February, the Angola Low is stationary at 17°S, while the highest surface temperatures move farther south, following the seasonal cycle in insolation. By February, the heat low (25°S), is separated from the Angola Low by 8° of latitude. The vertical structure of the troposphere in January and February is qualitatively similar to the structure in December. In March the region of

low 850 hPa geopotential heights in southern Africa moves to northern Angola and a weakened heat low remains over Namibia. While the Angola Low is still present, it is much weaker and not as obvious in the mean climatology. The lowest geopotential heights south of the Equator are now associated with tropical convection in the Democratic Republic of Congo (DRC) and northern Tanzania.

The seasonal cycle of the Angola Low provides some insight into whether the Angola Low, in its mean state, is a heat low or a tropical low. In mid- to late-spring (ON), the Angola Low and the subcontinental heat low are barely distinguishable. In the core of the summer season (DJF) however, the heat low shifts south into the Kalahari (now the Kalahari heat low) and is distinct from the Angola Low. At this stage in the season, the Angola Low is driven by moist instability. Given the different forms of the Angola Low in the spring and summer, it seems sensible to focus on just one season for the analysis of the CMIP5 ensemble. Given that the largest biases in rainfall are in the core of the summer season (Figure 4.1), and that a tropical low may have a more direct relationship with rainfall, we focus on this season (December to February; DJF) in our analysis.

4.4.2 Defining the Angola Low for intermodel comparison

We identify the Angola Low as the lowest 5% of DJF mean 850 hPa geopotential height values within a large southern African domain (5-55°E, 0-35°S). There is a sharp boundary at the southern limit of the subcontinent to avoid the detection of midlatitude low pressure associated with westerly disturbances. An Angola Low index is defined by

the mean geopotential height within this mask. We use this definition to compare Angola Low strength between models and reanalyses.

The lower tropospheric levels available in CMIP5 are 925 hPa, 850 hPa and 700 hPa. The 850 hPa surface corresponds to an approximate height of 1500m, slightly higher than height of average regional topography (Figure 4.3). Mean DJF surface pressure at the Grootfontein station is 854 hPa with a standard deviation of 2.9. The 850 hPa height is therefore suitable for capturing the near-surface low. In reanalyses, the 5% threshold accurately constrains the low to the Angolan-Namibian border; higher thresholds (e.g. 10%) include strong influences from the Kalahari heat low to the south and equatorial convergence to the north.

The vertical structure of the Angola Low is examined using vertical velocity (dP/dt) and geopotential height anomalies. Geopotential height anomalies are computed as a deviation from mean geopotential height over the large southern African domain for each pressure level.

4.5 The Angola Low in CMIP5 models

4.5.1 The near-surface Angola Low

The location of the Angola Low is reproduced well by the majority of CMIP5 models (Figure 4.7). All models, with exception of GISS-E2-H, simulate the location of Angola

Low at the confluence of the Namibian, Angolan and Botswanan borders. In the GISS model, there are two discrete minima in geopotential height; one in the Angola region, and another stretched zonally across the tropical subcontinent. In models other than GISS-E2-H, the latitude of the minimum geopotential height varies from 15-20°S, and the longitude varies from 18-22°E. In some models (e.g. NorESM1-M, GFDL-ESM2G, MPI-ESM-MR), the area of low pressure extends quite far south into Namibia. This could indicate a southward extension of austral summer rain band in these models. Nevertheless, the location of the Low as simulated by models is in broad agreement with reanalyses products and corresponds well with the area of enhanced moisture convergence identified by Cook et al. (2004), Reason and Jagadheesha (2005) and Reason et al. (2006).

The height of the 850 hPa surface varies by up to 20m between models. The variation is particularly evident as models progress from dry to wet; with drier models in the ensemble tending to simulate higher geopotential heights (weaker lows) than wetter models. The relationship between model Angola Low strength and simulated rainfall will be explored in detail in Section 4.6.

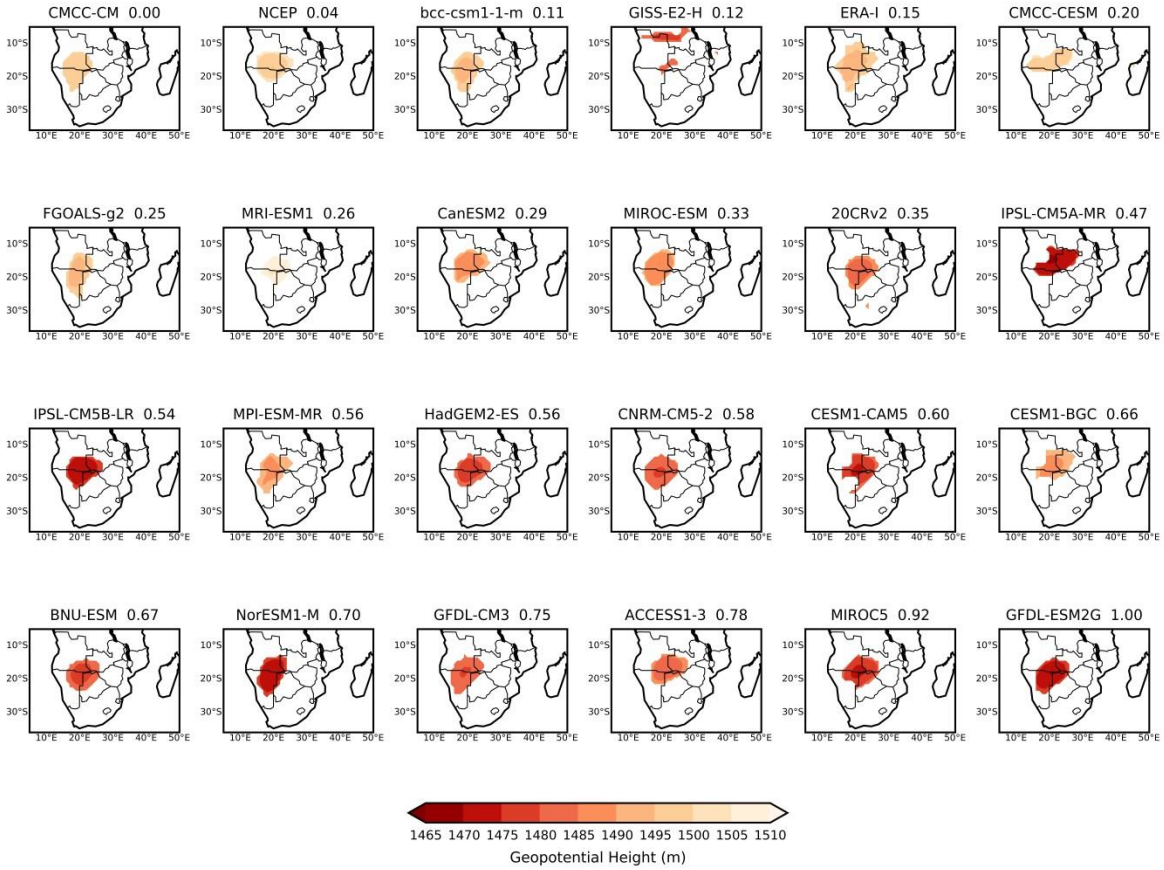


Figure 4.7 Mean DJF Angolan Low in CMIP5 models and reanalyses. Models and reanalyses are ordered from driest model (top left) to wettest model (bottom right). The Angolan Low is defined by lowest 5% of 850 hPa geopotential height. Model rainfall is expressed as an index between 0 and 1 based on mean DJF rainfall (Table 4.1) and is shown above each composite.

4.5.2 Vertical structure of the Angola Low

The vertical structure of the Angola Low is important for its influence on southern African climate. In both models and reanalyses, the center of the Angola Low coincides with negative geopotential height anomalies in the mid- to lower-troposphere and

positive geopotential anomalies at higher levels (Figure 4.8). This is accompanied by rising air throughout the tropospheric column up to 200 hPa. As proposed in Section 4.4, this suggests that in the DJF the Angola Low should be identified as a tropical low rather than a heat low, as it is not capped by mid-level subsidence.

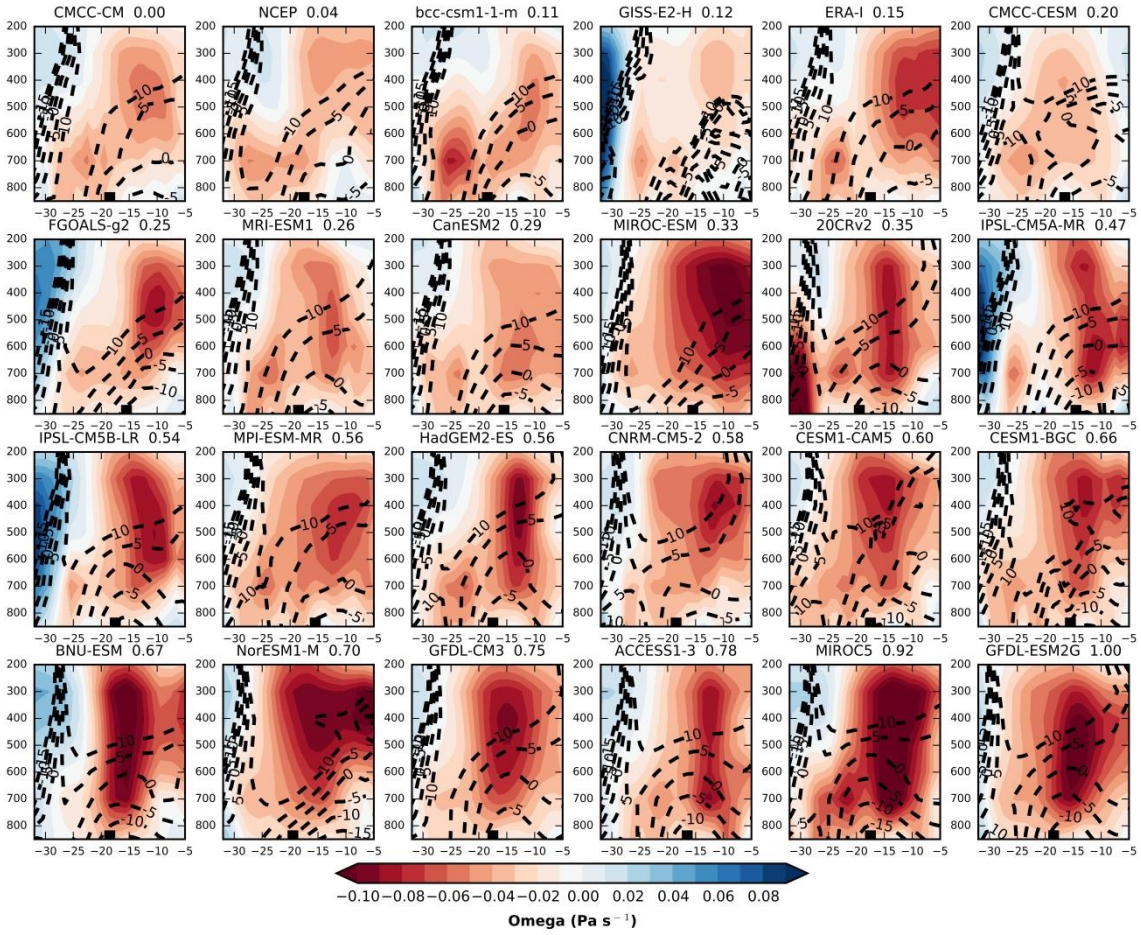


Figure 4.8 Mean DJF latitude-height cross sections of vertical velocity (Pa s^{-1}; shaded) and geopotential height anomaly (contours; interval 5m) for CMIP5 models and reanalyses. Models are ordered as in Figure 4.7. Longitudes are averaged over 18-24°E. The black rectangle in each composite represents the latitude of minimum 850 hPa geopotential height associated with the Angolan Low in each model or reanalyses.

In most models, the center of the Angola Low, indicated by the black rectangle, is located at the southern edge of maximum vertical velocity associated with tropical convection. There is significant variation between models in the magnitude of vertical velocity in the AL region. In drier models and reanalyses the rate of uplift is modest, between -0.04 and 0.06 Pa s^{-1}, while in the wettest models the rate of uplift is almost doubled; reaching -0.10 Pa s^{-1} over the Angola Low region. The latitudinal extent of the area of uplift also differs between models. In some models (e.g. NorESM1-M, MIROC-ESM) there is a wide band of very strong uplift spanning over 5-10° of latitude. In other models (e.g. ACCESS1-3, HadGEM2-ES)[5] there is a narrow band of strong vertical velocity, occupying less than 5° of latitude. The differences amongst models are also found between reanalyses. ERA-Interim and NCEP reanalyses simulate a relatively weak and wide band of rising air north of the Angola Low, while 20CRv2 simulates a stronger but narrower band of rising air.

The Kalahari Heat Low is evident in some of the models (e.g. CMCC-CM, bcc-csm1-1-m, IPSL-CM5A-MR, MIROC5) and in all three reanalyses. It is identified as the area to the south of the Angola Low (at c. 25°S) where ascent up to 600 hPa is capped by subsidence aloft (Figure 4.8) and surface heating reaches a subcontinental maximum (Figure 4.5). Geopotential height anomalies in these models and reanalyses take a domed form tilting downwards towards the Kalahari Heat Low. This implies that there could be some degree of interaction between tropical convection and the formation of the heat low, in a manner similar to the Sahara Heat Low (Adebiyi and Zuidema 2016; Lavaysse et al. 2009). If model simulation of rainfall and circulation in the African

[5] We note here that ACCESS1.3 is an early version of HadGEM3

tropics is linked to their simulation of southern African climate, biases in these regions could be related.

Other models (e.g. MIROC-ESM, NorESM1-M, GFDL-ESM2G) fail to reproduce subsidence aloft, and simulate rising air throughout troposphere in whole subtropical region. Synoptically, this is seen during some tropical temperate trough events when an elongated trough forms between the Angola region and northwest South Africa (Hart et al. 2010). If the same process were happening in models, this could help to explain biases in precipitation seen in Botswana and South Africa in a number of CMIP5 models (Dieppois et al. 2015 and Figure 4.2). The accurate reproduction of the Kalahari Heat Low could therefore be additional influence on the simulation of southern African rainfall. It is beyond the scope of this paper to explore this hypothesis.

4.6 The Angola Low and rainfall

There is a negative relationship between the Angola Low index and rainfall across CMIP5 models (Figure 4.9). Models with a stronger Angola Low (lower geopotential height) tend to simulate more rainfall over the subcontinent ($r=-0.67$; $p=0.0009$).There appears to be a strong coupling between model rainfall and the strength of their Angola Low; the slope of the regression line (-0.05) indicates that for every decrease of 5m geopotential height there is an approximate 0.25 mm d^{-1} increase in rainfall. This relationship is perhaps expected given the way in which the Angola Low influences the interannual variability of southern African rainfall (Section 4.2.1).

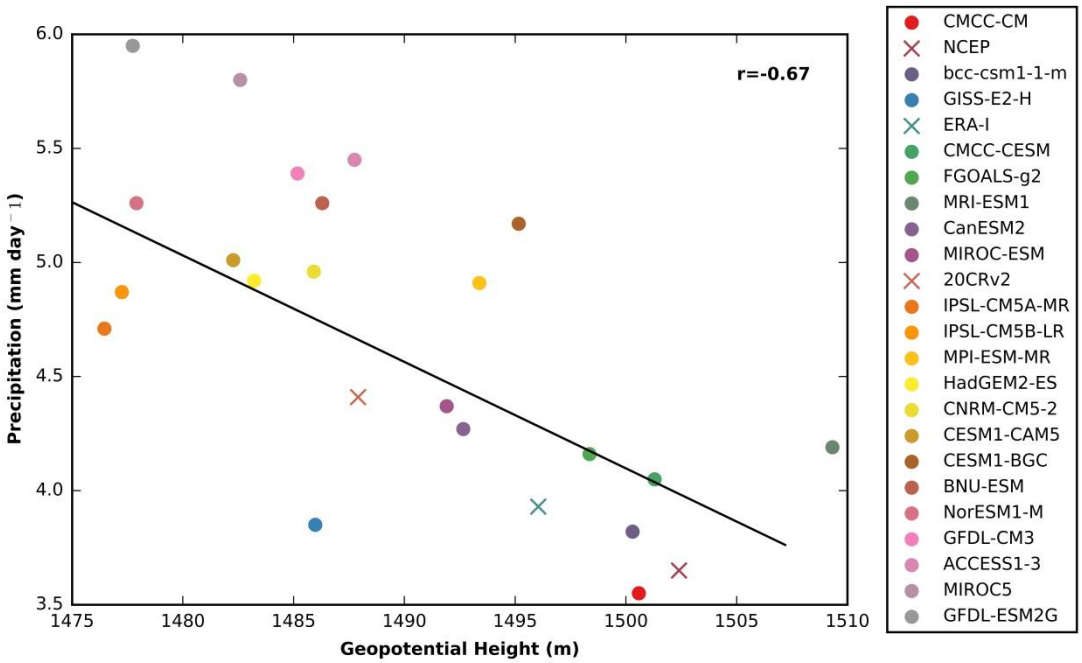


Figure 4.9 Relationship between DJF mean Angolan Low Index (see Section 4.4.2 for details) and southern African rainfall (10-35°S;10°E-52°E). Models are indicated by dots, reanalyses by crosses. Note that the linear regression and Pearson's test do not include reanalyses.

A few models do not conform to this relationship. For example, the GISS-E2-H model simulates relatively low 850 hPa geopotential heights (1486m) despite being relatively dry. This may be caused by the northward location of its geopotential trough shown in Figure 4.7. When the GISS model is removed from analysis (not shown) the correlation improves to 0.74. Reanalyses, indicated by crosses on Figure 4.9 conform to the overall relationship. NCEP is the driest amongst the reanalyses and also simulates the weakest Angola Low (1503m 850 hPa geopotential height). If the reanalyses are included in the Pearson's test, the correlation improves marginally (r=0.71). It is interesting that drier models (e.g. CMCC-CM, bcc-csm1-m, FGOALS-g2), which have rainfall amounts

similar to satellite-rain gauge products (Table 4.1), simulate the strength of the Angola Low in a similar way to reanalyses.

Figure 4.10 shows spatially how much of the variance between model rainfall is associated with the strength of the Angola Low. There is a strong relationship between the model Angola Low strength and grid-box rainfall in Angola and in the region stretching down to the south-east over the Mozambican Channel. In the core of the NW-SE band, the strength of the Angola Low is associated with between 40-60% of variance in model rainfall. The relationship between the Angola Low and rainfall in models weakens somewhat in the region of the Chimanimani mountains in Zimbabwe, and the Drakensburg in South Africa. In these areas, local differences in model orography may dominate over large scale circulation in influencing rainfall intensity. As model rainfall over large parts of southern Africa is associated with the simulation of the Angola Low, it follows that models which are poor at simulating the Angola Low are also likely to contain larger biases in their simulation of southern African rainfall.

The relationship between Angola Low strength and rainfall within the Angolan region is simple and can be explained by the enhanced vertical velocity in models with a strong compared to weak Angola Low (Figure 4.8). The northwest-southeast extension of the relationship is reminiscent of the structure of the South Indian Convergence Zone (SICZ; Cook, 2000) and could relate to increased southward export of moisture in models with stronger cyclonic circulation. This is explored in the following section.

There is a strong association between the modelled strength of the Angola Low and rainfall over the south-east Atlantic (Figure 4.10). Models with a stronger low tend to simulate more precipitation here. This is a region of low rainfall both in models and in reality (not shown), and moisture transport emanating from the Angola Low is unlikely to affect rainfall patterns. A more plausible explanation for this relationship might be a concomitant westward shift of the South Atlantic High in models with strong Angola Lows, weakening the inhibition of rainfall. This could be related to the strong warm SST bias observed in many CMIP5 models in the south-east Atlantic (Wang et al. 2014).

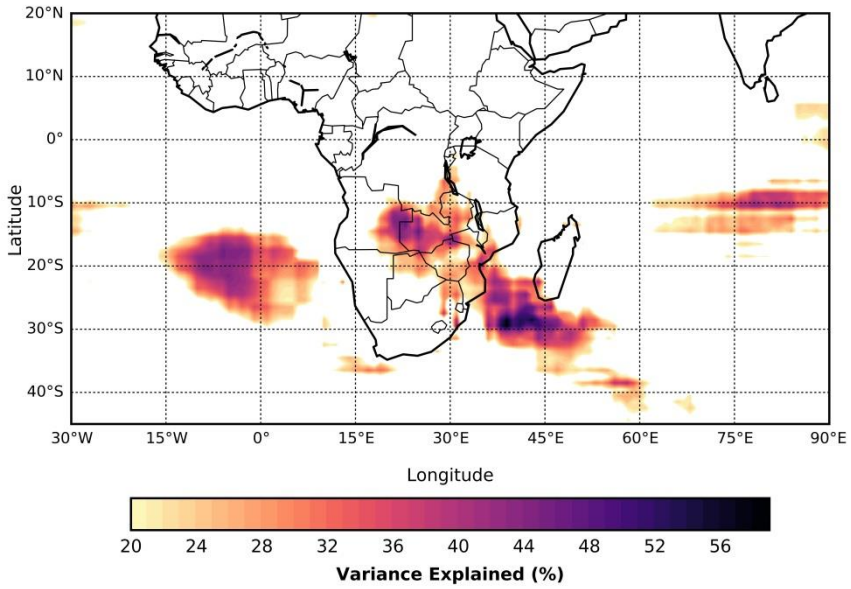


Figure 4.10 The percentage of inter-model variance in grid-box precipitation associated with the models' Angolan Low Index (see Section 4.4.2 for details). Relationship is for mean DJF and variance predicted is calculated based on r^2. Values below 20% are not significant at $p<0.05$ and are masked.

4.7 Moisture circulation and the Angola Low

On synoptic and interannual timescales a stronger Angola Low is associated with enhanced regional moisture circulation (Section 4.2.1). Figure 4.11 shows the differences in low-level (850 hPa) moisture flux and divergence between models with a relatively strong and weak Angola Lows. In models with a stronger low, there is enhanced moisture inflow (20-40 gkg^{-1} ms^{-1}) from the northwest which flows cyclonically around the low feeding the eastern portion of the subcontinent. This flow, originating in the central African convective region, enhances moisture convergence to the east of the low in north-west Zambia. The anomalous north-westerlies merge with an enhanced north-easterly moisture flow (20-50 gkg^{-1} ms^{-1}) out of southern Tanzania where moisture flux is strongly divergent. Together, these anomalous transport pathways increase the southward export of moisture, and act to both enhance moisture convergence in central areas and reduce the divergence of moisture across the Mozambican coast. It is noticeable that areas of comparatively enhanced convergence or reduced divergence in the strong Angola Low set of models correspond to the areas where the strength of Angola Low is correlated with increased rainfall (Figure 4.10). The magnitude of moisture flux anomalies in models with a strong Angola Low compared to those with a weak low is similar to the magnitude of differences in moisture flux between wet and dry years (Cook et al. 2004; their Figure 13).

The excessive monsoonal northeasterly flow into the subcontinent is accompanied by reduced, or even absent, northwesterly flow recurving towards Madagascar in models with a strong Angola Low. This acts to reduce moisture convergence in north-eastern Madagascar in these models and may explain, in part, the dipole pattern of dry precipitation biases over northern Madagascar, and wet biases over the Mozambican coast (Figure 4.2). The northwesterly flow toward Madagascar is also thought to be important for regional ocean dynamics, and in particular in the formation of the Seychelles-Chagos Thermocline Ridge (SCTR; Hermes and Reason 2008). Variations in the SCTR depth can influence the incidence of tropical cyclones forming in the south-western Indian Ocean (Hermes and Reason 2009b), and thus this deficiency in models could have important consequences for the modelling of extreme events and may impact on model rainfall climatology in regions prone to tropical cyclone formation.

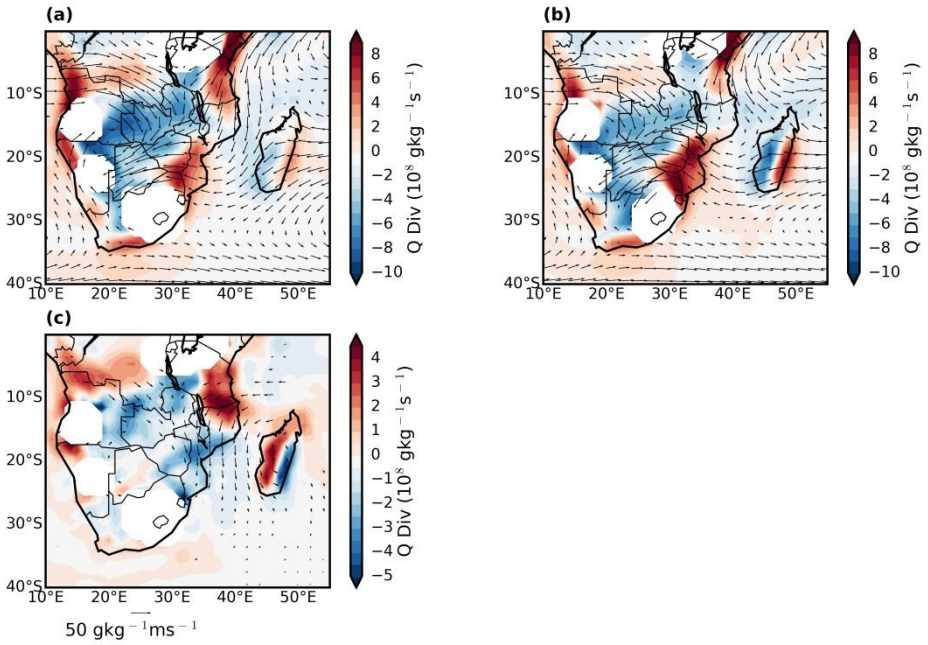


Figure 4.11 Mean DJF moisture flux and divergence at 850 hPa in (a) seven models with strongest Angolan Low, (b) seven models with weakest Angolan Low and (c) strongest Angolan Low models minus weakest Angolan Low models. In (c) we have only plotted moisture flux vectors where either meridional or zonal moisture flux values were significantly different between the two sets of models. Significance was calculated using Students t-test.

We assess quantitatively the relationship between inter-model variability in Angola Low strength and southward moisture export in Figure 4.12. The strength of the Angola Low is associated with 40-70% of the variability in meridional moisture flux in the Mozambican Channel. This corresponds with the enhanced north-westerly and north-easterly moisture transport in models with a strong Angola Low (Figure 4.11). Again, the strength of this relationship is improved if the anomalous GISS-E2-H model is removed from analysis (not shown). The north-west, south-east axis along which the relationship is strong is similar to the relationship between Angola Low strength and rainfall (Section 4.6; Figure 4.10). This suggests that the modulation of the strength of the Angola Low amongst models occurs contemporaneously with inter-model rainfall variability as a consequence of the increased southward export of moisture along the SICZ axis

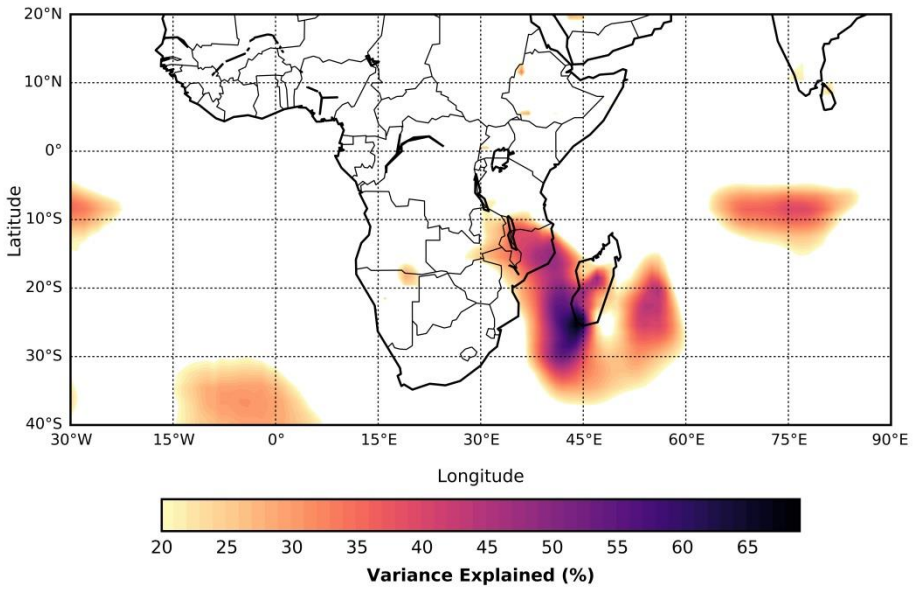


Figure 4.12 The percentage of inter-model variance in grid-box meridional moisture flux predicted by the models' Angolan Low Index (see Section 4.4.2 for details). Relationship is for mean DJF and variance explained is calculated based on r^2. Values below 20% are not significant at $p<0.05$ and are masked.

To the south-west of Madagascar this relationship is especially strong; the modelled strength of the Angola Low is associated with 65-70% of the variability in meridional moisture transport. In this region a topographically induced trough frequently forms (Figure 4.3). Easterly moisture transport from the south Indian Ocean is deflected northward on the western flank of this trough. In models with a weak Angola Low (Figure 4.11b) this effect is evident, with the easterly moisture feed deflected to the northwest across the Mozambican coast. In models with a strong Angola Low, this transport is zonal (Figure 4.11a), accounting for the greater poleward moisture transport. It is difficult to untangle cause and effect here. One explanation is that a poorly reproduced Mozambican trough could enhance strength of the low by increasing direct moisture inflow to the subcontinent. This may explain the very strong relationship found here, and suggests that the model representation of this feature warrants further study.

4.8 Discussion and Conclusion

4.8.1 Discussion

This paper explores the links between the Angola Low, regional circulation and rainfall in CMIP5 models and reanalyses. The Angola Low is an area of low surface pressure, located between 16-20°S and 18-22°E, which is evident in the mean climate from the start of austral spring (October). In the austral spring (ON), the Angola Low is a heat low, formed in response to high surface temperatures in the Angola region. As the season progresses into austral summer (DJF), its climatological structure changes, and is more similar to a near-equatorial trough. At this stage, it is characterized by strong negative gradients in θ_e in the lower troposphere.

There is significant variation in the strength of the Angola Low amongst CMIP5 models. Across a north-west to south-east orientated band, this variation in strength is associated with between 40-60% of the variation in rainfall amongst models. These results are consistent with the hypotheses of Reason and Jagadheesha (2005) and Dieppois et al. (2015), who suggest that the representation of the Angola Low in climate models might be associated with errors in summer rainfall in southern Africa. The elevated rainfall simulated in models with a stronger Angola Low corresponds to moisture circulation and divergence anomalies across the subcontinent. Models with a stronger low contain enhanced north-westerly and north-easterly moisture transport in the eastern portion of the subcontinent. This is accompanied by enhanced convergence in north-central areas of the subcontinent and enhanced (reduced) divergence in southern Tanzania (eastern

Mozambique). This supports Lazenby et al.'s (2016) hypothesis that CMIP5 biases in the strength of the Angola Low are associated with exaggerated moisture circulation patterns across the subcontinent. The moisture circulation biases have implications for poleward transport of latent energy and angular momentum, and could encourage more frequent or intense tropical temperate interactions in climate models.

The underlying drivers of model variation in the strength of the Angola Low remain unclear. One plausible candidate is model representation of topography. For a similar low pressure system on the Brazilian Plateau (20°S, 55°W), Grimm et al. (2007) and Kodama et al. (2012) emphasize the importance of local topography in the formation of the cyclonic anomaly. Model experiments which removed (Grimm et al. 2007) or smoothed (Kodama et al. 2012) the topographic gradients in the Plateau region demonstrated that the formation and intensity of the low is contingent on patterns of regional topography. However, amongst CMIP5 models, there is no simple relationship between model resolution (a proxy for topography) and the strength of the Angola Low (not shown). This indicates that while topography is likely to be important in the formation of the Angola Low, there are other model processes which may be more important for explaining model diversity in its strength.

Another candidate for intermodel variability in Angola Low strength is the representation of local surface-atmosphere feedbacks. For the Brazilian Plateau low pressure, Grimm et al. (2007) propose a mechanistic link between dry spring conditions and wet summer conditions over the Brazilian Plateau. They suggest that dry spring conditions can lead to high surface temperatures which encourage moisture convergence

over high elevations and a deeper Brazilian Plateau Low. They confirm the plausibility of this hypothesis by reducing soil moisture in a regional climate model in spring time, subsequently observing an increase in moisture convergence and rainfall in the following summer season compared to a control run. Precipitation over the Brazilian Plateau may then play a dominant role as an atmospheric heat source in sustaining the cyclonic circulation (Kodama et al. 2012). Similar processes could be at play for the Angola Low, as the seasonal cycle of the Angola Low (Figures 4.5 and 4.6) involves a transition from a heat low in spring, driven by high surface temperatures, to a tropical low in summer. Model variability in representing this seasonal cycle, including land-atmosphere feedbacks and convection, could play a role in the model diversity in the strength of the Angola Low. This is the subject of ongoing work.

The three reanalyses appear to conform to the relationship between the strength of the Angola Low and rainfall. NCEP is the driest amongst the reanalyses and has the weakest low, while 20CRv2 is the wettest and has a substantially stronger low. The circulation patterns between reanalyses differ slightly (e.g. Figures 4.4 and 4.8), with 20CRv2 simulating a more intense Angola Low which extends further south than the other two reanalyses. Despite this, the differences in rainfall between the reanalyses (<0.8 mm d^{-1}) is small compared to the intermodel range (2.4 mm d^{-1}). Differences amongst reanalyses reflect the observations used for assimilation and idiosyncratic model structure. The 20CRv2 reanalyses only assimilates synoptic surface pressure, monthly SST and sea ice distribution (Compo et al. 2011), whereas NCEP and ERA-Interim assimilate a larger range of variables (Kalnay et al. 1996; Dee et al. 2011). This could explain why NCEP and ERA-interim are more similar to each other than they are to 20CRv2.

Most of the drier models in the ensemble (excluding GISS-E2-H) are in better agreement with both the satellite/rain gauge estimates of regional rainfall magnitudes (Figure 4.1) and reanalyses simulations of the Angola Low (Figures 4.7 and 4.8) . It is tempting to conclude that these models are more reliable at simulating southern African precipitation than the wetter models in the ensemble. However, observational data in the Angolan region is scarce and satellite products, such as GPCP and CMAP, and reanalyses are not well constrained by station observations (Wilk et al. 2006; Zhang et al. 2013). It is therefore unclear which models are faithfully reproducing the Angola Low and related circulation. In the absence of long-term observations, a targeted observational campaign aimed at characterizing the Angola Low would be useful. Even if only for one season, rainfall data and vertical profiles of temperature, humidity and pressure obtained from radiosondes would help to assess the reliability of reanalysis products.

In DJF, the continental heat low forms over the Kalahari and is evident in latitude-height cross sections of subtropical southern Africa (Figures 4.6, 4.8). In reanalyses, this is present at between 25-30°S, and is characterized by weak uplift in the lower troposphere and subsidence aloft. It is similar in structure, to other heat lows, such as the Sahara Heat Low (Lavaysse et al. 2009), although less intense. Some models (e.g. bcc-csm1-m, IPSL-CM5A-MR) reproduce this feature well, while others simulate rising air throughout the troposphere across subtropical latitudes to the south of the Angola Low. This may be related to the excessive precipitation in the western half of the subcontinent

reported by Dieppois et al. (2015) and suggests that model reproduction of this feature is worthy of further study.

In the reanalyses, and in models where the Kalahari Heat Low is reproduced, contours of geopotential height anomalies suggest that there is some interaction between tropical convection and the formation of the heat low. Local axisymmetric circulation could create the clear skies needed for the strong surface heating associated with the heat low (Figure 4.5). This is consistent with Reason (2016) who suggests that the Botswana High, which lies above the heat low at 500 hPa, is generated in response to tropical precipitation to the northeast. This raises the possibility of connections between model biases in the Congo region and those in southern Africa. However, the lack of observational data in the Congo makes it very difficult to evaluate these biases (e.g. Washington et al. 2013) and process-based model evaluation is needed to help constrain model rainfall estimates (Creese and Washington 2016).

4.8.2 Conclusion

Coupled climate model biases are often difficult to understand due to the range of possible climatic influences which can operate on a number of spatial and temporal scales. This is particularly the case with the southern Africa climate system which extends through tropical and temperate regions, and is influenced by both regional and global SST dynamics. This paper has attempted to tackle this complexity by focusing on one circulation feature: the Angola Low, and relating it to the variation in model precipitation.

The results presented show a link between the strength of the Angola Low and rainfall in southern Africa. This implies that improvements to the simulation of the Angola Low will go hand-in-hand with improvements to the simulations of regional precipitation. As climate change in southern Africa is likely to be expressed through influences on regional circulation features, assessing the future changes to the Angola Low could place important constraints on the plausibility of future climate scenarios.

Acknowledgments

The first author is funded by the UK Natural Environmental Research Council (NERC) through the doctoral training programme (grant number: NE/L002612/1) and also through a Met Office CASE studentship (grant number: ACR00400). Richard Washington is partially supported by the NERC funded UMFULA (NE/M020207/1) and IMPALA (NE/M017206) African climate programmes. The climate model data used in this study was derived from the Earth System Grid Federation (ESGF) system (**https://pcmdi.llnl.gov/**). NCEP, 20CRV2 and ERA-Interim reanalyses data is provided by the NOAA/OAR/ESRL PSD, Boulder, Colorado, USA, at **http://www.esrl.noaa.gov/psd/**. Data from Grootfontein weather station in Namibia was sourced from the Okavango Basin Information System (**http://leutra.geogr.uni-jena.de/obis/metadata/start.php**) and USGS GTOPO30 global digital elevation model data from **http://earthexplorer.usgs.gov/**. The authors would like to thank Dr Neil Hart, Dr Rachel James, Amy Creese and Dr Sebastian Engelstaeder for helpful discussions.

5. Systematic climate model rainfall biases over southern Africa: links to moisture circulation and topography

C. Munday[1], R. Washington[1]

[1]School of Geography and Environment, University of Oxford.

Received 09/01/2018, Accepted 14/06/2018, Published Online 07/08/2018

J. Climate, 31, 7533–7548, https://doi.org/10.1175/JCLI-D-18-0008.1

Authorship declaration

I conducted all of the analysis and wrote the paper. Richard Washington contributed to the interpretation of the findings and helped with editing the manuscript during the preparation and revision stages.

Abstract

An important challenge for climate science is to understand the regional circulation and rainfall response to global warming. Unfortunately, the climate models used to project future changes struggle to represent present day rainfall and circulation, especially at a regional scale. This is the case in southern Africa, where models from the Coupled Model Intercomparison Project Phase 5 (CMIP5) overestimate summer rainfall by as much as 300% compared to observations and tend to underestimate rainfall in Madagascar and the southwest Indian Ocean. In this paper, we explore the climate processes associated with the rainfall bias; with the aim of assessing the reliability of the CMIP5 ensemble and highlighting important areas for model development. We find that the high precipitation rates in models which are wet over southern Africa are associated with an anomalous northeasterly moisture transport (~10-30 g kg^{-1} s^{-1}) which penetrates across the high topography of Tanzania and Malawi and into subtropical southern Africa. This transport occurs in preference to a southeasterly recurvature towards Madagascar which is seen in drier models and reanalysis data. We demonstrate that topographically related model biases in low-level flow are important for explaining the intermodel spread in rainfall; wetter models have a reduced tendency to block the oncoming northeasterly flow compared to dry models. The differences in low-level flow amongst models are related to upstream windspeed and model representation of topography, both of which should be foci for model development.

5.1 Introduction

The future evolution of the climate system under unprecedented human forcing is uncertain. Climate models are our only tools for projecting future climate change, and yet contain large errors relative to observations, particularly for societally important variables, such as rainfall (Biasutti 2013; Mehran et al. 2014; Yang et al. 2015; Lintner et al. 2017; James et al. 2018). Understanding the climate processes which underlie climate model errors is a first step toward assessing models' reliability for projecting future change, and can also help to guide future model development. This is particularly important in cases where an ensemble of models display a systematic bias compared to observations. A wide spread of model simulations around observations might be indicative of random error which will cancel in a multimodel mean (MMM), whereas a consistent direction of error implies some common structural error which will not cancel in an MMM (Sanderson and Knutti 2012).

In subtropical southern Africa (20-30°E; 20-30°S), climate models from the recent Coupled Model Inter-comparison Project (CMIP5; Taylor et al., 2012) systematically overestimate climatological summer rainfall (Figure 5.1a). Some models simulate three times more rainfall than satellite/rain gauge observations. The large and systematic rainfall bias drives excessive evapotranspiration (c. +0.5 mm d^{-1}) and cool temperature anomalies compared to observations (Mueller and Seneviratne 2014). The excessive rainfall is associated with a large off-equatorial diabatic heat source, and is therefore likely to influence the strength and character of regional overturning circulations (Chan and Nigam 2009). The problem has persisted through coupled model generations: from CMIP3 (Christensen et al. 2007; Moise and Hudson 2008) to CMIP5 (Figure 5.1 &

Dieppois et al. 2015) and is also present in atmosphere-only models (Goddard and Graham 1999; Cook 2000; Lazenby et al. 2016).

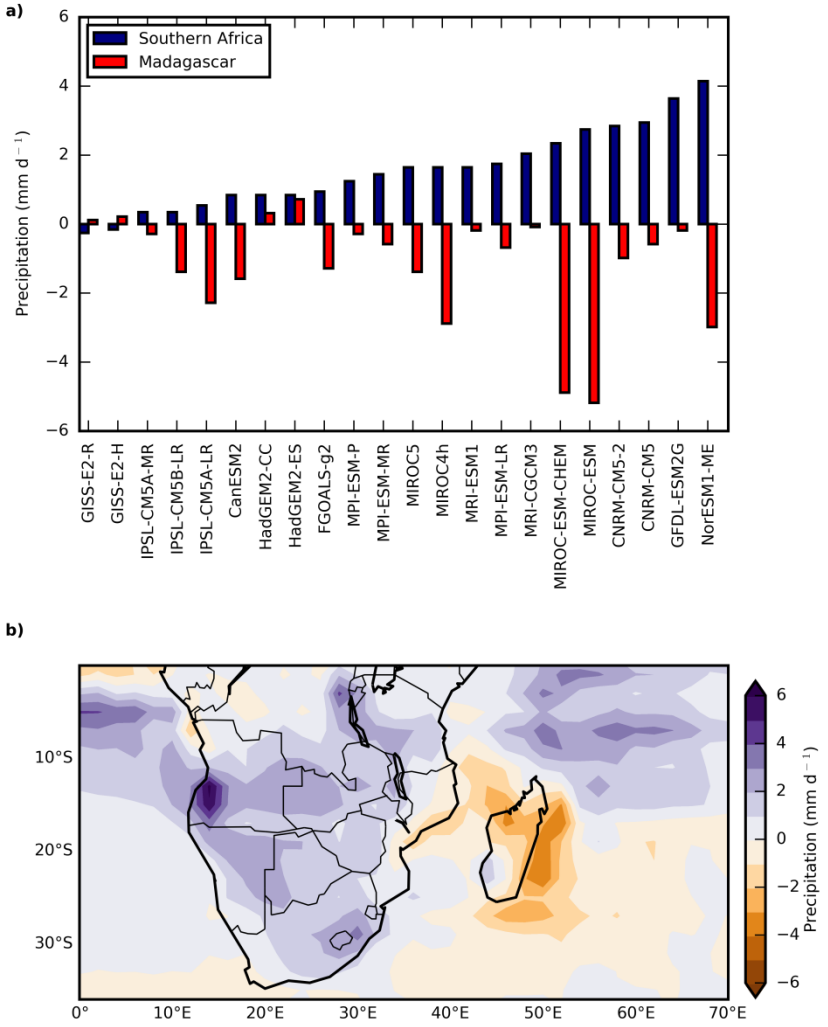


Figure 5.1 a) January-February (JF) climatological rainfall bias (1979-2005) in CMIP5 models relative to CMAP satellite-rain gauge product in subtropical southern Africa (20-30°E; 20-30°S: blue bars) and in Madagascar (44-56°E,12-28°S) b) JF multi-model mean precipitation bias (1979-2005) relative to CMAP.

The rainfall bias in the multi-model mean has a dipole structure with excessive rainfall over southern Africa (+40%) and a rainfall deficit over Madagascar and the south western Indian Ocean (-30%, Figure 5.1b). The dipole is a feature of 20 out of 22 models used in this study (Figure 5.1a), including two models which have a dipole of the opposite sign: diminished southern African rainfall and enhanced Madagascan rainfall. This raises the question of whether there is a common process error in models which encourages rainfall in southern Africa at the expense of rainfall over Madagascar. In this paper we aim to define this process.

5.2 Data

We estimate rainfall from the Climate Prediction Center Merged Analysis of Precipitation (CMAP; Xie and Arkin 1997), a satellite-rain gauge product, which has similar rainfall climatology (1979-2005) to other satellite products over southern Africa (Novella and Thiaw 2013). There are some significant differences between reanalyses products in their estimation of southern African circulation (Zhang et al. 2013). Here we use data from two reanalyses products NCEP2 (Kanamitsu et al. 2002) and ERA-Interim (Dee et al. 2011) to sample some of the uncertainty in the observed circulation. To get a different perspective on model performance in the subtropics we also use radiosonde data from Upington (21°E, 28°S), which spans 1976 to 1998 and from 2008 to 2017. To estimate the climatology we use data from 1979-1994 when the data record is 89% complete for 2am local time sounding and 61% complete for 2pm local time soundings.

Climate model data is from the recent Coupled Model Inter-comparison Project (CMIP5; Taylor et al. 2012). Topography data were only available for 23 models and one model did not have specific humidity fields available. Therefore, we evaluate 22 models (Table 5.1), using data from the first ensemble member for each model. All satellite, reanalysis and model data is in the form of the climatological mean from 1979-2005 for January-February (JF), the core of the austral summer season, and is remapped to a common 2°x 2° grid. Locations referred to in the text are included in a political map of southern Africa (Figure 5.S1; see Supplementary Material for Chapter 5).

Table 5.1 CMIP5 models. Models are ordered from dry to wet according to mean January-February precipitation (20-30°E; 20-30°S).

Model	**Modelling Group**
GISS-E2-R	*Goddard Institute for Space Studies*
GISS-E2-H	*Goddard Institute for Space Studies*
IPSL-CM5A-MR	*L'Institute Pierre-Simon Laplace*
IPSL-CM5B-LR	*L'Institute Pierre-Simon Laplace*
IPSL-CM5A-LR	*L'Institute Pierre-Simon Laplace*
CanESM2	*Canadian Centre for Modelling and Analysis*
HadGEM2-CC	*Met Office Hadley Centre*
HadGEM2-ES	*Met Office Hadley Centre*
FGOALS-g2	*State Key Laboratory Numerical Modelling for Atmospheric Sciences and Geophysical Fluid Dynamics*
MPI-ESM-P	*Max Planck Institute for Meteorology*
MPI-ESM-MR	*Max Planck Institute for Meteorology*
MIROC5	*National Institute for Environmental Studies (Japan), Atmosphere and Ocean Research Institute (University of Tokyo), Japan Agency for Marine-Earth Science and Technology*
MIROC4h	*See MIROC5*
MRI-ESM1	*Meteorological Research Institute*
MPI-ESM-LR	*Max Planck Institute for Meteorology*
MRI-CGCM3	*Meteorological Research Institute*
MIROC-ESM-CHEM	*See MIROC5*
MIROC-ESM	*See MIROC5*
CNRM-CM5-2	*Centre National de Recherches Météorologiques*
CNRM-CM5	*Centre National de Recherches Météorologiques*
GFDL-ESM2G	*Geophysical Fluid Dynamics Laboratory*
NorESM1-ME	*Norwegian Climate Centre*

5.3 Background

We hypothesise that the wetter than observed model climatology in southern Africa is linked to the drier than observed model climatology in Madagascar through a common mechanism. To understand why this might be the case, we briefly review the circulation associated with the observed summer rainfall climatology and its variability.

5.3.1 The observed rainfall climatology

The latitude of maximum African tropical rainfall is equatorward of the maximum in solar insolation throughout the year. In the austral summer, a broad region of enhanced rainfall orientated northwest to southeast is present between 8-22°S over southern Africa and Madagascar (Figure 5.2a). The land-based rainfall is not contiguous: there is one local maximum over northern Zambia (~6-8 mm d^{-1}) and another over Madagascar (~12-14 mm d^{-1}). The Madagascar rainfall maximum is the most poleward extension of the tropical rain band in the Southern Hemisphere. The broad pattern in the rainfall climatology is similar between CMAP and other rainfall datasets, although there are significant quantitative differences (Awange et al. 2015; Maidment et al. 2015). The drivers of the Madagascar rainfall maximum have not been fully demonstrated, with combination of orographic forcing by the ~1500m high topography and the warm sea surface temperatures of the southwest Indian Ocean and Mozambique channel likely to play a role.

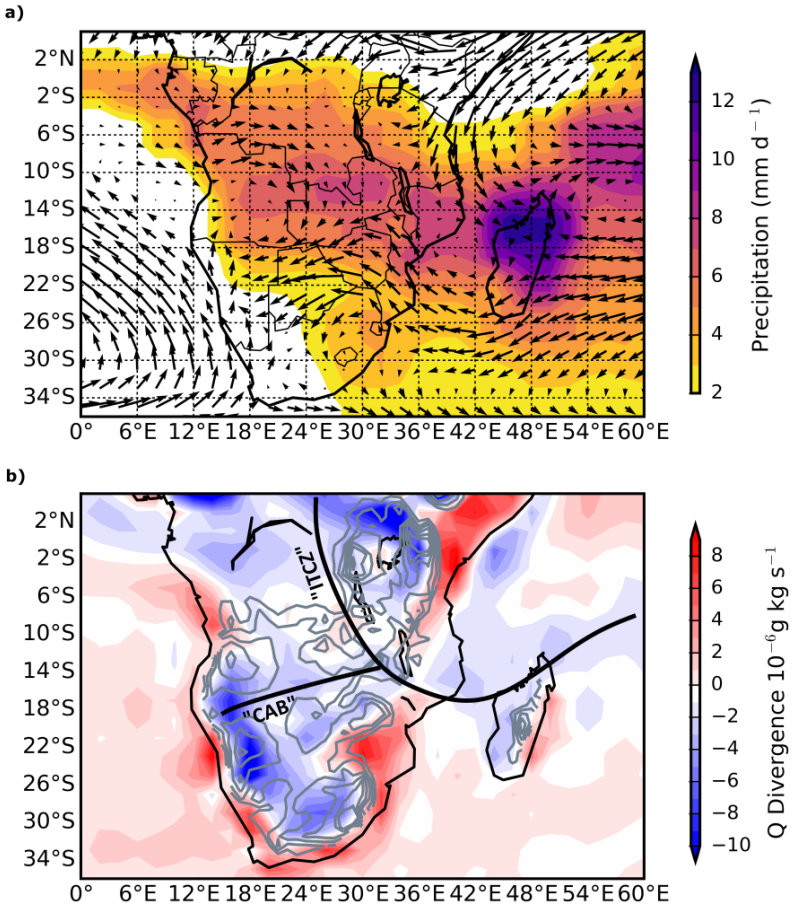


Figure 5.2 a) CMAP climatological precipitation (shaded) and ERA-Interim reanalysis 850 hPa moisture flux climatology for JF (1979-2005) b) Grey contours show topography above 800m (contour interval is 200m) and moisture divergence (g kg s^{-1} x 10^6) is shaded. The supposed positions of the Congo Air Boundary (CAB) and Intertropical Convergence Zone (ITCZ) are drawn following van Heerden and Taljaard (1998).

Reference to the peak austral summer low-level (850 hPa) moisture circulation suggests that the processes controlling the maxima over the tropical subcontinent and over Madagascar are different (Figure 5.2). In northern Zambia most of the moisture supply originates from the equatorial Congo Basin and flows cyclonically around a regional

low pressure system: the Angola Low. Some of this tropical northwesterly flow converges with subtropical southeasterlies, at the Congo Air Boundary (CAB; van Heerden and Taljaard 1998; Hachigonta and Reason 2006), although this convergence occurs predominantly to the south of the rainfall maximum (Figure 5.2b). The Katanga plateau in southern Democratic Republic of Congo (DRC) and The Muchinga mountain range in northeastern Zambia are more closely located with the rainfall maximum. A number of large inland waterbodies, including Lake Malawi, Lake Tanganyika and perhaps even Lake Kariba could also influence the rainfall distribution.

The location of the ITCZ is often invoked as an explanation for the seasonal cycle in rainfall distribution over Africa. In Figure 5.2b, we have drawn on the canonical position of the ITCZ along the eastern Congo Basin from Taljaard (1972) and van Heerden and Taljaard (1998). According to ERA-Interim data, the band of low-level convergence along the ITCZ is not continuous, with mean low-level divergence to the west and southwest of Lake Tanganyika. Counterintuitively, this area of low-level divergence is fairly closely located with the rainfall maximum, whereas the maximum in low-level convergence occurs to the northeast of the locus of tropical convection in the highlands of Tanzania, Kenya and Uganda. In agreement with a recent review by Nicholson (2018), we view this as evidence that the concept of the ITCZ may not be useful for explaining the rainfall distribution over continental Africa.

Cross-equatorial northeasterlies are an important moisture source for subtropical southern Africa during wet years (D'Abreton and Tyson 1995; Washington and Preston 2006). In the mean climatology, based on reanalyses with resolved topography reaching

~1200m, only a small proportion of the northeasterlies penetrate across the high topography of northern Malawi and southern Tanzania (which, in reality, reaches a maximum of ~3000m in the Kipengere range northeast of Lake Malawi). Instead, most of the northeasterly flow curves to the southeast in the vicinity of this topography towards the convection over Madagascar. The recurved flow converges with Indian Ocean easterlies in northern Madagascar, coinciding with the region of maximum summer rainfall.

The diminishing northeasterly flow with increasing latitude in subtropical southern Africa helps to set up a strong northeast to southwest rainfall gradient across the Kalahari Basin (Tyson and Crimp 1998). Rainfall across this gradient decreases from ~7 mm d^{-1} in northern Zimbabwe to less than 2 mm d^{-1} in southern Botswana, western South Africa and Namibia. The reduced moisture supply and high average surface temperatures (>25°C) result in low relative humidity which favours the formation of a thermal low over the western Kalahari in austral summer (Manatsa and Reason 2017). The thermal low is overlain by the Botswana (mid-level) High (Reason 2016). These conditions are clearly not present in some models (Figure 5.1)(also see Munday and Washington 2017; Figure 4.8).

5.3.2 The relationship between Madagascan and southern African rainfall

The dipole between Madagascan and southern African rainfall seen in the CMIP5 climatology (Figure 5.1) is similar to a well-established feature of observed rainfall variability (e.g Jury 1992; Washington 1999; Mutai et al. 1998). Wet years in

subtropical southern Africa are usually accompanied by relatively dry years over northern Madagascar and are associated with anomalous penetration of the cross-equatorial northeasterly flow into the Kalahari Basin (e.g. Hachigonta and Reason 2006; Washington and Preston 2006). Meanwhile, wet years in northern Madagascar are associated with a strengthening of the monsoonal northwesterlies towards northern Madagascar, and low geopotential heights in the southwestern Indian Ocean (Fauchereau et al. 2009a; Jury 2016). In southern Madagascar, rainfall tends to vary in phase with rainfall over southern Africa (e.g. Fauchereau et al. 2009; Randriamahefasoa and Reason 2017). With this in mind, we now evaluate differences in the mean circulation amongst CMIP5 models.

5.4 CMIP5 circulation

5.4.1 Zonal overturning circulation

We start our analysis of the CMIP5 models by examining the climatological zonal overturning circulation from 10-70°E averaged over 23-30°S during January-February (Figure 5.3). At 20-30°E in reanalysis data (top left), there is shallow overturning circulation comprising dry convection associated with the Kalahari Heat Low (20-30°E), and subsidence in eastern southern Africa and the Mozambican channel. Farther east, over Madagascar (50°E), deeper convection, up to 200 hPa, is coupled with the South Indian Ocean High (SIOH) and is part of the canonical Walker circulation.

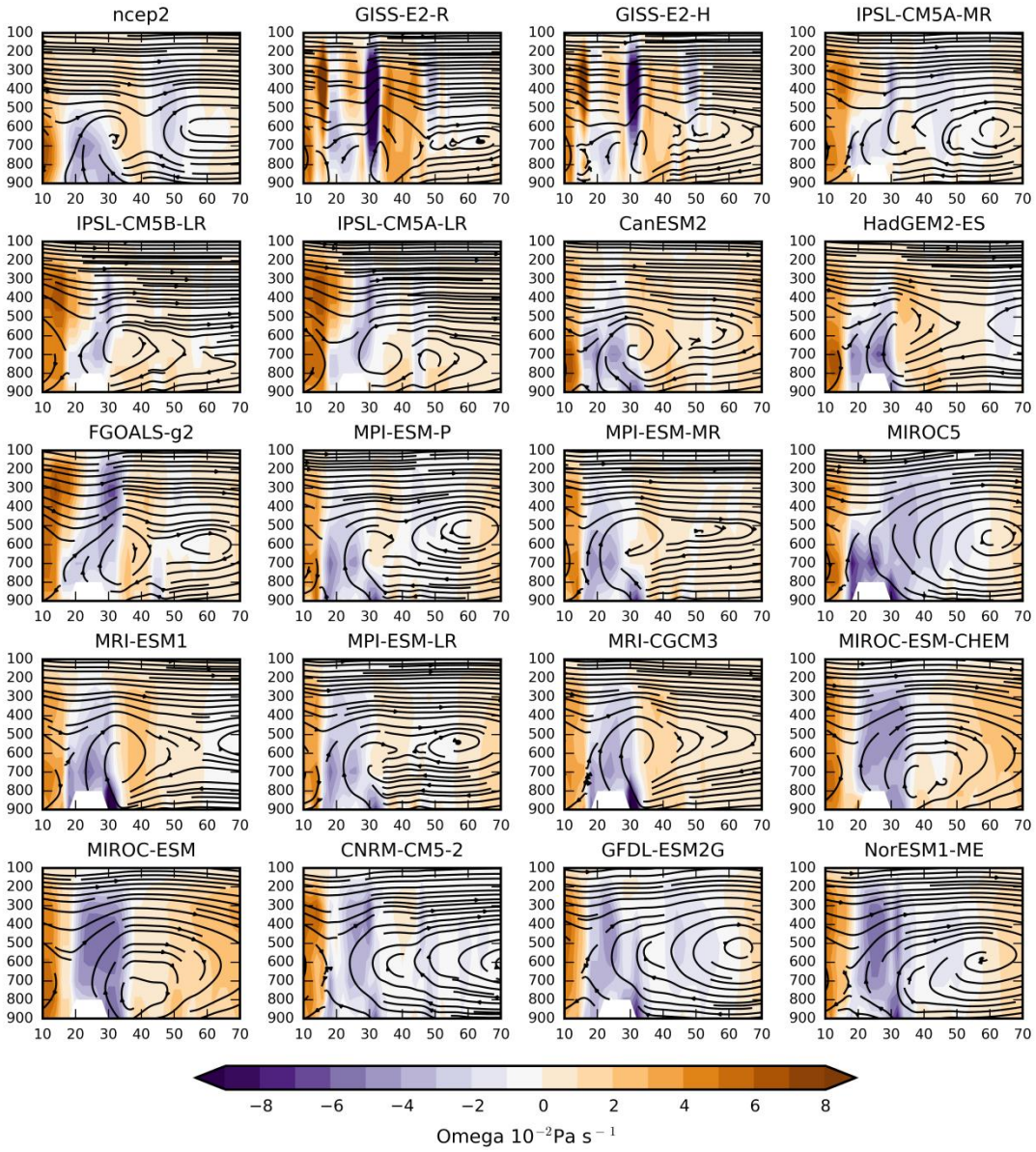


Figure 5.3 Longitude-height cross sections of streamlines (u; w x10^2) averaged over 23-29°S in NCEP2 (top left) and CMIP5 models ordered dry to wet (Table 5.1). Shading is vertical velocity (Pa s^{-1}x10^2), with purples as negative (upward) vertical velocity and oranges as positive (downward) vertical velocity. ERA-Interim is not included here but is qualitatively similar to NCEP2. HadGEM2-CC, MIROC4h and CNRM-CM5 did not have vertical velocity data available and are not included.

The CMIP5 ensemble does not reproduce this circulation. Most models, especially at the wetter end of the spectrum, simulate convection that is too deep over the subcontinent

where the shallow Kalahari heat low is present in reality. Meanwhile, more than half of the models (11/19) fail to simulate convection over Madagascar. This is consistent with the dipole rainfall bias amongst most models (Figure 5.1). Of the models which do simulate convection over Madagascar, only five show it as separate from subcontinental convection. One consequence of these errors is that the majority of models simulate a single overturning cell which links deep convection over land to subsidence over the South Indian Ocean. This is in contrast to the two cell system seen in both ERA-Interim and NCEP2 reanalyses.

To explore the deep convection bias in more detail we compare the vertical structure of moist static energy in models with radiosonde data at Upington (28.24°S; 21.16°E). Moist static energy is defined as:

$$MSE = CpT + gz + Lq \tag{5.1}$$

The first two terms on the right hand side represent the dry static energy (DSE) contribution; CpT is the sensible heat and gz is potential energy. The last term is the latent heat component; L is the latent heat of condensation and q is the specific humidity. For most models (solid lines), the vertical gradient in MSE between the surface and 700 hPa is too steep (Figure 5.4a) and ~75% of the models (16/22) simulate excessive surface MSE in the order of 5 - 10 kJ kg^{-1} compared to the radiosonde estimate (dashed lines). ERA-Interim and NCEP2 reanalyses (dotted lines) also have a positive MSE bias compared to the radiosonde data, although the MSE gradient in better reproduced.

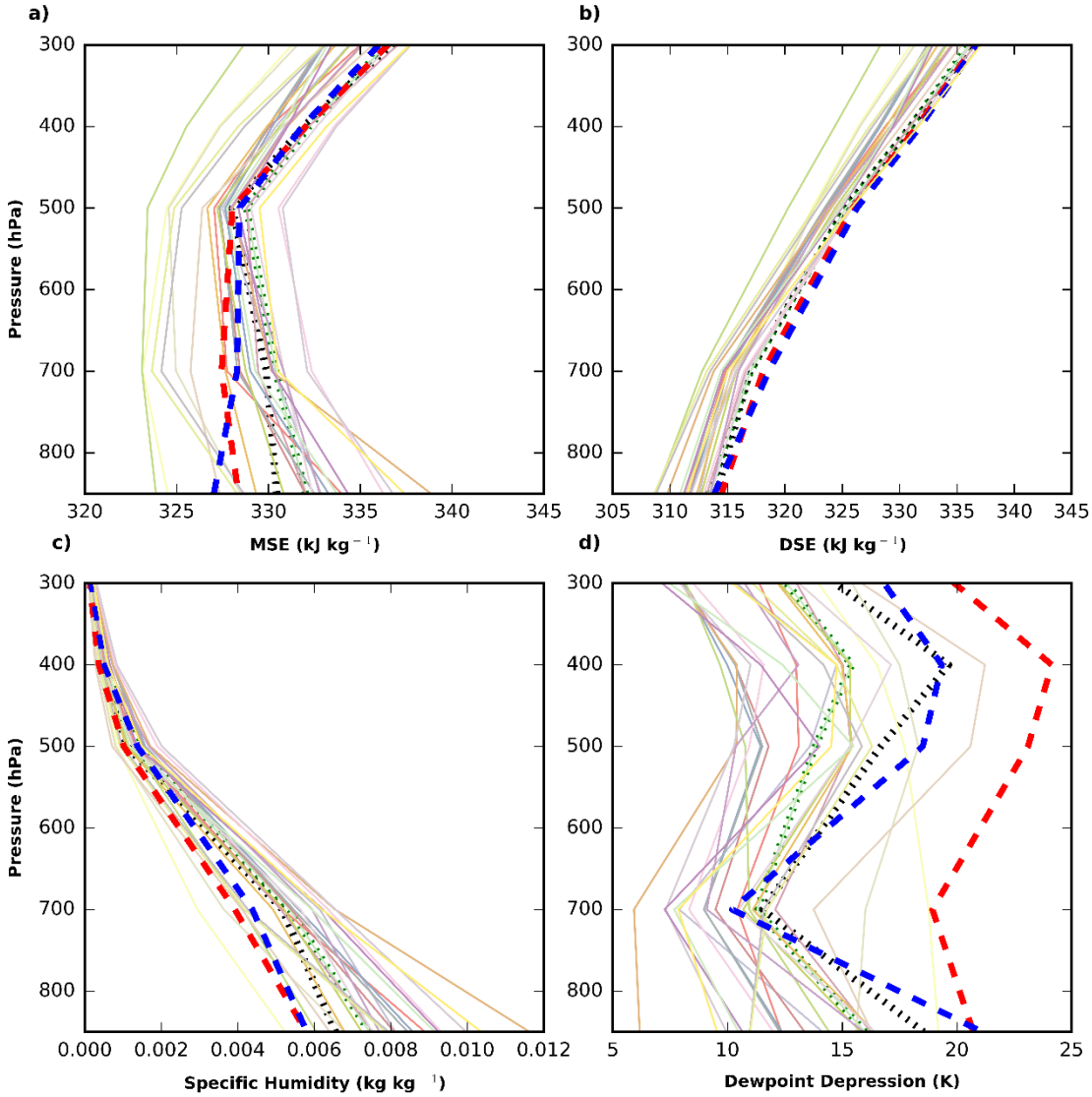


Figure 5.4 January-February climatological vertical profiles of a) moist static energy, b) dry static energy, c) specific humidity and d) dew point depression at Upington (28°S, 21°E). The red and blue dashed lines are average of 2pm and 2am local time radiosonde data, respectively. The solid lines are estimates of the daily mean vertical profile from CMIP5 models , the green (black) dotted lines is ERA-Interim (NCEP2) reanalysis. For reanalyses and models we have used data from the gridbox closest to the Upington station.

There is an opposite sign of model bias in the two components of MSE: the dry static energy component of MSE is underestimated in all models (Figure 5.4b) while specific

humidity is overestimated in all but one model (GISS-E2-R). At 800 hPa, the simulated specific humidity exceeds the radiosonde estimate by between 25 and 90% in 16 of 22 models (Figure 5.4c). The excessive moisture decreases the minimum dewpoint depression (the difference between the temperature and dewpoint temperature) in models (Figure 5.4d). Over half of models simulate a mean dewpoint depression at 700 hPa of between 6 and 11K, whereas in the radiosonde estimate the range in dewpoint depression between night and day is between 11 and 19K. This suggests that convection is much more likely in models compared to reality, consistent with Figure 5.3.

The biases compared to radiosonde data near Pretoria (Irene;28°E,26°S) at an elevation of 1526m are more complex than at Upington (not shown). In Pretoria, there is a tendency to underestimate specific humidity near the surface but overestimate specific humidity above 700 hPa. The overestimation of specific humidity at lower- to mid-levels in the atmosphere, coupled with an underestimation of dry static energy, results in an overall low bias in the dewpoint depression, which is especially prominent with respect to the daytime (1200UTC) radiosonde profile. Interestingly, the profile at 2am local time shows that the dewpoint depression near the surface at 850 hPa is low (2-3K), consistent with frequent dew formation previously reported by (Nagel 1962). The mean temperature profile at 2am is almost isothermal in the boundary layer suggesting efficient longwave cooling over the high plateau.

There is some uncertainty in comparing model grids (at 2°x2°) with a point observation; particularly as we only have a relatively short record available from the Upington radiosonde station (see section 5.2). However, our results are in agreement with previous

work which highlights the CMIP5 cool temperature bias and excessive specific humidity in southern Africa (Flato et al. 2013; Mueller and Seneviratne 2014). Since excessive specific humidity appears to be linked to the enhanced MSE, and by extension convection, our challenge now is to work out why there is excessive moisture in models compared to reality.

5.4.2 Moisture circulation in wet and dry models

We investigate the proximate causes of excessive moisture in models over the interior of subtropical southern Africa by examining the differences in low-level (850 hPa) moisture circulation between dry and wet models (Figure 5.5). In wet models, moisture penetrates farther into the subtropics from the northeast, and over the Tanzanian Escarpment, resulting in anomalous northeasterly flow across Zimbabwe and Botswana in the order of 10-30 g kg^{-1} ms^{-1}. This corresponds to enhanced MSE at 850 hPa of up to 9 kJ kg^{-1} in the Kalahari region (Figure 5.5c). The northeasterly moisture flux occurs in preference to the southeasterly recurvature of the monsoonal northeasterlies out toward the South Indian Ocean. As a consequence, south of 10°S there is almost no westerly moisture flow out into the subtropical Indian Ocean in wet models.

In dry models there is little penetration of moisture across the Tanzanian-Zambian border and some of the northeasterly flow slows and curves southeastward towards Madagascar. This prevents the penetration of easterly flow across the north of Madagascar and is associated with higher MSE (by 5 kJ kg^{-1}) in the South Indian Ocean in the dry set of models. Differences in dry static energy between wet and dry models

are negligible (not shown), emphasising the central role played by the provision of water vapour. The preferential supply of moisture into the subcontinent rather than into the southwestern Indian Ocean in wetter models could therefore be the leading contributor to the dipole precipitation bias (Figure 5.1).

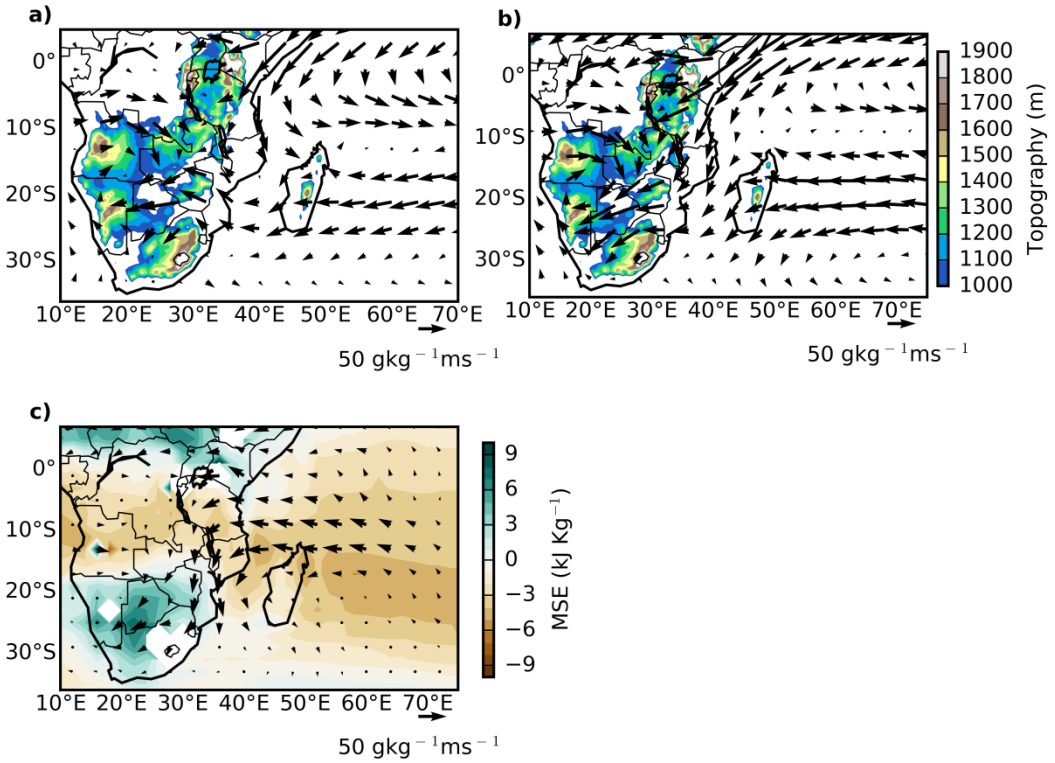


Figure 5.5 January-February climatological mean 850 hPa moisture flux (vectors) for an average of a) the set of six driest models b) set of six wettest models and c) the difference between wet and dry model sets. Shading in a) and b) is observed topography (USGS GTOPO30 dataset) above 1000m. Shading in c) is the 850 hPa moist static energy difference (kJ kg^{-1}) between wet and dry models.

We cannot demonstrate cause and effect in the context of the CMIP5 ensemble, as the relationship between convection and water vapour provision is two-way: convection moistens the troposphere and the diabatic heating associated with convection enhances

the large scale moisture inflow. Instead, our aim for the next section is to diagnose the link between the northeasterly flow and model rainfall.

5.4.3 Upstream circulation, topography and CMIP5 rainfall

5.4.3.1 Froude number in CMIP5 models

To reach the Kalahari Basin, the northeasterly moisture flow must overcome the barrier of the Tanzanian Escarpment. In the previous section we saw that this occurs in wet models but not in dry models or in reanalyses. As rotational effects are weak owing to the low latitude, the ability of the flow to pass over a barrier is primarily dependent on the balance of inertial and gravitational forces and can be estimated using the nondimensional mountain Froude number (Fn):

$$Fn = \frac{U}{Nh} \tag{5.2}$$

Where U is the mean wind velocity associated with upstream northeasterly flow at 850 hPa (averaged over 36-42°E; 3-11°S) and N is the moist Brünt-Väisälä frequency. The mean height of the modelled topography (h) is that orientated perpendicular to the northeasterly flow (30-34°E, 5-13°S, also shown in box Figure 5.7). When upstream flow is strong and stability weak, Fn is relatively large and the depth of blocked flow is

small. Conversely with relatively weak flow and strong stability, Fn is small and the blocking height is large. In this case, flow would be diverted around the barrier.

If blocking of the northeasterly flow is important for model rainfall variability, we would expect dry models over southern Africa to have a lower Froude number than wet models. Figure 5.6 demonstrates that this is the case; there is a strong positive correlation between model Froude number and precipitation over the Kalahari Basin ($r=0.85$; $p<0.0001$). Models with a high Froude number, indicative of a reduced tendency to block the northeasterly flow, tend to be wetter. The slope of the regression is steep: every increase of 0.1 in Froude number corresponds to a 1.6 mm d^{-1} increase in the simulated rainfall amongst models. The reanalyses data (diamonds in Figure 5.6) agree with drier models in the ensemble in estimating relatively low Froude numbers (0.27-0.33). The only two models (GISS-E2-H, GISS-E2-R) which simulate lower Froude numbers than reanalysis (NCEP2) are also the only two models with the opposite sign of rainfall dipole bias (dry southern Africa, wet Madagascar). This suggests that the Froude number is an effective diagnostic for southern African rainfall simulations.

The spatial correlation between the simulated Froude number and gridbox rainfall across models (Figure 5.7) provides support for our hypothesis that differences in the representation of the northeasterly flow are closely related to the dipole rainfall bias. After controlling for spurious gridpoint significance due to multiple hypothesis testing following Wilks (2016), we find strong positive correlations in the Kalahari region are accompanied by a region of strong negative correlations in the southwestern Indian

Ocean, to the east of Madagascar. Here, models with a greater tendency to block the northeasterly flow (lower Froude number) simulate more rainfall. This is consistent with composites of moisture flux (Figure 5.5), which show the southeastward recurvature and convergence of northeasterly flow to the north and east of Madagascar in the dry set of models.

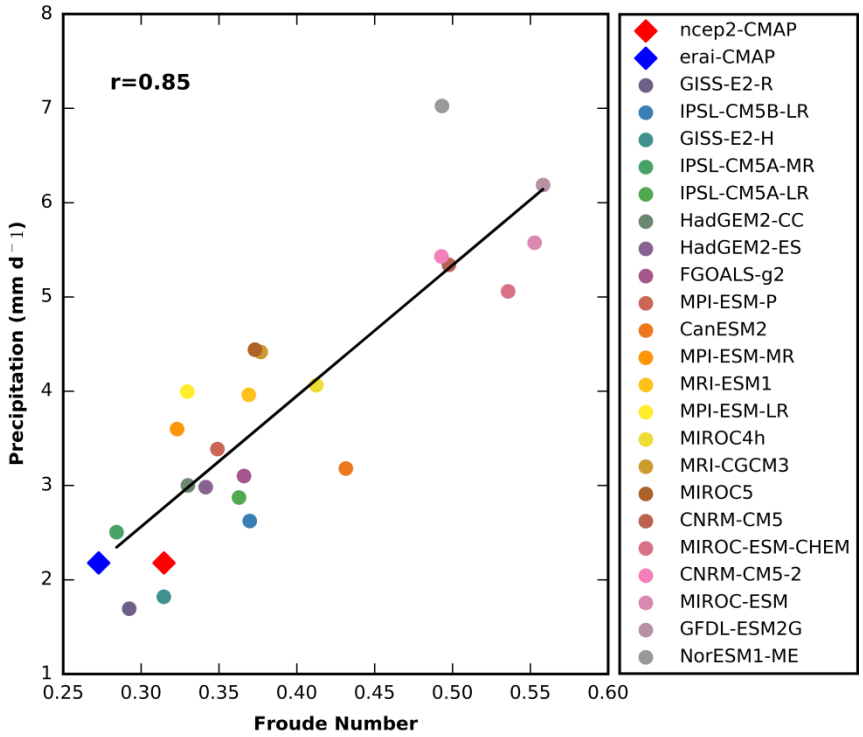


Figure 5.6 The relationship between JF climatological (1979-2005) model Froude number (details in text) and mean subtropical southern Africa precipitation (20-30°E, 20-30°S). Diamonds represent reanalyses and satellite-rain gauge estimates.

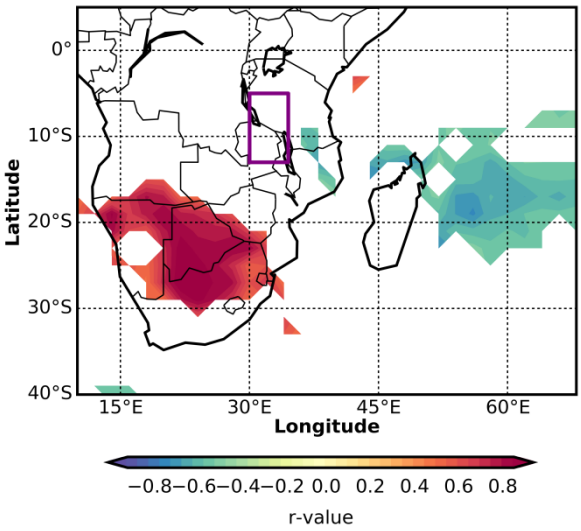


Figure 5.7 Pearson's correlation coefficients for the relationship between JF climatological (1979-2005) model Froude number (details in text) and gridbox rainfall over southern Africa. We control for the false discovery rate (FDR) of significant correlation following Wilks (2016), with a conservative control FDR value of α_{FDR}=0.10 yielding a threshold level of significance as p_{FDR}=0.026. Non-significant values are masked. The purple box shows the Tanzanian Escarpment region.

5.4.3.2 Components of the Froude number

The intermodel spread in simulated Froude number contains contributions from the different terms; U, N and h. The relative importance of these contributions can be estimated by calculating their coefficient of variation (multi-model mean divided by intermodel standard deviation). The intermodel coefficient of variation is 17%, 9% and 2% for U, N and h respectively. This implies that differences in model circulation, and especially in upstream windspeed, are particularly important for model variability in Froude number and rainfall. In the following we discuss the model biases for each component in turn; with the aim of making the potential future model improvements more tractable

Static stability

There is no relationship between the model variability in the simulated moist Brünt-Väisälä frequency and precipitation in southern Africa (not shown). The moist Brünt-Väisälä frequency in 14 out of 22 models falls within the range of the NCEP2 and ERA-Interim estimates. This suggests that the upstream wind speed or topography, or a combination of the two, is responsible for the high simulated Froude numbers and penetration of moisture over the Tanzanian topography. The differences in static stability are, however, relatively large and do modulate the relationship between Froude number and precipitation.

Upstream wind speed

Figure 5.8 shows that the differences amongst models in wind speed upstream of the Tanzanian domain are large, and mostly overestimated in models compared to reanalyses. In the wettest models, the northeasterly flow is 2-3 m s^{-1} faster than reanalysis and only one model (GISS-E2-R) simulates slower wind speeds than the reanalyses. Conspicuously, the GISS-E2-R model is the only one of two models with rainfall dipole of opposite sign (dry southern Africa, wet Madagascar). The systematic overestimation of the strength of the northeasterlies has serious implications for cross-equatorial mass flux. For example, in the boreal summer the reversed jet (Findlater Jet), which is of similar magnitude to the jet in wet models during austral summer (~7 m s^{-1}), is responsible for roughly half global atmospheric cross-equatorial mass flux (Findlater 1969).

While rotational effects are likely to be weak owing to the low latitude, we note here that the intensified upstream wind speed will tend to increase the Rossby number in models:

$$Ro = \frac{U}{Lf} \tag{5.3}$$

Where L is length scale of cross equatorial flow of magnitude 10^6 m and f is the Coriolis frequency. The Rossby number varies between models from 0.25 to 0.5 with increasing wind speed (as L and f are approximately constant between models). The relatively low Rossby number (lower wind speed) in dry models compared to wet models implies a greater role for rotational effects which could encourage the eastward deflection of the flow toward Madagascar. Rotational effects are less important in wet models with higher Rossby numbers.

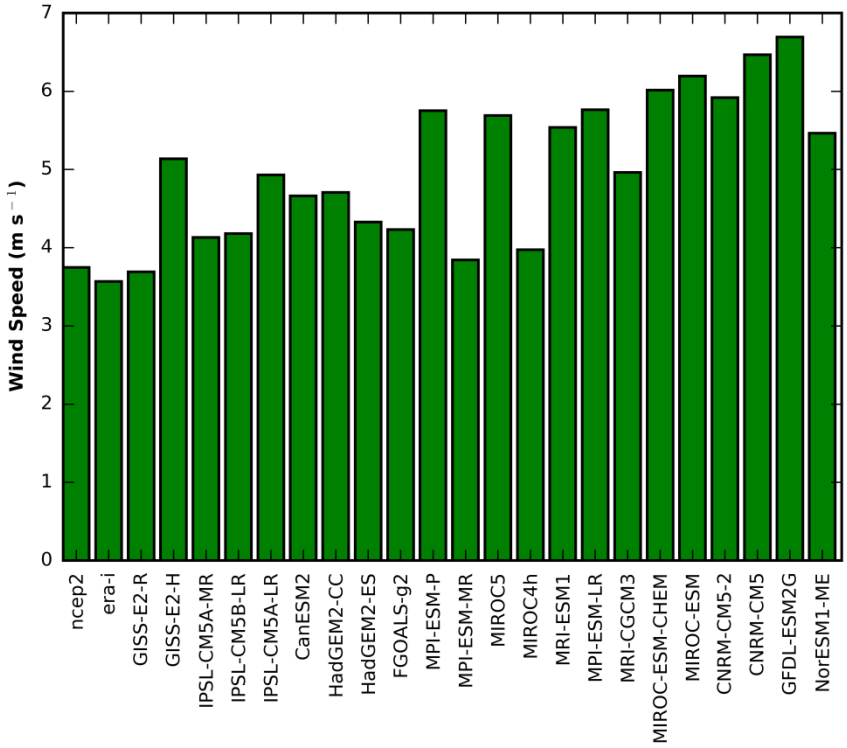


Figure 5.8 Wind speed (m s^{-1}) upstream of Tanzania at 36-42°E; 3-11°S in reanalyses (first two bars) and CMIP5 models (ordered dry to wet; see Table 5.1).

Topography

Although the circulation components dominate the model variability in Froude number, the model representation of topography could also be important. Figure 5.9 shows the longitudinal cross section of surface height at 10°S across the African continent (10-45°E) for CMIP5 models compared to the observed height as estimated by a global digital elevation model (GTOPO30) at sixth of a degree resolution. In the Tanzanian Escarpment region (30-36°E), limits on model resolution result in a lower, smoother barrier to the northeasterly flow. At some longitudes (e.g. 35°E), the resolved topography in the median model is a third of the height of the observed topography (c. 600m difference) and all models produce just one peak in topography associated with the Tanzanian Escarpment, whereas there are four peaks in reality.

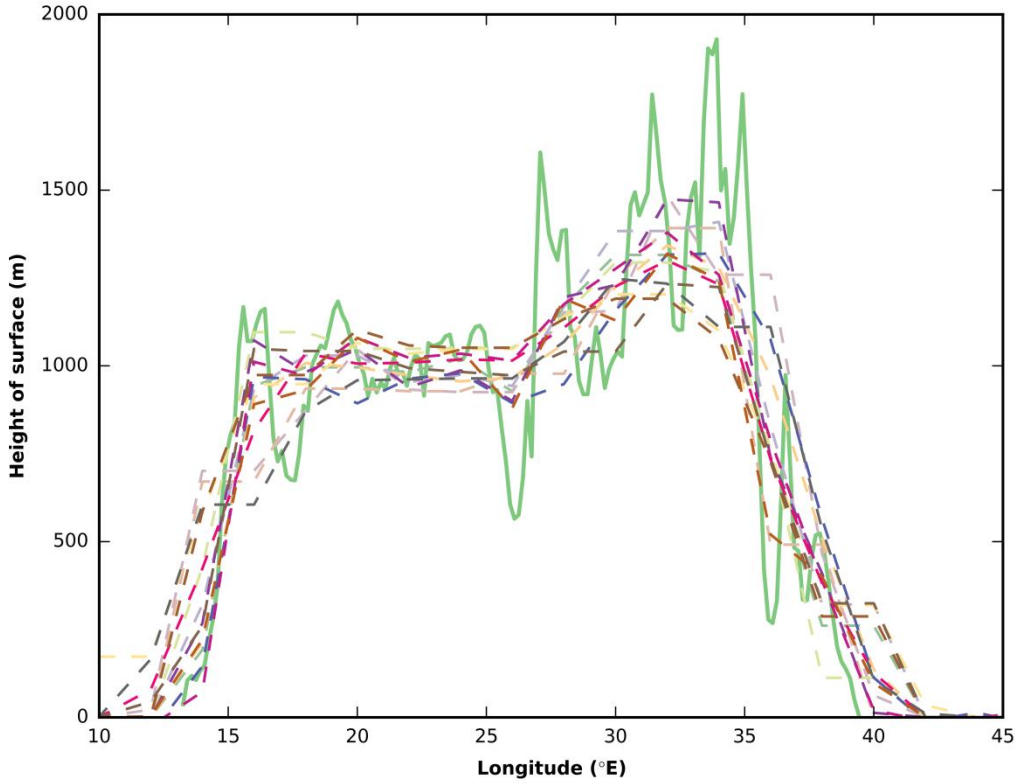


Figure 5.9 Longitudinal cross-section of surface height across southern Africa at 10°S for CMIP5 models (dotted lines) and NASA GTOPO30 (green solid line).

The lower and smoother barrier is likely to be less effective in blocking the northeasterly flow. Figure 5.10 shows that models with lower resolved topography in the Tanzanian Escarpment region (30-36°E, 5-13°S); tend to simulate greater downstream (20-42°E,20-30°S) northeasterly flow (r=-0.65, p=0.001), and more rainfall in the Kalahari Basin (r=-0.59, p=0.004). The difference in rainfall between an average of six models with the highest and lowest topography over the Tanzanian Escarpment supports this result (Figure 5.11). Models with low topography tend to simulate more rainfall over subtropical southern Africa and less rainfall over northern Madagascar. Improving the resolved topography may, therefore, improve the model simulation of climatological rainfall over southern Africa.

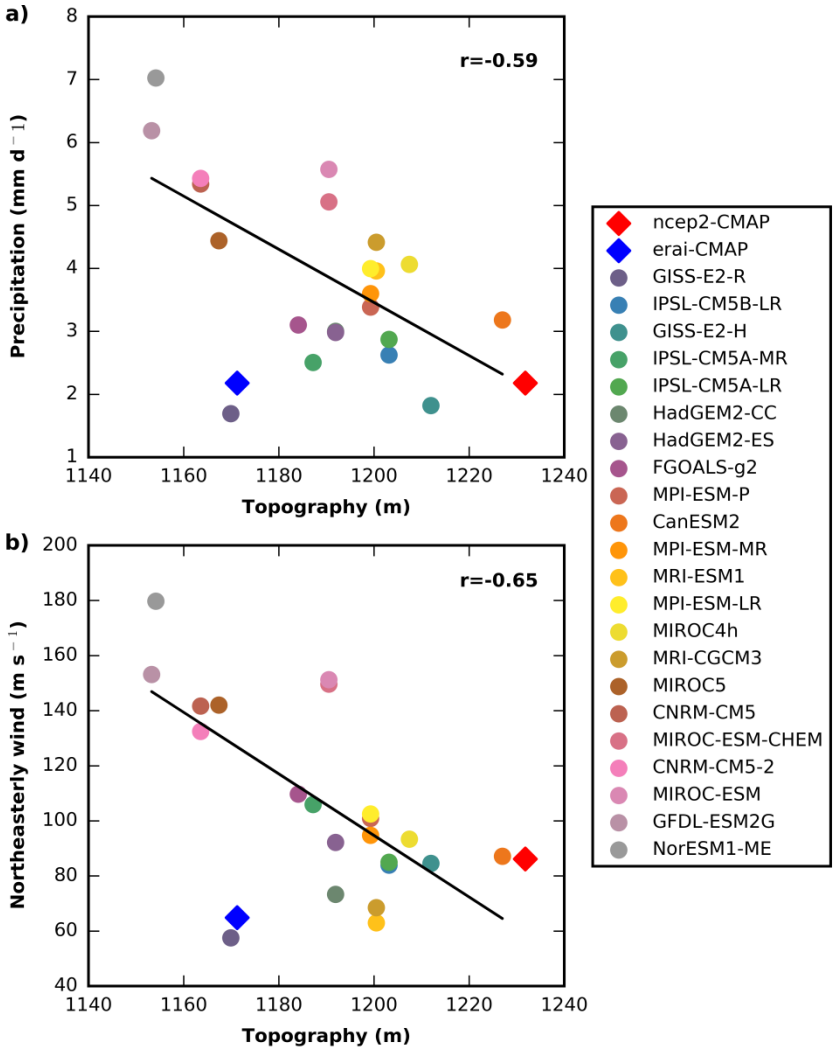


Figure 5.10 The relationship between the Tanzanian Escarpment topography (5-13°S,30-36°E) and a) Kalahari Basin precipitation (20-30°E,20-30°S) , and b) total downstream wind speed (850hPa) in a northeasterly direction (20-42°E,20-30°S). To compute total downstream northeasterly flow we mask grid boxes with westerly and southerly flow, compute wind speed at remaining grid boxes and sum the wind speed across these grid boxes.

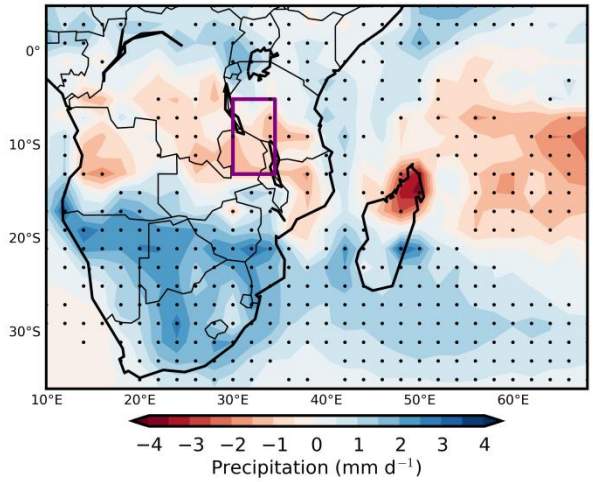


Figure 5.11 The difference in climatological January-February rainfall between the six models with the lowest average topography and the six models with the highest average topography over the Tanzanian Escarpment (purple box). Stipples indicate gridboxes where at least 5 out of 6 models with low topography over the Tanzanian escarpment are wetter (blues) or drier (reds) than all of the models with relatively high topography.

Given the large differences between the observed and simulated topography, the intermodel spread in the magnitude of low-level blocking will also depend on how unresolved orographic drag effects are represented in parameterisation schemes (Lott and Miller 1997). Such schemes are only implemented in some CMIP5 models (Pithan et al. 2016), and yet have been shown to dramatically alter circulation and precipitation on a global scale (e.g. Pithan et al. 2016; van Niekerk et al. 2016). In southern Africa, the influence of model topography parameterisations are not known, although model experiments have demonstrated that the regional topography can influence key climatic features, including the cross-equatorial northeasterly flow (Slingo et al. 2005) and the cold sea surface temperature (SST) of the Benguela upwelling zone (Potter et al. 2017).

5.5 Summary and discussion

5.5.1 Summary of the processes associated with intermodel rainfall variability

CMIP5 models simulate too much summer rainfall over southern Africa, but too little over Madagascar. This paper shows that the dipole bias is related to some fundamental errors in the modelled regional circulation. Most models simulate the ascending branch of subtropical Walker circulation over the subcontinent, whereas in reanalyses the main region of ascent is over Madagascar (Figure 5.3). As a consequence, most models simulate just one single overturning cell which links convection over southern Africa with subsidence over the Indian Ocean. The observed picture is more complicated, with shallow convection associated with the Kalahari heat low comprising one part of a two cell overturning system in the subtropical southern Africa- Indian Ocean sector (Figure 5.3). The presence of this two cell Walker circulation over southern Africa can also be inferred from Schwendike et al. (2014) (their Figure 2).

The wettest models over southern Africa simulate an enhanced northeasterly moisture flux which penetrates across the high topography of Malawi and Tanzania and into the Kalahari Basin. In dry models and in reanalysis the northeasterly flux curves to the southeast in the vicinity of this topography and towards the convective centre over Madagascar. The model variation in simulated Froude number, a measure of the flow's ability to pass over the Tanzanian topography, is strongly associated with intermodel rainfall variability over southern Africa ($r=0.85$, $p<0.0001$). Models with reduced tendency to block the oncoming northeasterly flow simulate more rainfall over southern Africa. This is accompanied by a reduction in rainfall over southwestern Indian Ocean

in those models with a higher Froude number. The model biases in the northeasterly moisture flow are similar to the anomalies observed during wet years in the interannual record (e.g. Washington and Preston 2006).

In subtropical southern Africa, a high proportion of summer rainfall falls during infrequent weather events including tropical-temperate cloud bands (Harrison 1984; Hart et al. 2013), cut-off lows (Favre et al. 2013), mesoscale convective complexes (Blamey and Reason 2013) and tropical lows (Mudenda and Mumba 1996; Reason and Keibel 2004; Howard and Washington 2018). The CMIP5 biases in the mean climatology might influence, or be influenced by, their simulation of these weather events although this has not yet been investigated in any depth. One exception is a study by James et al. (2018) who find that the seasonal cycle of tropical temperate cloud bands (TTCBs) is misrepresented in a recent version of the Met Office unified model (HadGEM3-GC2). The model simulates too many cloud bands in winter and too few in the summer, while there is too much rainfall associated with TTCBs in December. Understanding why this occurs, and whether it is a common bias across models is a logical next step from the present study, and may give further insights into the mean state biases we have investigated here.

5.5.2 Foci for model development

Our results highlight two foci for model development which may improve the simulation of southern African summer rainfall amongst climate models. The first is the model representation of the cross-equatorial northeasterly flow. Most models

overestimate the strength of the flow compared to reanalyses (by over 50% in some cases) and the variation in its strength amongst models is linked with intermodel rainfall variability both in southern Africa and the southwestern Indian Ocean. The link between southern African precipitation and cross-equatorial moisture transport is consistent with model experiments which have shown that the accurate representation of cross-equatorial energy transport improves representation of precipitation both globally and in southern Africa (Hwang and Frierson 2013; Hawcroft et al. 2017). Understanding what drives the bias in northeasterly flow should be a priority.

Previous work on southern African rainfall biases in climate models also highlights the importance of understanding causes of climate model differences in low-level moisture circulation (Moufouma-Okia and Jones 2014; Lazenby et al. 2016; Munday and Washington 2017). Moufouma-Okia and Jones (2014) show in an atmosphere-only model that errors in simulated vertically integrated moisture flux in southern Africa are correlated with errors in rainfall over the period 1980-2008. Munday and Washington (2017), meanwhile, show that some of the CMIP5 intermodel variability in low-level moisture flux and rainfall in tropical and eastern southern Africa is related to the strength of the Angola Low pressure system.

Our results demonstrate a link between the mean height of resolved topography in the Tanzania-Malawi region and rainfall over southern Africa ($r=-0.59$, $p=0.004$). Models with lower topography tend to simulate faster downstream northeasterly flow and more rainfall compared to those with high topography. This implies that improving model representation of topography either through increased model resolution or improved

parameterisations of topographic effects could improve model rainfall, a claim that is consistent with a number of studies using both regional and global climate models (Mason and Joubert 1997; Mehran et al. 2014; Favre et al. 2016; Pinto et al. 2016).

5.6 Conclusions

The organisation of the mean regional circulation over subtropical southern Africa is fundamentally different in a majority of CMIP5 models compared to reanalyses. When these models are used to simulate future climate, a climate forcing is imposed on a mean state which is not observed. Evaluating the uncertainty in the climate change signal from this background state is therefore difficult, especially since we do not know ahead of time whether or how the present day bias might influence the response to forcing. It will be interesting to investigate whether the models analysed here which do simulate a reasonable precipitation and circulation climatology (e.g IPSL-CM5A-MR) project a distinct climate change response in southern Africa compared to other models in the ensemble. This is the subject of our current work.

In addition to highlighting the potential importance of the cross-equatorial northeasterly flow and of topography for model rainfall biases, the analysis of the CMIP5 ensemble raises interesting questions about how the southern African climate system works in reality. Amongst models, there is a trade-off between moisture supply to the continent and into the south-western Indian Ocean (Figure 5.5). In the present day, most models tend to supply too much moisture into the subcontinent and this is tightly coupled with an increase in subcontinental convection at the expense of precipitation over northern

Madagascar. The observed balance of moisture supply in favour of northern Madagascar, in addition to the warm SSTs and proximity to tropical cyclone tracks, may contribute to its relative wetness compared to subtropical southern Africa at the same latitudes.

Acknowledgements

The first author is funded by the UK Natural Environmental Research Council (NERC) through the doctoral training partnership (NE/L002612/1) and also through a Met Office CASE studentship (ACR00400). Richard Washington is partially supported by the NERC- DfID funded UMFULA (NE/M020207/1) and IMPALA (NE/M017206) African climate programs. The climate model data are downloaded from the Earth System Grid Federation (ESGF) (https://pcmdi.llnl.gov/). NCEP2, ERA-Interim and CMAP data were sourced from NOAA/OAR/ESRL PSD, Boulder, Colorado, USA at http://www.esrl.noaa.gov/psd/. Radiosonde data from Upington is available from the Integrated Global Radiosonde archive (IGRA) (https://www.ncdc.noaa.gov/data-access/weather-balloon/integrated-global-radiosonde-archive) and the USGS GTOPO30 global digital elevation model data from http://earthexplorer.usgs.gov/. In addition to three reviewers, whose comments improved the manuscript, we would like to thank members of the SOGE climate lab and Annelize van Niekerk for useful discussions.

Supplementary Material for Chapter 5

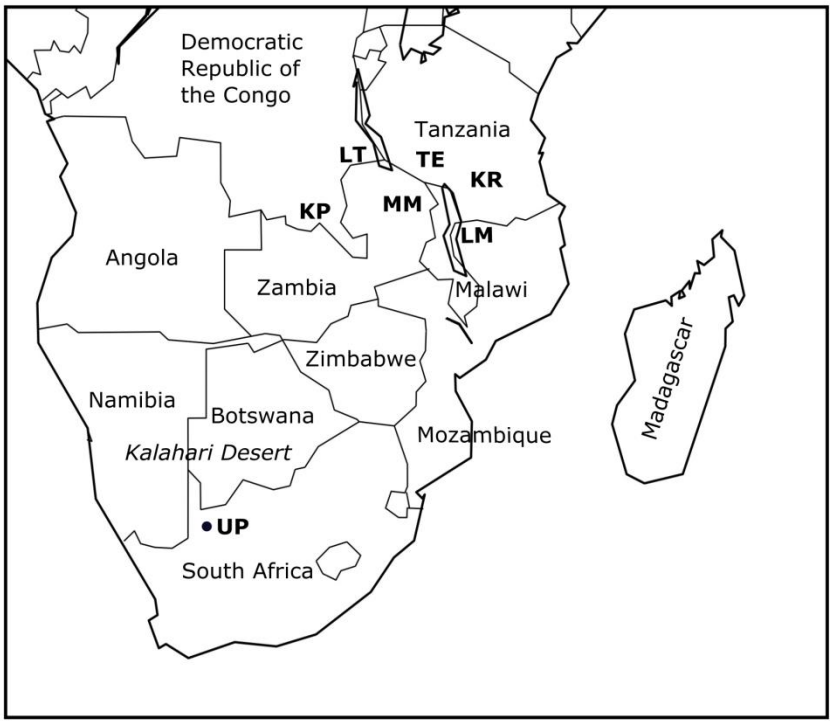


Figure 5.S12 Political Map of southern Africa showing countries and place names mentioned in Chapter 5

6. Controls on the diversity in climate model projections of early summer drying over Southern Africa

C. Munday[1], R. Washington[1]

[1]School of Geography and Environment, University of Oxford.

Submitted J. Climate, 19/07/2018

Authorship declaration

I conducted all of the analysis and wrote the paper. Richard Washington contributed to the planning of the methodology, interpretation of the findings and helped to edit the manuscript.

Abstract

Ninety-five percent of climate models contributing to the Coupled Model Intercomparison Project phase 5 (CMIP5) project early summer rainfall declines over southern Africa. The intermodel consensus underlies the Intergovernmental Panel on Climate Change (IPCC) assessment that rainfall declines are 'likely' and implies that significant climate change adaptation may be needed. However, model consensus is not necessarily a good indicator of confidence, especially given that there is an order of magnitude difference in the scale of rainfall decline among models (from < 10 $mm.season^{-1}$ to ~100 $mm.season^{-1}$), and that the CMIP5 ensemble systematically overestimates present day precipitation over southern Africa, (in some models by a factor of two). In this paper we investigate the uncertainty in the early summer drying signal by evaluating the climate mechanisms which underlie the diversity in model rainfall projections. Local diagnosis of the drying signal indicates that models projecting the highest magnitude drying simulate the largest increases in tropospheric stability associated with increases in upper-level subsidence, reduced evaporation and amplified surface temperature change. Intermodel differences in rainfall projections are in turn related to the large scale adjustment of the tropical atmosphere to emissions forcing; models with the strongest relative warming of the northern tropical sea surface temperatures compared to the tropical mean warming simulate the largest rainfall declines. These models also tend to simulate the largest present day biases in rainfall and in tropical sea surface temperatures, leading the authors to suggest that high magnitude early summer drying over southern Africa is an unlikely scenario.

6.1 Introduction

Climate models consistently project declines in rainfall over southern Africa in the 21st century in response to rising global temperatures (Christensen et al 2007; Shongwe 2009; Collins et al. 2013; He and Soden 2016). The signal-to-noise ratio of the drying is particularly high in the early summer season from October to December (OND), when models from the Coupled Model Intercomparison Project phase 5 (CMIP5) project an average decrease in rainfall over southern Africa (15-40°E,15-30°S) of 42 mm.season^{-1} by the end of the century under high emissions forcing (RCP8.5). Predicated in part on the confidence implied by the intermodel consensus in rainfall projections, hundreds of climate impact studies have outlined the potentially negative effects of climate change in the region, including its effects on agriculture, water supply, energy production, human health and biodiversity (e.g. Schlenker and Lobell 2010; Midgley and Thuiller 2011; Gosling and Arnell 2016; Conway et al. 2015; Serdeczny et al. 2017).

However, agreement between models in the sign of a climate projection is not necessarily a strong argument for confidence in that projection (Parker 2011). This is especially true under conditions where the magnitude of projected change between models varies widely (Parker 2011) and where models contain systematic biases in their estimation of present day climate (Knutti et al. 2010). Both of these conditions are met in the case of projections of southern African drying. First, despite strong consensus among ~95% of models that rainfall will decline in the future, there is an order of magnitude difference in the scale of decline, from less than 10 mm per season to nearly 100 mm (Figure 6.1). Second, the large intermodel spread in future projections occurs in the presence of systematic overestimations of present day rainfall over southern Africa

(Mueller and Seneviratne 2014; Dieppois et al. 2015; Lazenby et al. 2016; Munday and Washington 2017). In ~80% of models in OND, the magnitude of their present day bias exceeds the future change, by a median factor of 2.5 (Figure 6.1). The large intermodel variation in the projections and present day climatology of rainfall suggests that the foundation on which the many impact studies rest is not secure.

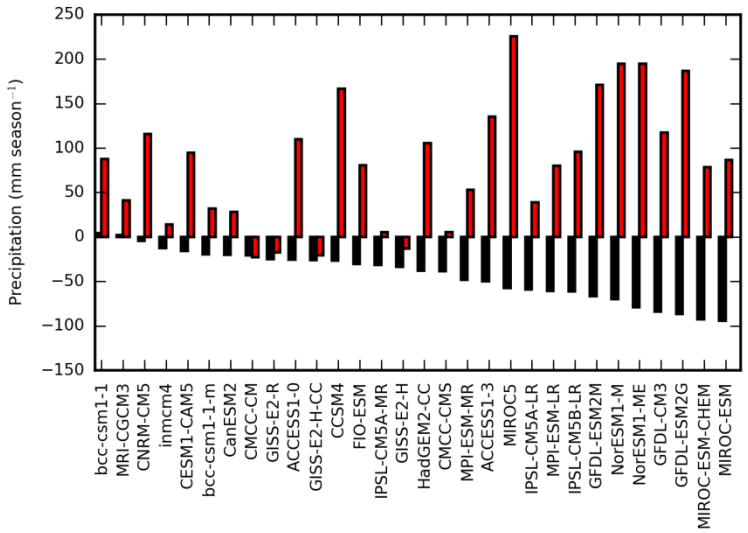


Figure 6.1 CMIP5 future rainfall change (mm.season^{-1}) over southern Africa (15-40°E; 15-30°S) (black bars) for OND (2073-2099 minus 1979-2005) and the present day bias (red bars) in mm.season^{-1} relative to the CMAP dataset.

One way to build confidence in projections is to assess the mechanism of drying among models. Over southern Africa, several studies have done this for both regional and global climate models, providing a useful starting point for assessing confidence in the projections (e.g. Shongwe et al. 2009; Engelbrecht et al. 2013; Cook and Vizy 2013; Lazenby et al. 2018; Pinto et al. 2018). In a regional model driven by the CMIP3 ensemble mean to the mid-21st century, for example, Cook and Vizy (2013) suggest that the rainfall decline occurs as the South Indian Ocean Convergence Zone (SIOCZ) shifts

northeastward in association with a strengthened thermal low and weakened subtropical high. Meanwhile, Pinto et al. (2018) show that annual mean drying trends among four CMIP5 models are associated with an increase in frequency of high pressure systems across southern Africa in lieu of continental and midlatitude lows. These studies are useful in that they relate projections of rainfall change to specific climate processes, the realism of which could be evaluated in comparison with observations (e.g. James et al. 2015) or which could be tested with simpler, idealised models (Held 2005). If the processes are judged to be plausible and are consistent across a range of climate models, this would add evidence to support the reliability of the drying trend. As a contribution to this effort, the purpose of this paper is to understand in more detail the physical processes associated with the divergence in early summer drying projections among 30 of the CMIP5 models, and to consider these processes in light of present day model biases.

6.2 Background: Potential mechanisms of change

A number of mechanisms have been proposed to explain rainfall change in the global tropics. At a zonal mean scale, increases in water vapour content of the atmosphere due to warming may amplify existing patterns of moisture convergence (precipitation-minus-evaporation; P-E), resulting in increases in rainfall in areas of climatological deep convection (the wet-get-wetter mechanism) and decreases in precipitation in climatologically dry regions (Chou and Neelin 2004; Held and Soden 2006; Chou et al. 2009; Seager et al. 2010). Although this thermodynamic increase or decrease in rainfall is likely to be offset by a (dynamical) weakening of overturning circulations (Held and Soden 2006; Vecchi et al. 2006; Ma et al. 2012; Ma and Xie 2013; Chadwick et al.

2013), it helps to explain the observed large scale increases in P-E (E-P) in regions of climatological ascent (descent) over recent decades (Allan et al. 2010).

The wetting of regions with high climatological precipitation by enhanced moisture advection could lead to dynamical rainfall decreases at convective margins (Neelin et al. 2003; Chou and Neelin 2004). In subtropical regions, such as southern Africa, increases in low level moist static energy may be insufficient to keep pace with the near-uniform increases in dry static energy in the upper tropical troposphere due to warming of the oceans (Neelin et al. 2003). Giannini (2010) applies this moist-static energy perspective to explain rainfall projections in the Sahel. She finds that ocean-warming induced increases in upper level moist static energy, affect moist stability from the top down and are related to rainfall declines in some CMIP3 models. This is consistent with simulations of Sahelian rainfall variability in the 20th Century, which is affected by periodic warming of the tropics during El Niño events (Held et al. 2005; Giannini 2010).

Seth et al. (2011, 2013) extend the analysis of Giannini (2010) to explain future early summer drying trends in the ensemble mean CMIP3 and CMIP5 models across global monsoon regions, including over southern Africa. For southern Africa, they show that upper tropospheric warming during the early summer presents an enhanced convective barrier, which is not overcome by increases in moisture supply after a warmer and drier dry season. The enhanced moist stability is associated with decreased evaporation and increased moisture divergence, which combine to exacerbate the rainfall decline (Seth et al. 2013).

In addition to spatially uniform oceanic warming, which is assumed by the mechanisms discussed above, patterns of sea surface temperature (SST) change are also likely to influence future oceanic rainfall change (Xie et al. 2010; Huang et al. 2013; Ma and Xie 2013) and, through atmospheric teleconnections, could be critical for model diversity in terrestrial rainfall change in the tropics (Biasutti and Sobel 2009; Park et al. 2015; Brown et al. 2016; Rowell and Chadwick 2018). In the Sahel, evidence that the pattern of SST warming affects future change comes from associations between the enhanced warming of the northern hemisphere extra-tropics relative to tropics and rainfall projections in CMIP5 (Park et al. 2015), as well as a delayed seasonal cycle of SSTs which contributes to early summer rainfall declines in CMIP3 models (Biasutti and Sobel 2009). Meanwhile, for the East African "long rains" (OND), Rowell et al. (2018) show that the pattern of SST change in the tropics is a major driver of uncertainty in rainfall projections in CMIP5.

The pattern of sea surface temperature change is also likely to be important for southern African rainfall projections. In the CMIP5 ensemble mean model, Lazenby et al. (2018) find a northeastward shift of the South Indian Ocean Convergence Zone (SIOCZ) towards East Africa and the western Indian Ocean. By decomposing the future rainfall change into dynamic and thermodynamic components following Chadwick et al. (2013), they demonstrate that the precipitation decline in OND is a consequence of both dynamic change in the location of convection and thermodynamic changes induced by decreasing relative humidity. While declines in ensemble mean rainfall are driven equally by both thermodynamic and dynamic terms, intermodel uncertainty in the rainfall decline appears to be driven mostly by the dynamical term. The authors go on to

argue that uncertainty in the future evolution of dynamical precipitation changes may be related intermodel differences in the pattern of SST change in the Indian Ocean.

In what follows we diagnose changes to the southern African climate system associated with early summer drying (Section 6.4) and trace how they might arise through differences in the extent and pattern of warming of tropical oceans among models (Section 6.5). In Section 6.6 we comment on these results in light of present day biases before concluding in Section 6.7.

6.3 Data

We analyse future change projections in 30 models forming part of the CMIP5 dataset (Table 6.1; Taylor et al. 2012). Future change for each model is calculated by subtracting their present day climatology (1979-2005) in the historical experiment (ensemble r1i1p1) from their future climatology (2073-2099). The future change experiments in CMIP5 use the representative concentration pathways (RCPs) developed by van Vuuren et al. (2011). To maximise the signal-to-noise ratio for examining mechanisms of change, we use the most extreme of these pathways (RCP8.5) in which the global net radiative forcing by 2100 is 8.5 Wm^{-2}. The RCP8.5 experiment is comparable to the previous Coupled Model Intercomparison Project (CMIP3) SRES A2 scenario, which is based on a 'business as usual' approach to climate change mitigation.

We use composites of six models which project highest magnitude (HM) drying and six models which project low magnitude (LM) drying (OND). The models used for composites are marked in Table 6.1, along with their future OND rainfall change and present day rainfall bias. All model data is remapped to a common 2°x 2° grid.

In Section 6.6 we discuss potential links between model projections and their present day biases in precipitation and SST. Our comparison dataset for precipitation is the Climate Prediction Center Merged Analysis of Precipitation (CMAP; Xie and Arkin 1997), a satellite-rain gauge product. The rainfall climatology of the CMAP dataset is in good agreement with other satellite and rain gauge-based datasets over southern Africa (Novella and Thiaw 2013), although there are relatively few rain gauges with which to confront the satellite datasets in tropical regions of southern Africa (Washington et al. 2006). For observed SST we use the National Oceanic and Atmospheric Administration (NOAA) Extended Reconstructed Sea Surface Temperature version 5 (ERSSTv5) (Huang et al. 2017), which is based primarily on in situ measurements. Previous versions of this product (e.g. ERSSTv3) are similar in their climatology to other SST products which use different measurement techniques (Kennedy 2014). The present day climatology for both CMAP rainfall and ERSSTv5 SST is calculated over 1979-2005 and both datasets are remapped to a 2°x 2° grid for comparison with CMIP5 models.

Table 6.1 CMIP5 models used in this study, their future OND rainfall change over southern Africa (15-40°E; 15-30°S) and their precipitation bias relative to the CMAP dataset. Models are ordered by precipitation change (ΔP) under RCP8.5 (2073-2099 minus 1979-2005), models in bold are those included in the low magnitude (LM) and high magnitude (HM) change composites. Stars indicate the 10 models with highest present day bias, crosses indicate models with lowest present day bias.

Model	**Δ P**	**P bias (mm.seas^{-1})**
bcc-csm1-1	4.2	87.8
MRI-CGCM3	2.1	41.2
CNRM-CM5*	-4.3	115.6
inmcm4^{+}	-12.4	13.8
CESM1-CAM5	-15.7	94.7
bcc-csm1-1-m^{+}	-19.5	31.6
CanESM2^{+}	-20.0	28.2
CMCC-CM^{+}	-20.8	-22.8
GISS-E2-R^{+}	-24.7	-17.4
ACCESS1-0*	-25.7	109.5
GISS-E2-H-CC^{+}	-25.9	-20.8
CCSM4*	-26.4	166.7
FIO-ESM	-30.5	80.5
IPSL-CM5A-MR^{+}	-31.7	5.2
GISS-E2-H^{+}	-33.6	-13.3
HadGEM2-CC	-37.8	105.2
CMCC-CMS^{+}	-38.5	5.2
MPI-ESM-MR	-48.0	53.0
ACCESS1-3*	-49.7	134.9
MIROC5*	-57.5	225.5
IPSL-CM5A-LR^{+}	-59.0	38.6
MPI-ESM-LR	-60.6	79.9
IPSL-CM5B-LR	-61.3	95.5
GFDL-ESM2M*	-66.9	171.1
NorESM1-M*	-70.0	194.9
NorESM1-ME*	-79.2	194.5
GFDL-CM3*	-84.2	117.4
GFDL-ESM2G*	-86.6	186.8
MIROC-ESM-CHEM	-92.8	78.2
MIROC-ESM	-94.2	86.3

6.4 Local diagnosis of southern African rainfall projections

In this section we examine changes to the vertical structure of the atmosphere, moisture circulation and water balance.

6.4.1 Changes to the vertical atmospheric structure

The future drying signal among CMIP5 models (Figure 6.1) is likely to be related to changes in tropospheric stability. Changes in stability can be diagnosed through examining alterations to the vertical profile of moist static energy (MSE). MSE is defined as:

$$MSE = CpT + gz + Lq \quad (6.1)$$

The first two terms on the right hand side represent the dry static energy (DSE) contribution; CpT is the sensible heat and gz is potential energy. The last term is the latent heat component; L is the latent heat of condensation and q is the specific humidity.

If the remote effect of SST warming is important for determining the magnitude of rainfall decline we would expect to see larger increases in upper tropospheric MSE over southern Africa in the HM compared to LM models. This is because warming of the oceans would tend to increase convection over water because moisture is readily

available through evaporation (Chou and Neelin 2004). Moist static energy is imported through moisture convergence at low-levels into the convective (ascent) regions over the oceans and is then exported at upper levels through the divergence of high-MSE air. Greater increases in warming (and convection) over oceans would therefore lead to a greater increase in the export of MSE at upper-levels. Figure 6.2 shows that this could be important in distinguishing between models with low and high magnitude rainfall changes over subtropical southern Africa. In a longitude-height cross section averaged over 15°-30°S HM models simulate a ~25-30% larger increases in MSE between 300 and 200 hPa compared to LM models.

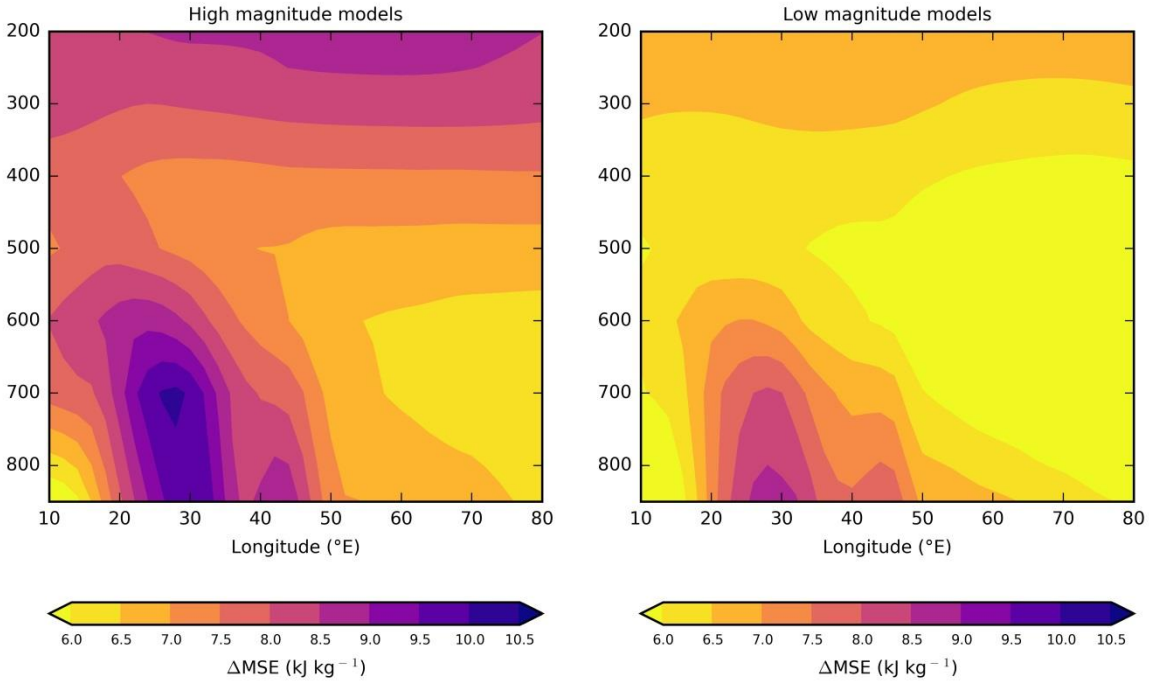


Figure 6.2 Longitude-height (in hPa) cross section (averaged between 15 and 30°S) of future change in moist static energy (kJ.kg^{-1}) in high magnitude drying (left) and low magnitude drying (right) sets of models.

The increased upper level MSE in the HM models is accompanied by large MSE anomalies (10 $kJ.kg^{-1}$) near the surface centred on 28°E. The increase in surface MSE is mainly associated with an increase in the dry static energy term (not shown), and lies to the east of the location of the climatological Angola heat low. This suggests a future deepening and broadening of the thermal low, in accordance with results from previous studies (Cook and Vizy 2013; Lazenby et al. 2018). The strengthened heat low sets up a steeper low level MSE gradient between the southern African landmass and the adjacent Indian Ocean. The pattern of change is qualitatively similar in the LM models, although less intense.

To highlight the effect of the altered MSE profile on vertical motion, we examine the cross sections of vertical velocity (dP/dT) averaged over the same latitudes (Figure 6.3). Consistent with the large increase in upper level MSE, there is anomalous upper level subsidence which reaches a maximum at between 400 and 300 hPa in the HM set of models. Over the continent, the anomalous subsidence overlies an increase in shallow convection near the surface. The preferential increase in shallow convection over deep convection supports the view that the continental thermal low is deepening in response to warming. The main differences between the LM and HM models follow this structure, with HM models simulating 70% larger increases in upper level subsidence than LM models, and greater low-level uplift associated with a relatively strengthened thermal low.

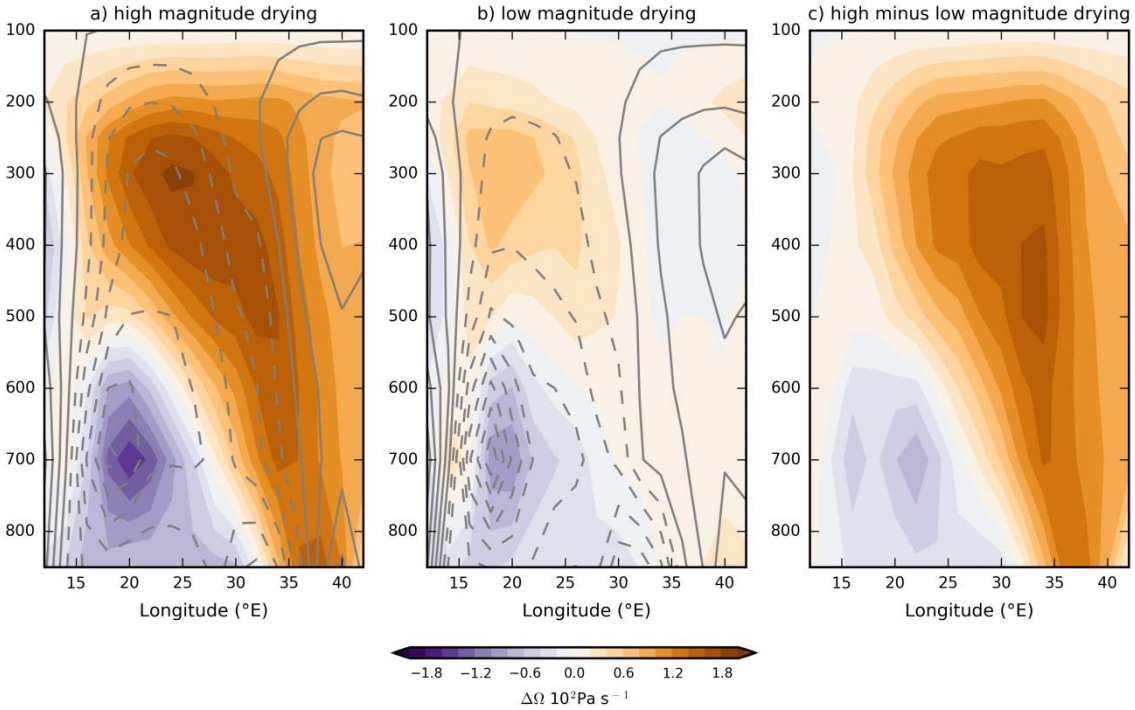


Figure 6.3 Longitude-height (in hPa) cross section (averaged between 15 and 30°S) of future change in vertical velocity (10^2 Pa.s^{-1}) (shading) in high magnitude drying (left) and low magnitude drying (middle) models, and their difference (right). The contemporary climatology (1979-2005) in HM and LM models is shown by grey contours.

Comparison between the present day climatology of vertical velocity and future change raises two further points worthy of note (Figure 6.3). First, in both sets of models there is an eastward shift in the location of the low level uplift from ~18°E to ~20°E, indicating an eastward shift or broadening of the thermal low. Second, the contemporary climatology of vertical uplift in the HM models is deeper than that in reanalysis data (Adebiyi and Zuidema 2016). The LM models, in contrast, have a vertical velocity structure that resembles reanalysis. That the larger future response in vertical velocity occurs in the HM models is the first indication that the present day bias might influence the magnitude of future drying and is evidence we will return to in Section 6.6.

6.4.2 Changes in moisture circulation

The differences between HM and LM models in Figures 6.2 & 6.3 indicate increased stability is being set from the top down, rather than from changes in the low-level circulation. This view of precipitation declines is consistent with the mechanism set out by Giannini (2010) and applied to southern Africa by Seth et al. (2013), but could be complicated by changes in the low-level moisture circulation between models. For example, HM models may simulate reduced moisture supply into southern Africa in the future compared to LM models, thus influencing atmospheric stability from the surface up.

In both sets of models, future anomalies in 850 hPa moisture flux and convergence (Figure 6.4, *middle row)* are superimposed on their existing pattern of convergence (Figure 6.4, *top row*). Across both model sets, moisture convergence increases (2-5 10^8.kg $kg^{-1}.s^{-1}$) in the central subcontinent while moisture divergence increases (1-4 10^8.kg.$kg^{-1}.s^{-1}$) across the eastern coast in Tanzania, Mozambique and eastern Zimbabwe. The intensification of the existing pattern of convergence/divergence is associated with greater moisture flux from the Indian Ocean and the equatorial Congo Basin region. This is likely associated with the strengthened Angola thermal low which is evident in both model sets (Figures 6.2 & 6.3).

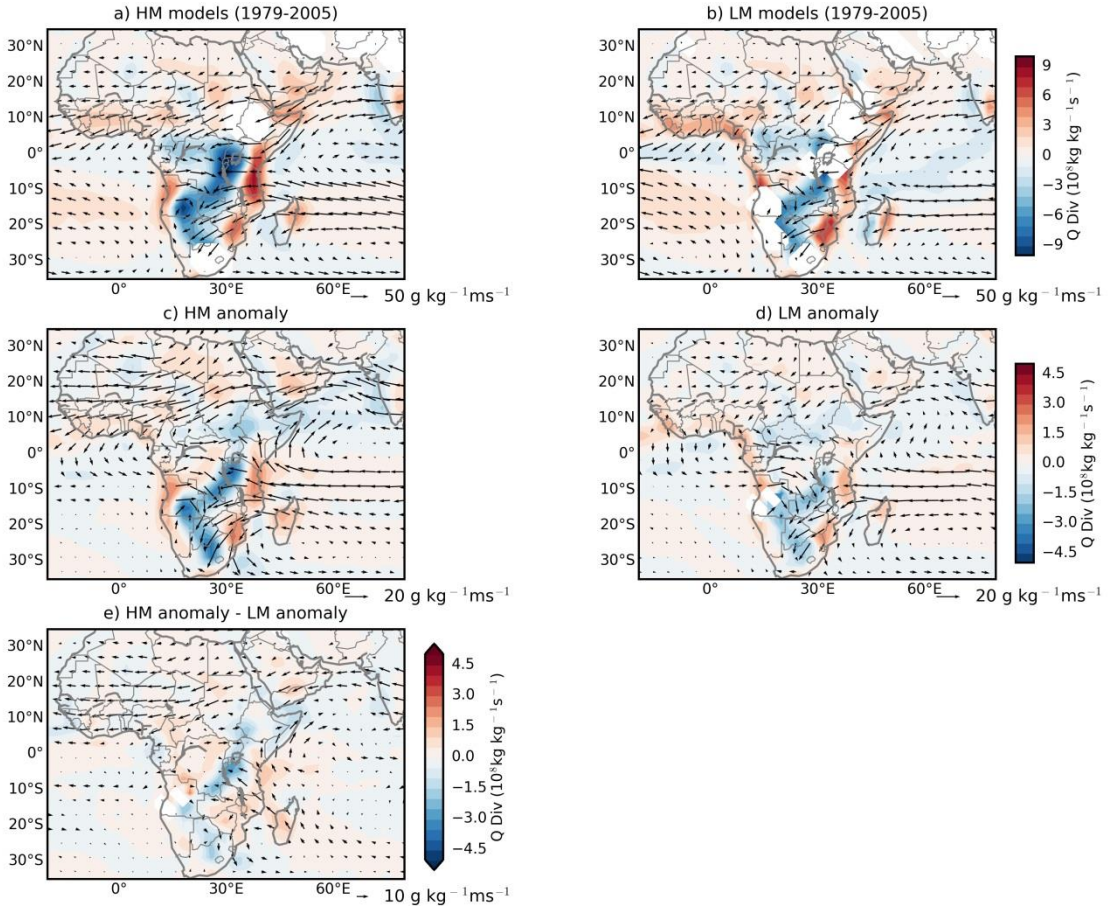


Figure 6.4 Low-level (850 hPa) moisture divergence (shading; 10^8kg.kg^{-1}.s^{-1}) and moisture flux (vectors; barb in lower right corner of plots shows scale). The first row is the present day climatology (1979-2005) in a) high magnitude drying models and b) low magnitude drying models. The second row is the future change for c) high magnitude drying models and d) low magnitude drying models. The last plot, e), is the difference in future change between high and low magnitude drying models

If intermodel variation in projections of moisture circulation influences the intermodel spread in precipitation change, we would expect to see less moisture convergence in the continental interior in the HM models compared to the LM models given the greater drying evident in the HM models. This is not evident in Figure 6.4. Moisture convergence over the continental interior increases more (by 2-4 10^8.kg.kg^{-1}.s^{-1}) in the HM compared to LM models (Figure 6.4, *bottom row*). The larger increases in moisture

convergence are consistent with the greater intensification of the Angola heat low in HM compared to LM models. This emphasises the primacy of a top down mechanism of stabilisation in controlling differences between model projections, as the additional moisture supply in HM compared to LM models is not sufficient to mitigate the rainfall decline. We do note, however, that larger increases in low-level moisture divergence in HM compared to LM models may contribute to rainfall declines in eastern parts of southern Africa and especially in Mozambique.

6.4.3 The relationship among projections of rainfall, surface temperature and evaporation

Figures 6.2 to 6.4 present evidence which suggests that the intermodel spread in projections of early summer drying is controlled primarily by the degree of increase in upper level subsidence. Since increased stability is associated with clearer skies and enhanced net surface solar radiation (Giannini 2010), one way of diagnosing this relationship at a regional scale is to examine the relationship between surface temperature change and rainfall change over southern Africa amongst CMIP5 models.

After normalising temperature change by each models' tropical mean change to account for different climate sensitivities, Figure 6.5a shows how projections of surface temperature over southern Africa are closely associated with projections of rainfall in CMIP5 models. Models projecting high magnitude drying also project larger surface temperature amplification over southern Africa ($r=-0.60$, $p<0.001$**)**. This could indicate that the uncertainty in the precipitation change is driving uncertainty in the local temperature change through cloud feedbacks, although causation cannot be

demonstrated in this context. A similar intermodel association between rainfall and temperature change has been noted for future changes to the Australian monsoon in CMIP5 models (Brown et al. 2016).

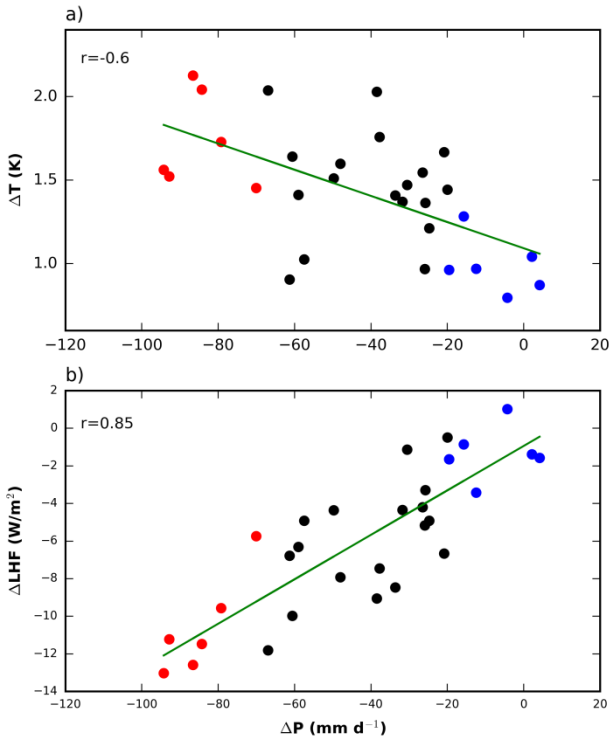


Figure 6.5 The intermodel relationship between future rainfall change over southern Africa (15-40°E; 15-30°S) and a) future surface temperature change (K) over southern Africa relative to the tropical mean temperature change (180°W-180°E; 20°N-20°S), and b) future latent heat flux change (W.m^{-2}) over southern Africa. The blue (red) dots represent models which are part of the LM (HM) composites

Southern Africa is a semi-arid region and evapotranspiration (latent heat flux) tends to be precipitation limited (Mueller and Seneviratne 2014). This implies that as precipitation declines so should evaporation, notwithstanding the increases in moisture supply (Figure 6.4). We show this relationship in Figure 6.5b: there is a strong positive correlation between decreasing precipitation and decreasing evapotranspiration among models ($r=0.85$, $p<0.001$**)**. In turn the reduced evapotranspiration increases the ratio of sensible to latent heat fluxes (the Bowen ratio, not shown), which could further contribute to the amplification of temperature change over southern Africa. The

relationships among future projections of precipitation, temperature and evaporation imply that uncertainty in projections of temperature and rainfall should be considered together.

6.5 Connections with tropics-wide projections

The enhanced atmospheric stability over southern Africa could be connected to changes in tropics-wide circulation and warming through the mechanisms outlined in the background section. Here, we investigate how the intermodel diversity in rainfall decline may be related to changes in tropical rainfall and patterns of sea surface temperature change.

6.5.1 Spatial changes in southern African and tropical rainfall

HM models project future reductions in rainfall across much of southern Africa, with the largest decreases, of up to 170 mm.season^{-1}, occurring along an axis orientated from northwest to southeast; similar to the climatological location of the SIOCZ (Figure 6.6). In LM models, by contrast, there is little change in rainfall across much of subtropical southern Africa, with only small decreases in rainfall over Angola and Zambia (<40 mm.season^{-1}). As we noted in the introduction, the difference between these projections would require substantially different approaches to climate change adaptation. Interestingly, models which project high magnitude drying over southern Africa also do so over South America and parts of northwest Australia. This could indicate the

presence of a common mechanism responsible for drying across southern hemisphere land regions during the early summer.

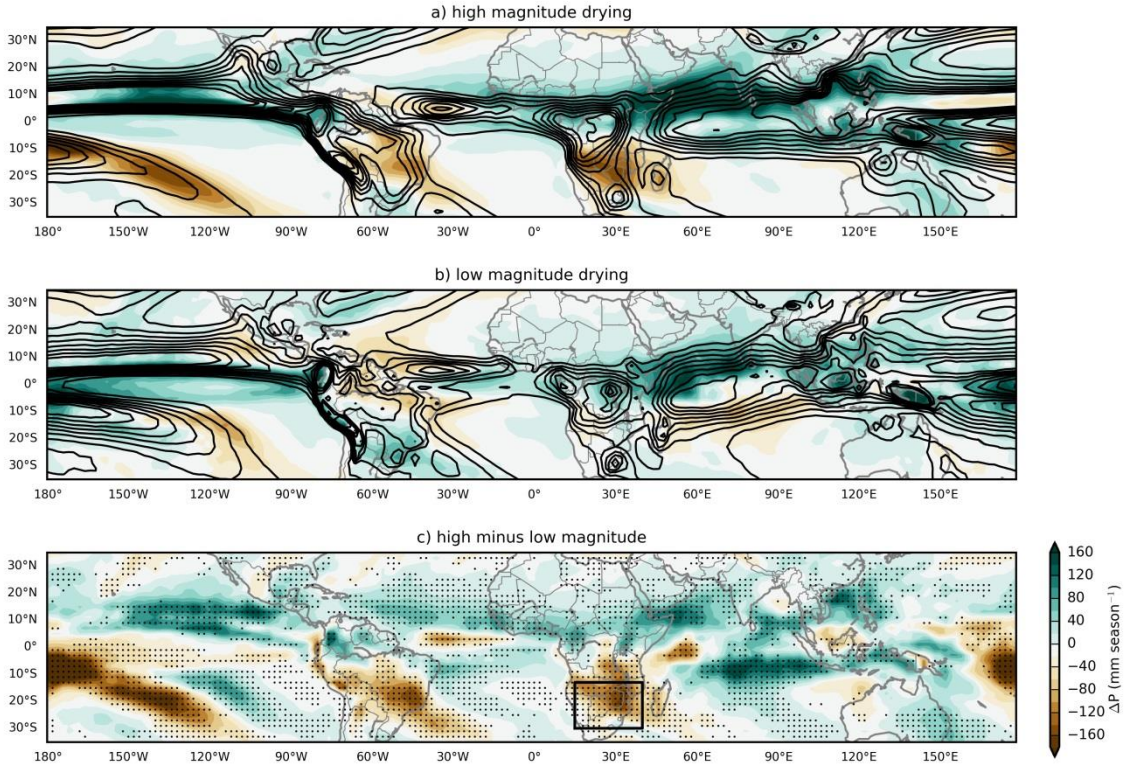


Figure 6.6 Future tropical rainfall change in mm.season^{-1} (shading) averaged over the set of a) HM models, b) LM models and c) the difference in future rainfall change between HM and LM models. Black contours in a) and b) show the present day rainfall climatology in HM and LM models respectively, contours start at 180 mm.season^{-1} and the contour interval is 90 mm.season^{-1}. The stippling in c) is a metric of model agreement, a stipple indicates that all models in the→ HM composite simulate lower or higher magnitude changes relative to all models in the LM composite (e.g. over southern Africa, all models in HM composite project greater drying than those in LM composite).

In both sets of models, the rainfall decline over southern Africa is accompanied by large increases in rainfall in other parts of the tropics, especially to the north of the equator. In the Indian Ocean the largest increases in rainfall in both sets of models (120-160 mm.season^{-1}) occurs to the northwest of the climatological maximum precipitation. In

the Atlantic Ocean, there is an eastward shift in location of convection towards the Gulf of Guinea (Bakassi Peninsula), while in the Pacific Ocean there are broad increases in rainfall which maximise in the northern tropics, especially in the HM models.

The difference in rainfall projections between HM and LM models shows evidence of a north-south tropical contrast (Figure 6.6, *bottom*). HM models simulate greater increases in precipitation over large parts of the northern tropics compared to LM models while generally projecting greater declines in subtropical regions of the southern hemisphere. South of the equator in the Pacific Ocean, for example, HM models project future decreases in precipitation in areas of high climatological rainfall, whereas LM models project modest increases in precipitation. The consistency of response between models (indicated by the stipples in Figure 6.6) within HM and LM groups in areas remote from southern Africa provides some indication that rainfall declines over southern Africa are primarily a consequence of the large scale adjustment of the tropical atmosphere to warming.

The areas where rainfall increases most strongly in the northern tropics are generally displaced relative to the areas of maximum climatological rainfall. This implies a role for the pattern of future SST warming, which is what we investigate next.

6.5.2 Changes in tropical SSTs and southern African rainfall

Figure 6.7 shows SST warming relative to the mean tropical SST warming for OND in HM and LM models. In both model sets, the northern tropics warm more than the tropical mean while the southern tropics warm less. This is consistent with observations and historical model simulations of global annual temperature change which show a

faster rate of warming in the northern compared to southern hemisphere (Friedman et al. 2013), perhaps due to the greater land fraction in the northern hemisphere (Stouffer et al. 1989) and the cooling of the Southern Ocean by vertical mixing (Manabe et al. 1991; Xie et al. 2010).

Of particular interest here is the difference between the SST warming pattern in the HM and LM models (Figure 6.7, *bottom*). Models projecting the highest magnitude drying over southern Africa also simulate stronger relative warming of the northern tropics compared to the tropical mean warming. This is true across almost all longitudes in the tropical band from 10-25°N, with particularly high agreement between models in the northern tropical Pacific and Atlantic basins. This raises the possibility that model variability in the differential warming of the northern tropics, and associated adjustment of tropical convection (Figure 6.6), could explain the intermodel diversity in rainfall response over southern Africa.

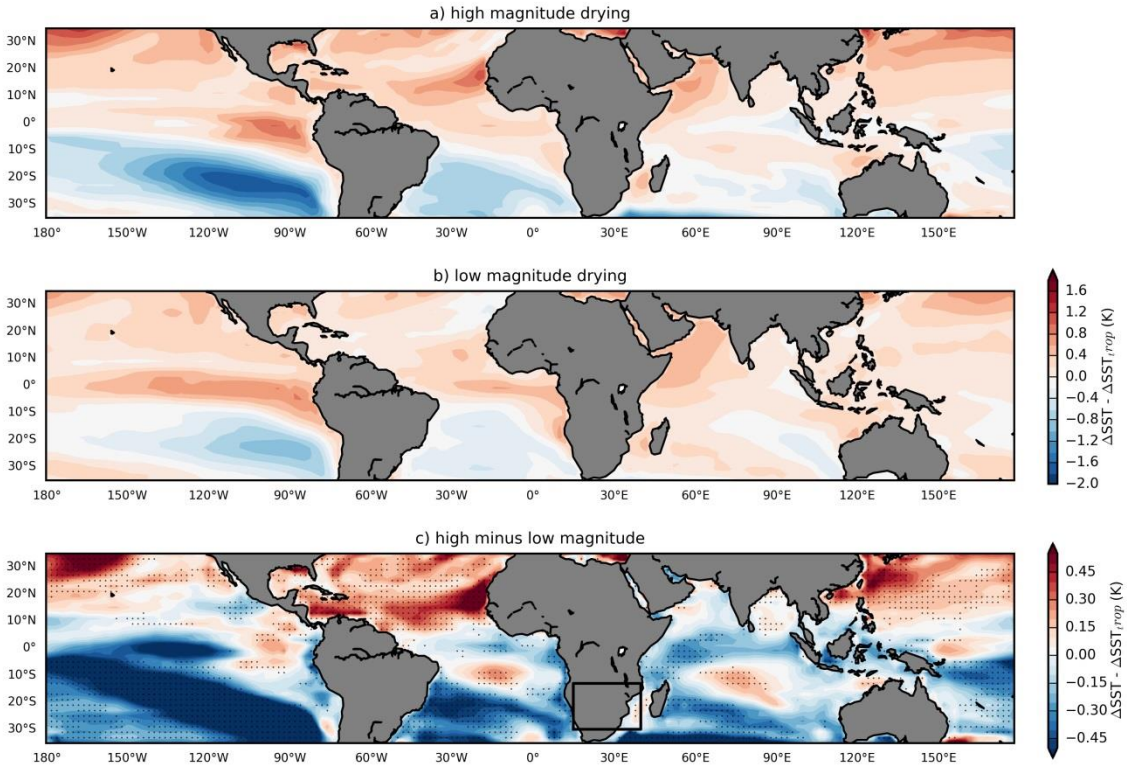


Figure 6.7 Future SST change (K) at each grid point minus the tropical mean (180°W-180°E; 20°N-20°S) SST warming averaged over the set of a) HM models, b) LM models and c) the difference in relative future SST change between HM and LM models. Stipples are applied in same way as in Figure 6.6.

In support of this hypothesis, we find a negative correlation between the relative warming of the northern tropics and rainfall change over southern Africa amongst models ($r=-0.57$, $p<0.001$) (Figure 6.8a). Models simulating greater relative warming of the northern tropics tend to project larger precipitation declines over southern Africa. This relationship is further strengthened if the FIO-ESM model (marked with an x) is not included in the analysis ($r=-0.63$, $p<0.001$). In this model the northern tropics warm at a much slower rate than the tropical mean (~0.4K), which is inconsistent with present day observational trends (Friedman et al. 2013).

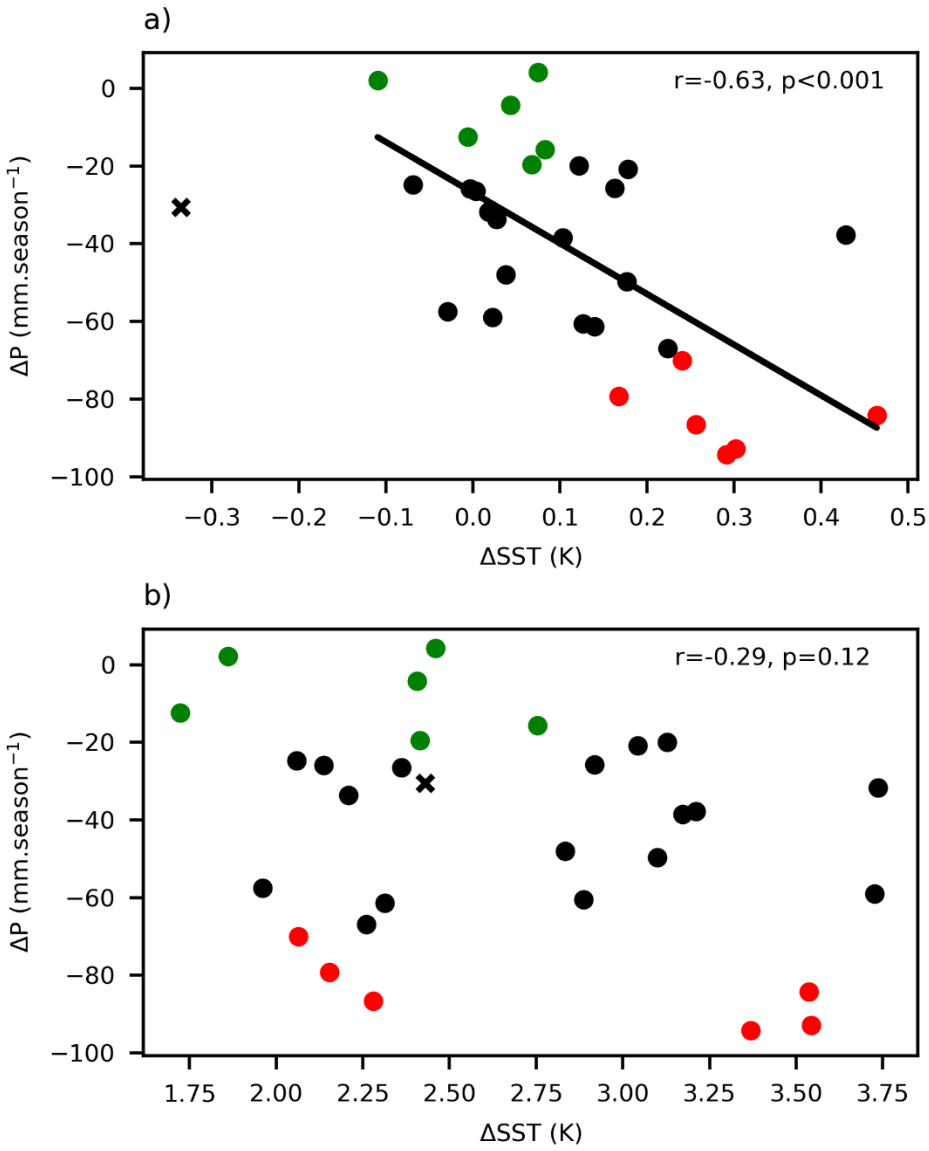


Figure 6.8 The intermodel relationship between a) warming of northern tropical SSTs (10-25°N;180°W-180°E) minus tropical mean warming (20°N-20°S; 180°W-180°E) in K and rainfall change (mm.season^{-1}) over southern Africa (15-40°E; 15-30°S) and b) tropical mean warming (20°N-20°S; 180°W-180°E) and rainfall change over southern Africa. Blue (red) dots indicate models which are part of the LM (HM) composites. The cross marks the outlying FIO-ESM model, note that the linear regression in a) (green line) excludes this model.

By definition, the rate of relative SST warming of the northern tropics depends partially on the tropical mean SST warming. To ensure that the relationship in Figure 6.8a is tied to the pattern of warming and not just the average change, we also examine the relationship between tropical mean SST change and rainfall change. We find no relationship between the mean oceanic warming and rainfall change. This is evidence

that the pattern of SST change is particularly important for explaining the diversity in CMIP5 rainfall projections over southern Africa. It is not, however, evidence that the mean oceanic warming is unimportant for rainfall change in individual models.

Since the models projecting strong drying in southern Africa are the same set of models which project the strongest drying over South America (Figure 6.6), we also examine the relationship between tropical SST warming and rainfall change over South America (60°-40°W,25°-10°S) in Figure 6.9. We find the same result. With FIO-ESM excluded, there is a strong and significant correlation between the differential warming of the northern tropics and rainfall change over South America ($r=-0.59$, $p<0.001$), and no relationship between mean tropical warming and rainfall change. This suggests that understanding the drivers of the differential warming of the northern tropics is important for understanding the model diversity in early summer rainfall decline across the southern hemisphere.

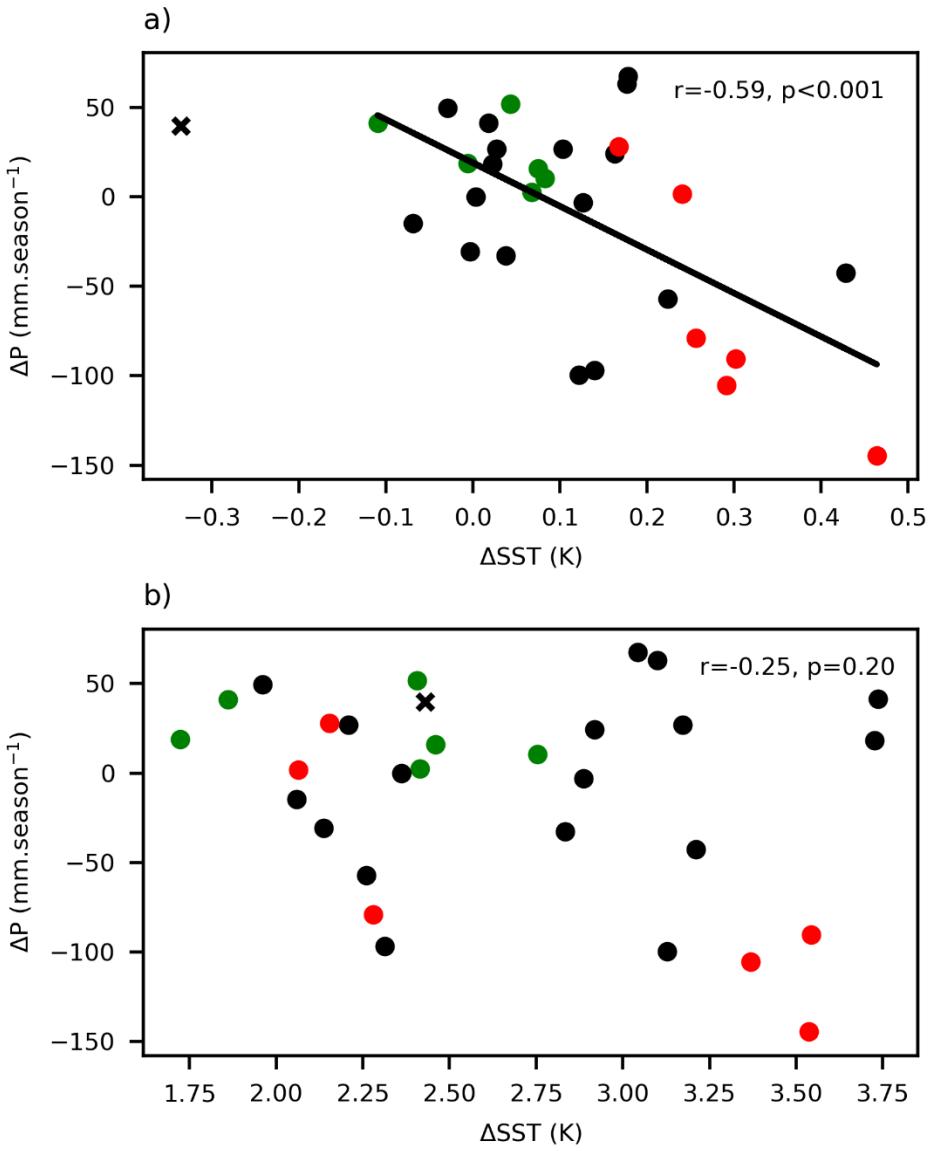


Figure 6.9 As in Figure 6.8, but for future rainfall change (mm.season^{-1}) in South America (60-40°W; 10-25°S).

6.6 Potential connections with present day rainfall biases

Our main aim in this paper is to consider the processes associated with the diversity in precipitation projections. Prior to summarising and discussing our results, it is useful to briefly consider these processes in the light of present day biases, especially given the differences in the present day structure of vertical velocity in HM and LM models (Figure 6.3).

Figure 6.10 shows the current day precipitation bias in HM and LM models compared to the CMAP satellite/rain gauge product. While both sets of models tend to overestimate precipitation over southern Africa, the bias is much more severe in HM models, reaching up to 300 mm.season^{-1} in areas of Angola and eastern South Africa. In the LM models the precipitation bias is much weaker over most of southern Africa (<100 mm.season^{-1}). The difference in severity of bias over southern Africa is made clear in the composite anomaly of the rainfall bias between HM and LM models (Figure 6.10c). Interestingly, HM models also tend to simulate too little rainfall over northern Madagascar. This dipole bias is also a feature of many models in the main rainy season (January-March; JFM), and is related to poor representation of topography and moisture circulation (Munday and Washington 2018). The large future rainfall declines in HM models relative to LM models results in a future rainfall climatology across models which converges towards the present day observed climatology. The average HM bias is 143 mm.season^{-1} and reduces by 170% over nine decades to 58.5 mm.season^{-1}, while there is only an 8% reduction in the average LM model bias from 64.1 mm.season^{-1} to 56.6 mm.season^{-1}. Only eight models simulate a future rainfall climatology which, in an absolute sense, is drier than the observed present day climatology.

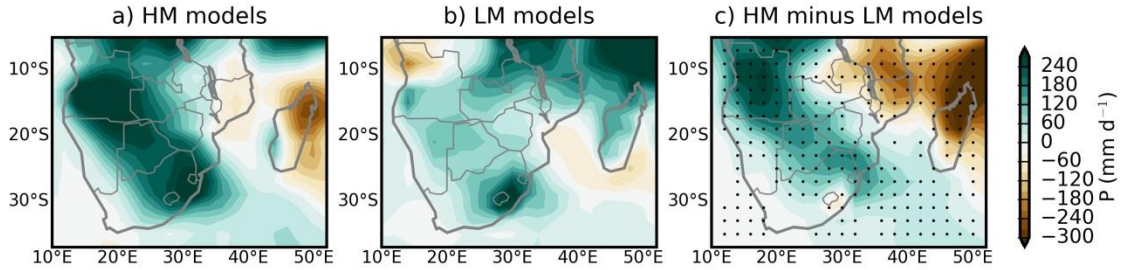


Figure 6.10 Climatological (1979-2005) precipitation bias (mm.season^{-1}) relative to the CMAP dataset averaged across a) HM models, b) LM models and c) their difference. The stipples in c) indicate where all HM models are either wetter or drier compared to LM models (e.g. the green areas with stipples show that all HM models are wetter than all LM models in the present day)

Given that HM models simulate larger present day biases in rainfall compared to LM models, it is worth investigating whether the highest magnitude declines in rainfall over southern Africa are *only* found in models with a large present day bias. If true, this is basis for questioning the credibility of models projecting high magnitude change. To do this we alter our sampling base and consider the difference in rainfall projections between the third of models with highest present day bias over southern Africa (n=10) and third of models (n=10) with lowest present day bias relative to CMAP. While both sets include models which project low magnitude drying, seven of the ten high bias models simulate OND rainfall declines of more than ~50 mm.season^{-1}, whereas only one model in the low bias set projects a 50 mm.season^{-1} or greater rainfall decrease (IPSL-CM-5A-MR; -59.0 mm.season^{-1})(Table 6.1). The models projecting the highest magnitude drying, MIROC-ESM and MIROC-ESM-CHEM, are not included in the high bias set of models, but it is worth noting that they also overestimate rainfall by 40-45%. These findings suggest that we should treat projections of high magnitude early summer drying with caution.

The spectrum of model rainfall projections is connected to simulated changes in the pattern of tropical SST (Figure 6.8), which are superimposed on the present day climatology. It is useful, therefore, to consider whether there are differences in the present day biases in tropical SSTs between HM and LM models (Figure 6.11). Compared to ERSSTv5, HM models simulate a cold bias in the present day climatology across much of the tropics; apart from in upwelling regions on the western coasts of South America and Southern Africa. In LM models there are also very severe biases throughout the tropics. In addition to warm biases in the upwelling regions, LM models also simulate a warm bias across the subtropical oceans, particularly in the Atlantic and Indian Oceans. Given the large biases present in both model sets there is no clear case to be made in linking present day SST biases with the rainfall projections, at least based on this initial analysis.

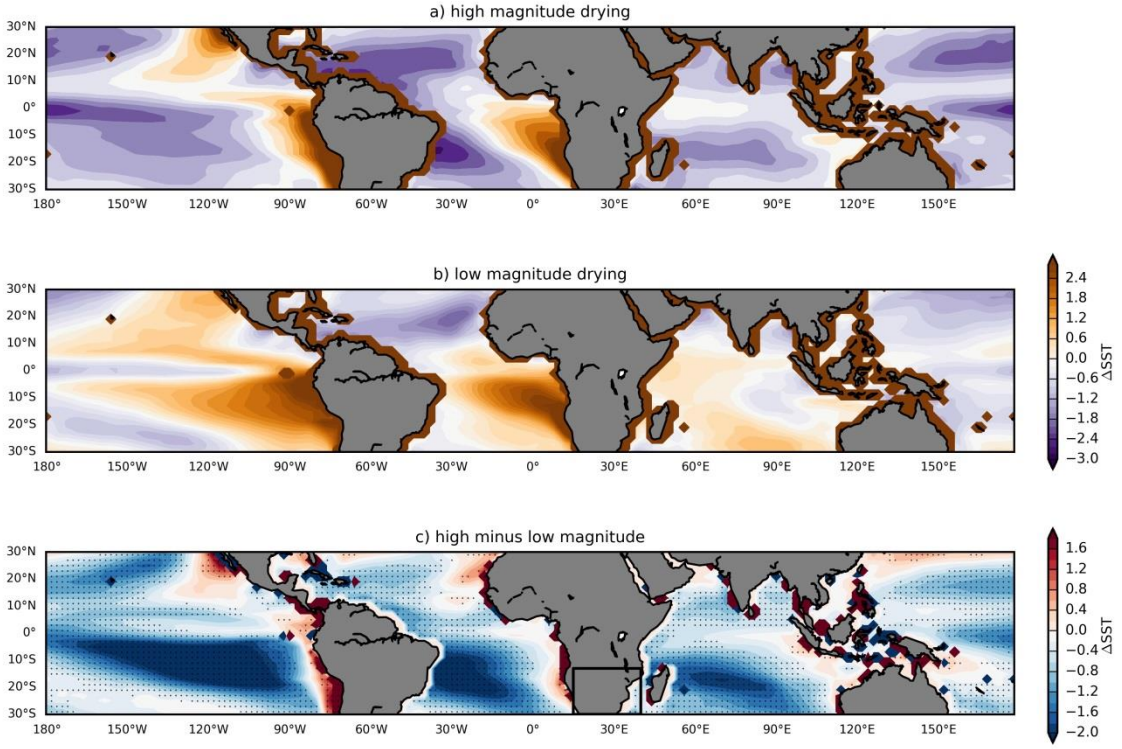


Figure 6.11 As in Figure 6.10, but for climatological (1979-2005) SST biases (K) relative to ERSSTv5

6.7 Discussion and Conclusions

6.7.1 Summary and Discussion

Climate models consistently project rainfall declines in the early summer season (OND) over southern Africa, but there is an order of magnitude difference in the scale of the decline between models. In this paper we investigate the physical processes underlying differences in the projections of rainfall decline among 30 CMIP5 models.

In all models there is an increase in stability over southern Africa by the end of the 21st century. The increase in stability is associated with enhanced upper level subsidence, and occurs in spite of increases in low-level moisture flux supply and convergence which are especially pronounced in models projecting the highest magnitude drying. The future increase in stability and in moisture flux convergence are linked with amplified surface temperatures over southern Africa relative to the tropical mean, and a strengthened thermal low. These finding are consistent with previous work on the early summer drying signal (Seth et al. 2013; Cook and Vizy 2013; Lazenby et al. 2018). Seth et al., (2013) found that the rainfall decline in the multi-model mean of CMIP5 models is associated with enhanced MSE at upper levels in the atmosphere, and reduced evaporation. Meanwhile, Cook and Vizy (2013) found that a strengthened and enlarged Angola heat low was associated with rainfall decline in a regional model driven by an ensemble mean of CMIP3 models into the mid-21st century.

Differences in the strength of top-down stabilisation account for the key differences between models simulating high and low magnitude drying. We link future changes in rainfall with local surface temperature change, since increased subsidence is linked to clearer skies and higher net solar radiation. Models projecting larger precipitation declines simulate greater surface temperature amplification over southern Africa (relative to the tropical mean). The greater surface temperature amplification in models projecting drying may also arise in part from projections of decreasing evaporation and enhanced water vapour supply. In high magnitude drying models the ratio of sensible to latent heat fluxes increases strongly, as does the water vapour supply, which could contribute to the temperature enhancement through a direct radiative effect. The coupling between future projections of precipitation and temperature has also been noted for other semi-arid regions, including the Sahel (Giannini 2010) and northern Australia (Brown et al. 2016), and indicates that uncertainties in the two variables should be considered together.

We find that the magnitude of the rainfall decline among models is also linked with changing patterns of tropical sea-surface temperatures. There is a strong negative correlation between precipitation change over southern Africa and the relative warming of northern tropical SSTs compared to the tropical mean oceanic warming. Models projecting high magnitude drying tend to project much stronger warming of the northern tropics relative to the tropical mean, whereas model projecting low magnitude drying simulate more spatially uniform SST warming across the tropics. The role of the pattern of SST changes indicates that dynamical mechanisms of change are important for explaining the uncertainty in future projections of rainfall, a claim consistent with studies investigating rainfall change at a tropics-wide scale (e.g. Chadwick et al. 2013;

Kent et al. 2015; Huang et al. 2013). Over southern Africa, our findings support Lazenby et al.'s (2018) hypothesis that uncertainty in CMIP5 rainfall projections during the early summer is linked with changes in the north-south SST gradient in the Indian Ocean.

Our results show that there is a strong coherence between models in the rainfall change over southern Africa and the rest of the tropics (Figure 6.6). Models projecting high magnitude changes over southern Africa also project consistent declines over South America and the southern tropical Pacific, while projecting consistent increases in rainfall north of the equator in the Sahel, Indian Ocean, Atlantic Ocean and Pacific Ocean. For the CMIP3 ensemble, Chou et al. (2007) and Biasutti and Sobel (2009) suggest that this pattern of rainfall change is due to a delay in the global seasonal cycle of SSTs under warming. Examining the plausibility of the delay in seasonal cycle in SSTs, as well as how it relates to rainfall over specific regions should be a focus of future work.

The projections of future rainfall decline could be affected by large present day biases in precipitation over southern Africa (Figures 6.1, 6.10, & Table 5.1). The precipitation biases are especially pronounced in the models which project high magnitude drying over southern Africa (and South America) relative to those projecting low magnitude drying. The overestimation of precipitation in CMIP5 models in southern Africa is related to the simulation of the Angola Low (Munday and Washington 2017), the position and orientation of the SIOCZ (Lazenby et al. 2016) and to the representation of the complex southern African topography (Munday and Washington 2018). These key

errors in model circulation and topography suggest that we should treat the future drying signal with caution, especially in the case of models projecting high magnitude drying over southern Africa. This claim is supported by observational evidence, which indicates that there is no clear early summer drying trend in the last 30 years over southern Africa (Maidment et al. 2015).

6.7.2 Conclusion

Large ensemble mean rainfall reductions in early summer are driven primarily by the response of more extreme members of the CMIP5 ensemble, a third of model project modest declines of less than 30 mm across the whole October-December season. This paper provides an insight into the controls on the intermodel diversity in early summer rainfall declines. We find that members of the ensemble projecting high magnitude rainfall decreases simulate large increases in tropospheric stability associated with strong relative warming of the northern tropics compared to the tropical mean. The rainfall declines across models occur in the context of systematic rainfall biases in the present day climatology, and the models projecting the highest magnitude rainfall declines also tend to be those with the largest positive present day rainfall biases. The results, therefore, emphasise the need to evaluate the connections between present day model simulations and future rainfall projections in more detail. For the moment, this paper suggests that extreme future early summer drying in southern Africa is an unlikely scenario.

Acknowledgements

The first author is funded through a Met Office CASE studentship (ACR00400) and through the doctoral training partnership of the UK Natural Environmental Research Council (NERC) (NE/L002612/1). Richard Washington is supported by the NERC and Department for International Development (DfID) funded Future Climate for Africa (FCFA) UMFULA (NE/M020207/1) and IMPALA (NE/M017206) African climate programs. We source the climate model data from the Earth System Grid Federation (ESGF) (https://pcmdi.llnl.gov/). CMAP and ERSSTv5 data are downloaded from NOAA/OAR/ESRL PSD, Boulder, Colorado, USA at http://www.esrl.noaa.gov/psd/

7. Conclusions

7.1 Introduction

Climate models are the only tools we have to investigate how regional rainfall may change in response to global warming. While much work has considered what climate models project in the future, relatively little work has considered whether those projections are trustworthy. This is necessary, especially since climate models can contain systematic and severe biases in their representation of the climate system in the present day. This thesis investigates the reliability of climate models in southern Africa. Southern Africa is a region of considerable climatological complexity, which provides a good test bed for the climate models used to project rainfall change on a global scale. Moreover, the regional population is thought to be highly vulnerable to potential changes in the hydrological balance owing to manifold societal and physical stressors. Assessing the likelihood of projections of rainfall change with different magnitudes and signs is therefore important.

The primary aim of the thesis is to understand the reasons for differences in the simulation of rainfall over southern Africa among the latest generation of state-of-the-art climate models (the CMIP5 ensemble). This aim is achieved through investigating the physical processes which give rise to the differences between models, and which also may help to explain the differences between model simulations and observations. This approach is based on the premise that a better understanding of the physical processes which underlie model simulations can provide a more meaningful assessment of model reliability as compared to a judgement based on comparison with observations alone. Moreover, a physical understanding of model simulations could guide essential areas for

model improvement and lend insights into the functioning of the southern African climate system in reality.

This concluding chapter draws together the evidence in support of these arguments, structured by the aims in outlined in Section 1.2 and with reference to analysis of present day model simulations (Chapters 4 and 5) and analysis of future rainfall change (Chapter 6) over southern Africa. The final section (7.8) discusses the future prospects for climate modelling and climate model evaluation in southern Africa.

7.2 The climate processes underlying the simulation of present day rainfall over southern Africa

The CMIP5 models simulate a large range of rainfall climatologies over southern Africa. Overall, the ensemble tends to overestimate summer rainfall over southern Africa, in some cases by a factor of three, but underestimate rainfall over Madagascar and the southwest Indian Ocean. The overestimation of rainfall over southern Africa is a persistent problem among many different model types including atmosphere-only and coupled models, as well as some regional climate model versions. In recognition of this issue, the first aim of the thesis is **to understand the climate processes associated with the intermodel spread in rainfall in the present day.** Chapter 4 and 5 provide a key insight into the controls on model rainfall simulation by examining the links between model rainfall and their simulation of the Angola Low, moisture circulation and topography. The results from these chapters are discussed in this section.

7.2.1. The role of the Angola Low

The Angola Low is a low-pressure system situated over south-east Angola, northern Namibia, northern Botswana and eastern Zambia. At 850 hPa, it is the nadir in African geopotential height during the austral summer, and, together with the subtropical highs in the southern Indian and Atlantic Oceans, is a key player in the moisture circulation patterns over southern Africa. In Chapter 4, intermodel differences in the simulation of the Angola Low are hypothesised to be important in distinguishing between model simulations of rainfall over southern Africa.

In support of this hypothesis, Chapter 4 demonstrates that models which simulate the strongest Angola Lows tend to simulate the most rainfall over southern Africa. The simulated Angola Low explains 45-60% of the intermodel variability in rainfall across a large southern African region extending from the tropics (10°S) to the subtropics (35°S), and from the western coast (10°E), to the eastern coast of Madagascar (55°E). Models which simulate the strongest Angola Lows tend to also simulate increased low level moisture convergence in tropical, central regions of southern Africa. This is associated with a strengthened northeasterly moisture transport emanating from the southern Indian Ocean, and an enhanced northwesterly moisture transport originating the Congo Basin convective region. Compared to models with weak Angola Lows, rate of northerly moisture transport is increased by 20-50 g kg^{-1} m s^{-1}. The anomalous northerly transport pathways tend to increase moisture convergence and reduce moisture divergence along the eastern coast of southern Africa and into the Mozambican channel. Here too, models

with a stronger Angola Low simulate more rainfall compared with those models simulating weak Angola Lows.

Models with relatively weak Angola Lows and drier rainfall climatologies are in better agreement with the Angola Low as estimated by three different reanalysis datasets. This could suggest that those models are the most realistic in the ensemble. However, the reanalysis data is not well constrained by observations over Angola, and strength of the Angola Low, as measured by 850 hPa geopotential height, varies by 20m between reanalysis estimates. Therefore, while the evidence presented indicates that improving model simulations of the Angola Low will help to reduce the intermodel spread in rainfall, the lack of observations leaves us uncertain as to how the Angola Low manifests in reality.

The importance of the Angola Low in distinguishing between model estimates of rainfall is consistent with earlier studies which investigate rainfall biases in global (Lazenby et al. 2016) and regional (Kalognomou et al. 2013) models. In these studies, the authors note that models tend to simulate excessive moisture circulation in the vicinity of the Angola Low. Chapter 4 presents the first direct evidence which explicitly links the rainfall biases with the excessive moisture circulation, and with the strength of the low pressure system.

7.2.2 Moisture circulation and topography

While the model simulation of the Angola Low is effective in explaining the intermodel diversity over tropical and eastern areas of southern Africa, it does not explain why models overestimate rainfall in subtropical southern Africa (by a factor of three), and underestimate rainfall over Madagascar and the Southwest Indian Ocean. This dipole bias has been present in a number of different climate model versions since the early 1990s, and deserves explanation. In Chapter 5, this bias is investigated with reference to the model representation of the regional pattern of low-level moisture circulation, and how it is modified by the complex southern African topography.

The dipole rainfall bias is associated with large errors in the simulation of zonal overturning circulations in subtropical southern Africa, with a majority of CMIP5 models failing to reproduce key qualitative features of the vertical atmospheric structure. In reanalysis data, two overturning cells are present, one shallow associated with the continental heat low, and one deep associated with convection over Madagascar. In ~60% of models the shallow convection and overlying subsidence associated with the thermal low and mid-level high is replaced by deep convection with typical rates of uplift in the order of 5-8 10^{-2}Pa s^{-1} at 400 hPa. Meanwhile, the deep convection over Madagascar is not reproduced at all, with subsidence throughout the atmospheric column in more than half of models.

The deep convection bias over the subcontinent is associated with a pattern of low-level moisture circulation which is not seen in reanalysis data. The wettest models in the

ensemble simulate an anomalous climatological northeasterly moisture transport (10-30 g kg^{-1} ms^{-1}), which penetrates across the complex topography of Tanzania and Malawi and into the Kalahari Basin. In the observed climatology, this northeasterly moisture transport recurves to the southeast upwind of southern Africa, and becomes the northwesterly transport towards the convective centre over Madagascar. Chapter 5 (Section 5.4.3) diagnoses this northeasterly moisture transport bias by investigating the degree to which the northeasterly flow is blocked by the Tanzanian Escarpment, using the nondimensional Froude number. The Froude number takes into account the balance of inertial forces (wind speed) to gravitational forces (height of topographic barrier and the static stability). Models simulating the largest wet bias over southern African tend to underestimate the amount of low-level blocking (high Froude number), and there is a strong correlation between the Froude number and precipitation ($r=0.85$, $p<0.001$). Since the northeasterly moisture transport occurs in preference to the southeasterly recurvature toward Madagascar, the models with a strong wet bias over the subcontinent also simulate less rainfall over Madagascar and the Southwest Indian Ocean.

The excessive northeasterly moisture transport in GCMs has been noted before (e.g. Moufouma-Okia and Jones 2014; Lazenby et al. 2016), but Chapter 5 provides the first evidence that the north-easterly moisture transport bias is linked to the representation of topography upstream of the southern African domain. Moreover, the strong intermodel relationship between the northeasterly moisture transport and rainfall over both southern Africa and the Southwest Indian Ocean (Figure 5.7) suggests that it is the key to explaining the dipole rainfall bias.

7.2.3 Implications of present day process biases for model reliability

Based on our findings in Chapters 4 and 5, Figure 7.1 shows schematically the circulation in a typical wet CMIP5 model compared to a typical dry model or reanalysis data. The crucial point here is that there exist significant qualitative (as well as quantitative) differences in the mean summer circulation of a wet CMIP5 model as compared to the reanalyses data (Figure 7.1), whereas dry models are generally in better agreement with the observed circulation. In wet models, the northeasterly moisture transport penetrates across a smoother and less complex Tanzanian escarpment, the northwesterly moisture transport to Madagascar is barely reproduced, the mid-level Botswana High is weakened and is shifted away from the subcontinent, the Kalahari Heat Low is either weak or not simulated at all, and the strengthened Angola Low leads to anomalous penetration of the northwesterly moisture transport from the Congo Basin. These circulation characteristics are associated with the overestimation of rainfall over much of southern Africa and the underestimation of rainfall in the southwest Indian Ocean.

The implications of these findings for the adequacy of the CMIP5 ensemble for projecting future change are troublesome. The future climate change experiments impose progressive emissions forcing through the 21st Century on to the simulated present day state. Over southern Africa this present day state is not realistic in a number of CMIP5 models. Therefore, if we are to trust envelope of uncertainty implied by the range of future projections from these models, we must make the assumption that the response to future forcing is not dependent on the present day climatology. This is a

considerable assumption to make given the evident process biases, and is one that is tested in Chapter 6.

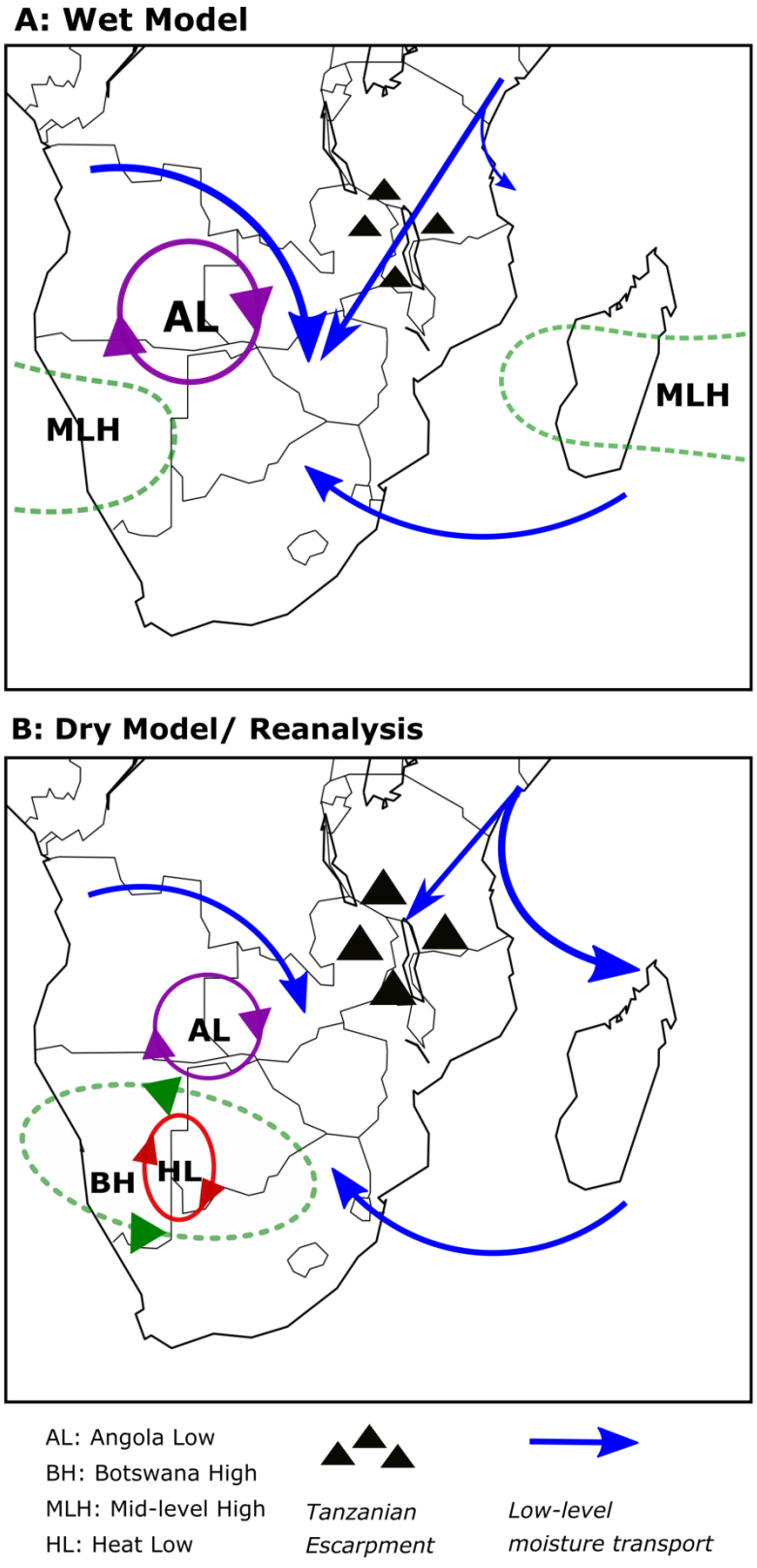


Figure 7.1 Schematic of austral summer circulation in wet models (top) and dry models/reanalysis (bottom)

7. 3 Mechanisms of rainfall future change in CMIP5

The second aim of the thesis is **to assess the mechanism of future rainfall change in the CMIP5 ensemble**. The results from Chapter 6 provide evidence of the mechanism of change in CMIP5 models, and are discussed in this section.

A few studies have considered the mechanisms of future rainfall change over southern Africa, in the ensemble mean CMIP5 model (Seth et al. 2013; Lazenby et al. 2018), in selected CMIP3 models (Shongwe et al. 2009) and in other models (Engelbrecht et al. 2009, 2013; Cook and Vizy 2013). These studies find that future rainfall declines in austral summer are associated with strengthened mid-level high pressure systems (Engelbrecht et al. 2009), increased moist stability (Seth et al. 2013), a stronger thermal low and a northeastward shift in the main summer rain band (Cook and Vizy 2013; Lazenby et al. 2018).

By the end of the century (2070-2100) under high emissions forcing (RCP8.5), CMIP5 models tend to agree that rainfall will decline in the early austral summer (OND), with an average rainfall decrease of 42 $mm.season^{-1}$. The rainfall reductions are associated with increases in moist stability due to large increases in dry static energy (DSE) of 7-10 $kJ.kg^{-1}$ at upper levels in the atmosphere. This is in accordance with results based on the ensemble mean CMIP5 and CMIP3 models (Seth et al. 2011, 2013). Increases in DSE at upper levels are a signature of oceanic warming and are associated with anomalous upper level subsidence over southern Africa (0.2 to 2 $10^{-2}Pa.s^{-1}$) across all CMIP5 models. The future increase in stability occurs in spite of increases in convergent low-

level moisture fluxes (2-5 10^8.kg $kg^{-1}.s^{-1}$) in the central subcontinent in the models projecting the highest magnitude drying. That rainfall declines in spite of increased moisture supply is strong evidence that the increased stability is being set from the top down rather than through changes to the low-level circulation.

Future increases in stability and moisture flux convergence are linked with amplified surface temperatures over southern Africa relative to the tropical mean, and to a strengthened Angola Heat Low. The reduction in precipitation also is strongly linked with decreasing evaporation across the subcontinent ($r=0.85$, $p<0.01$), which could in turn contribute to the amplified temperature change by increasing the ratio of sensible to latent heat fluxes (the Bowen ratio). The results, therefore, expand on the mechanism of change outlined in previous work on the CMIP5 ensemble (Lazenby et al. 2018; Seth et al. 2013), and demonstrate a link between the future projections of rainfall and of local temperature change.

7.4 Controls on intermodel diversity in rainfall projections

While there is agreement across over 90% of models that rainfall will decline in response to future emissions forcing, the magnitude of rainfall reductions in OND ranges from less than 10 mm.$season^{-1}$ to nearly 100 mm.$season^{-1}$ (Figure 6.1). Such large differences in rainfall projections imply substantially different approaches to climate change adaptation. The third aim of the thesis is therefore **to understand the controls on the diversity of future rainfall projections.** This section presents findings

from Chapter 6 which advance our understanding of the intermodel spread in rainfall projections.

Differences in the operation of the mechanism of rainfall change, summarised in Section 7.3, accounts for the intermodel spread in rainfall projection. Models projecting the largest future rainfall declines simulate the largest increases in upper level subsidence over southern Africa (+2 10^2Pa.s^{-1}), the greatest amplification of surface temperatures (+2°C relative to tropical mean), the largest increases in strength of the thermal low and greatest reductions in surface evapotranspiration (-12 W.m^{-2}). Additionally, the models projecting the highest magnitude drying simulate the largest increases in water vapour flux into the subcontinent, which, through a direct radiative effect could contribute to the amplified surface temperatures.

There is a strong coherence between the rainfall change among models over southern Africa and the rest of the tropics. Models which project severe drying over southern Africa, which exceeds 170 mm.season^{-1} in parts of Angola and Zambia, also project the largest rainfall declines over South America and parts of northwestern Australia. This is in addition to simulating large increases in rainfall north of the equator in the Sahel, Indian Ocean, Atlantic Ocean and Pacific Ocean. This raises the hypothesis that the intermodel spread in the rainfall change over southern Africa is associated with the large scale adjustment of the tropical atmosphere to warming.

This hypothesis is tested by examining the pattern of SST change in models projecting strong drying versus those projecting low magnitude drying. Models projecting strong

drying both over southern Africa and South America tend to simulate the greatest relative warming of the northern tropics (0.3-0.5K greater than the tropical mean warming), whereas those models projecting the weakest rainfall declines simulate a more spatially uniform SST increase in the tropics. The high correlation between model projections of rainfall decline over Southern Africa (and South America) and the amplified future warming of northern tropical SSTs is highly unlikely ($p<0.001$) if the changes were not linked.

The pattern of future SST change, whereby the northern tropics warm at a faster rate than the tropical mean, has previously been linked with a delay in the global seasonal cycle of SSTs (Chou et al. 2007; Biasutti and Sobel 2009), and is associated with precipitation declines in the early boreal summer in the Sahel (Biasutti and Sobel 2009; Park et al. 2015). Chapter 6 demonstrates that a similar control on model rainfall projection diversity might be important in both Southern Africa and South America in the early austral summer. This is consistent with Lazenby et al. (2018) who link the uncertainty in future rainfall decline in southern Africa with intermodel variability in alterations to the meridional SST gradient in the Indian Ocean.

7.5 Links between present day model simulations and their future rainfall change

Chapters 4 and 5 demonstrate key errors in the model circulation as they relate to the simulated rainfall climatology. An important question, therefore, is whether model biases in the present day are linked to their simulation of future change. This is the

fourth aim of the thesis: **to evaluate whether models' simulation of the present day climate system influences their projections of rainfall change**. In this section we discuss evidence from Chapter 6 that suggests that model biases in the present day are important for the rainfall projections.

Chapter 6 finds that the models which project the largest 21st century decreases in rainfall (of over 60 mm.season^{-1}) are those which simulate the largest positive rainfall biases compared to observations in the present day (of over 40% relative to satellite/rain-gauge estimates; Table 6.1, Figure 7.2). These models also simulate the largest present day positive biases in evaporation and in upper-level uplift. Recalling the results from the analysis of the present day model simulations (Figure 7.1); the models with large future declines in rainfall are also those with very strong Angola Lows as compared to reanalysis data (Chapter 4), with poor representation of low-level moisture circulation patterns (Chapters 4 and 5) and with the coarsest representation of topography over southern Africa (Chapter 5). These include models from the MIROC group (MIROC-ESM, MIROC-ESM-CHEM, MIROC5), from the GFDL group (GFDL-ESM-2G, GFDL-ESM-2M, GFDL-CM3) and from the Norwegian Climate Centre (NorESM1-M, NorESM1-ME). Together, therefore, the thesis provides evidence that projections of severe future declines in austral summer rainfall are unlikely.

In the early summer, the model rainfall climatologies converge towards the observed present day climatology by the end of the 21st Century (Figure 7.2). Only a quarter of models simulate, in an absolute sense, a rainfall climatology which is drier in the future than is observed in the present day. While this indicates that the change to the rainfall

climatology may be modest, there are no projections of significant future increases in rainfall. The lack of rainfall increase is in contrast to generally high confidence in the increase of regional temperatures at a faster rate than the global mean, underpinned by analysis of contemporary temperature trends (Engelbrecht et al. 2015). This could result in conditions of exacerbated water stress over southern Africa even without significant rainfall declines, and should be considered in the interpretation of these results in a policy context.

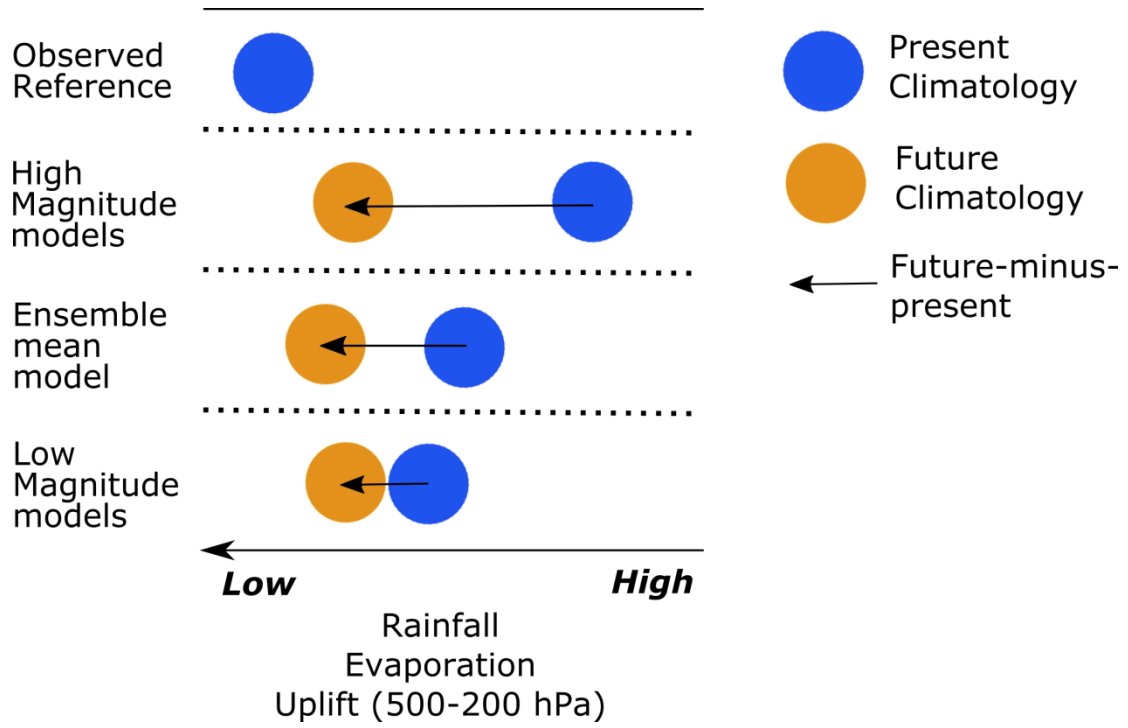


Figure 7.2 Schematic of the present day and future climatologies of OND rainfall, evaporation and upper-level uplift. Models are grouped according to the magnitude of future change (black arrows).

7.6 Targets for model improvement

Given the links between the present day biases and the future rainfall projections, especially in models with a high present day bias, it seems that model improvement is necessary ahead of achieving a defensible estimate for the uncertainty in the future rainfall projections from GCMs. The fifth aim of the thesis is therefore **to identify specific processes or features which, if improved, could enhance the simulation of southern African rainfall**. Based on the analysis of present day simulations, summarised in Figure 7.1, three key areas for model improvement emerge: model representation of the Angola Low; of topography; and of the northeasterly moisture transport. This section discusses these features in turn.

7.6.1 The Angola Low

The Angola Low is the dominant circulation feature of the southern African summer. Chapter 4 demonstrates that models vary widely in their estimation of the strength of the Angola Low based on 850 hPa geopotential heights in southern Angola. The variation in strength of the Angola Low explains up to 60% of the intermodel rainfall variability across parts of tropical and eastern southern Africa. This in turn is associated with greater southward export of moisture (30-50 g.kg m.s^{-1}) across southern Africa in models with stronger Angola Lows. Drier models in the ensemble, with rainfall climatologies more similar to the satellite-rain gauge observations, simulate a relatively weaker Angola Low (850 hPa geopotential height of ~1495m), which is more similar in strength to the reanalysis estimates. This is in contrast to models with a large rainfall bias, which simulate very deep Angola Lows (~1470m). Improvements to the

representation of the Angola Low are likely therefore to go hand in hand with improvements to the rainfall climatology. Advances in the simulation Angola Low will rely on a better understanding of its dynamics in climate models and in reanalysis data at timescales finer than the monthly mean. This process has already begun (Section 7.7).

7.6.2 Northeasterly moisture transport

Reanalysis data all simulate a northeasterly moisture feed which recurves to the southeast upstream of southern Africa (Figure 1.2, Figure 7.1). In the models with the largest rainfall biases the northeasterly moisture transport penetrates into southern Africa, with almost no northwesterly transport out toward the Indian Ocean. Chapter 5 shows that part of the reason for the penetration into southern Africa is the anomalously high wind speeds at 850 hPa, of up to 7 $m.s^{-1}$, in the region upstream of southern Africa. These wind speeds are 2-3 $m.s^{-1}$ faster than they are in reanalysis data, and are similar in magnitude to the strength of the austral winter southerly (Findlater) jet. The Findlater jet is responsible for nearly half of the global atmospheric cross-equatorial mass flux (Findlater 1969) in austral winter, and ultimately feeds the Indian Monsoon.

The bias in the cross equatorial mass flux, which manifests over the eastern Indian Ocean, may be related to hemispheric-scale biases in energy fluxes (Hwang and Frierson 2013; Hawcroft et al. 2017). For example, in models experiments which artificially reduce the interhemispheric energy balance, precipitation biases are alleviated both globally and in southern Africa (Hawcroft et al. 2017). It could be the case, therefore,

that addressing the rainfall bias over southern Africa may rely in part on reducing global scale energetic biases in models.

7.6.3 Topography

The simulated downstream northeasterly moisture transport is correlated with the mean topographic height over the Tanzanian Escarpment region across models. Models with lower topography (~1150m) simulate greater downstream northeasterly flow ($r=-0.65, p<0.001$) and enhanced precipitation over southern Africa ($r=-0.59, p<0.01$). This implies that improving the representation of topography in models can reduce the positive southern African rainfall bias. The call to improve topography in GCMs is consistent with a number of studies which report that the rainfall biases present in GCMs worsen in the vicinity of complex and high topography over southern Africa (Mason and Joubert 1997; Engelbrecht et al. 2013; Pinto et al. 2016). Indeed, the move towards using nested regional models in southern Africa, as exemplified by the use of the CORDEX ensemble (Giorgi et al. 2009; Nikulin et al. 2012), is in part a response to the perceived need to adequately represent the complex southern African topography (Kalognomou et al. 2013). This approach has yielded some success, with positive rainfall biases over southern Africa generally reduced among regional models compared to their global counterparts. The extent to which improving the representation of topography within GCMs can improve the precipitation climatology over southern Africa remains to be seen.

7.7 CMIP5 based insights into the southern African climate system

The final aim of the thesis is **to explore how process-based approaches to evaluation can be used to generate hypotheses regarding the operation of the southern African climate system**. In this section, evidence is presented from Chapters 4 to 6 which suggests that, at least in a southern African context, process-based analysis has provided this generative value.

The finding that the Angola Low is strongly related to intermodel rainfall variability raised a number of questions concerning the real southern African climate system. The first question is simply, what is the Angola Low? In the existing literature on the Angola Low, reference is made to the Angola Low as a thermal low and as a tropical low. In Chapter 4, this confusion is addressed by investigating the basic mean state of the Angola Low through the seasonal cycle. In the early austral summer, the Angola Low, identified as a low geopotential height anomaly, is collocated with the maximum surface temperatures and with a vertical equivalent potential temperature profile which is stable to deep convection. Together, this suggests that the Angola Low in October and November has structure more similar to a thermal low rather than a tropical low. In the late summer, from December onwards, the maximum in surface temperatures moves southward over the Kalahari Basin while the geopotential height anomaly remains in the Angola region. The vertical profile over Angola at this time demonstrates the Low is collocated with negative gradients in equivalent potential temperature, indicative of moist instability. In the late summer, therefore, the Angola Low is more similar to a tropical low.

The analysis of the monthly mean climatology and seasonal cycle of the Angola Low has now been expanded upon in the last year through the work of Howard and Washington (2018). They analyse the different synoptic states of the Angola Low, showing two distinct clusters of heat low and tropical low events based on the threshold levels of dry static stability. Consistent with Chapter 4 they demonstrate that the heat low phase of the Angola Low occurs predominantly in the early austral summer (October-November), whereas tropical lows are a feature of the late summer climatology. Moreover, they demonstrate a strong interannual relationship between an index of the Angola Tropical Low and rainfall over southern Africa, which helps to explain the rainfall variability between the three strongest El Niño events.

In Chapter 4, it is evident that different reanalyses datasets do not agree in their estimation of the strength of the mean circulation associated with the Angola Low. This is consistent with a recently published paper which highlights significant variation between different reanalysis datasets in representing the synoptic states of the Angola Low (Crétat et al. 2018). It is also in accordance with work which suggests that the reanalysis datasets perform poorly in comparison to ground-based observations in the period 1960-1974, before the Angola Civil War disrupted the observational base (Pombo et al. 2017). On the basis of these findings, and together with its clear importance for the modelled and observed southern African rainfall climatology, it would be useful to conduct an observational campaign which samples the vertical atmospheric structure of the Angola Low. Even if only for one season, radiosonde data coupled with key surface observations could provide important constraints on reanalysis and model estimates of the circulation. New observational data coupled with bespoke

model experiments will be necessary to test key hypotheses and to advance our understanding of the Angola Low.

In Chapter 5, the dipole rainfall bias in CMIP5 models is shown to relate to model representation of the topography of the Tanzanian Escarpment. Models with relatively low and coarse topography tend to simulate a strongly positive rainfall bias over southern Africa, yet a negative rainfall bias over Madagascar. The effect of the low topography is to encourage an anomalous northeasterly moisture transport to penetrate into subtropical southern Africa. This suggests that the presence of the complex and high topography of the Tanzanian Escarpment, by blocking the tropical easterly moisture source, might contribute to the relative aridity of southern Africa compared to Madagascar in reality. This hypothesis has yet to be tested, although there is preliminary evidence that the eastern boundary topography in general may be important in setting the east-west rainfall gradient. For example, a recent study has shown that compared to a control simulation, model experiments which remove the Drakensburg Mountains in eastern South Africa, simulate higher rainfall rates (by ~6 $mm.day^{-1}$) over the normally arid western Kalahari and eastern Namib Deserts (Koseki and Demissie 2018). This is due to an enhanced southeasterly moisture flux in the simulation without the Drakensburg (Koseki and Demissie 2018). A similar result could apply when the topography further north in tropical latitudes is reduced, especially since a strengthened northeasterly moisture transport is a key feature of wet years in the interannual record.

Chapter 6 uncovered the intriguing result that models projecting the most severe rainfall declines in OND simulate the largest increases in low-level moisture convergence over

southern Africa. This suggests that in future projections, the stability of the southern African atmosphere is set remotely by upper level subsidence, rather than by changes in the low-level moisture circulation. This is analogous to a proposed mechanism of El Niño impact on southern Africa through the propagation of Rossby waves in association anomalous warming of the Pacific Ocean (Cook 2000; Ratnam et al. 2014). It is, however, in contrast to a large body of literature on the interannual variability of southern African rainfall which emphasises the control of year-to-year variation by changes to key moisture transport pathways (e.g. Washington and Preston 2006). This raises the possibility that the processes controlling future change in rainfall are different from those which influence present day interannual variability.

The three chapters which analyse the intermodel diversity in rainfall simulations, therefore, raise a number of important questions concerning how the mean state of the southern African climate system is maintained in reality. The results suggest that more work is needed to understand how variability in the Angola Low and rainfall are connected, how topography influences the distribution and magnitude of rainfall, and whether the balance of controls on interannual variability will remain constant in the future. Finally, the large difference between model and reanalysis estimates of tropical circulation particularly in connection with the Angola Low strongly motivates a targeted observational campaign which seeks to constrain estimates of the circulation. The generative role fulfilled by process-based analysis of the CMIP5 ensemble in a southern African context could be useful in other regions, and should be emphasised during the design and implementation of model evaluation studies.

7.8 Future outlook for modelling southern African rainfall

After a brief phase of process-based model evaluation of southern African rainfall in the 1990s (Mason and Joubert 1997; Joubert 1995; Mullan and McAvaney 1995; Joubert and Hewitson 1997), the literature on modelling in a southern African context largely turned its attention towards performance-based model evaluation (e.g. Moise and Hudson 2008) or towards regional modelling approaches (e.g. Hewitson and Crane 2006; Tadross et al. 2006). While reemphasising persistent errors in models and demonstrating the potential value of regional modelling, this latter phase of research was not able to identify the causes of key model biases or to produce defensible constraints on the envelope of uncertainty in future rainfall change. This thesis returns to the task started in the 1990s of assessing GCMs on the basis of their representation of key processes related to the simulation of rainfall. The intention of this final section is to use the key conclusions from this thesis to outline priorities for further process-based model evaluation.

For present day model simulations, the representation of the Angola Low, moisture circulation and topography all help to account for the intermodel diversity in rainfall. The intermodel variation in the Angola Low is associated with up to 60% of the variability in the climatological rainfall in tropical regions, and the Froude number, calculated over the Tanzanian escarpment, explains 72% of the intermodel rainfall spread in the subtropics. A better understanding of these features and their influence on model simulations is therefore a research priority. In addition to these important climatic influences, the analysis highlighted the potential importance of other features of the

southern African climate system in maintaining the simulated rainfall climatology. These include the model representation of the Botswana High (Chapter 4 & 5), of the Mozambique trough (Chapter 4) and of the Madagascan highlands (Chapter 5). In ongoing work within the School of Geography in Oxford, we are seeking to understand the model simulation of these features, and to ascertain whether they influence the simulated rainfall climatology.

The thesis has focussed on model representation of the mean state of the southern African climate systems along with projections of change to the mean climatology. The focus on the mean state, as opposed to higher orders of variability, is intended as a starting point for the evaluation of model performance. It is likely that biases in simulation of modes of interannual variability or of synoptic weather events will be affected by or may affect the large biases in the mean circulation uncovered here. There is evidence, for example, that mean-state CMIP5 model biases over southern Africa may lead to the wrong sign of rainfall anomalies in response to the El Niño events over parts of southern Africa (Dieppois et al. 2015). On a synoptic timescale, meanwhile, Pinto et al. (2018) show that four GCMs which contribute to the CMIP5 ensemble tend to overestimate the frequency of synoptic systems associated with the Angola Low. Linking the mean state circulation biases with those on synoptic and interannual timescales will be an important stage in evaluating model reliability and guiding improvement.

We cannot observe the future, and so evaluating the reliability of the tools used to simulate future climate is an important task. This thesis approaches this task by

investigating links between model performance in the present day and their simulations of future change. Models which simulate key features of the circulation related to rainfall poorly in the present day simulate a distinct and extreme signal of rainfall decline compared to other, better performing models. While the physical explanation for this connection is unclear, this finding suggests that the common 'delta factor' approach to assessing regional change, where the ensemble-derived signal of change is applied to the present day observed state, is not suitable over southern Africa. A future research priority should be to investigate fully the physical links between the model simulation of the present day climate and the simulation of future change. This may yield more robust constraints of future climate change, which can be used to inform planning decisions under an uncertain future.

The conclusions of this thesis apply specifically to the CMIP5 ensemble. The key controls on the simulation of southern African rainfall found here could also apply across a wider range of climate models. Further research which investigates the processes underlying modelled southern African rainfall across other global and regional models could add value to this thesis, and provide additional evidence to bolster our conclusions. Research along this path is in progress via research projects at the School of Geography in Oxford, and could also occur within the framework of the forthcoming CMIP6 model experiments. Similarly, it will be interesting to investigate whether model simulation of the mean state southern African climate system is fundamentally different in very high resolution models which explicitly represent convection, compared to the parameterised versions analysed here.

In the context of model intercomparison it is not possible to demonstrate cause and effect, and the approach through the thesis has been to highlight important relationships between the simulation of precipitation and circulation among a range of models. Some of the conclusions here could therefore usefully be tested in a model experiment framework. For example, experiments which progressively degrade the representation of topography within a single model could lend support to the hypothesis that the poor representation of topography causes an overestimation of rainfall over southern Africa. Such model experiments, guided by the findings in this thesis, could advance our understanding on the controls on the mean state climate over southern Africa.

Faced with continued political inertia in dealing with the root causes of climate change, successful adaptation to its potential effects is a central challenge for 21st century society. Climate models are the only tools available to evaluate possible future regional climate change, and a key responsibility for climate science is to extract the greatest possible value from them. This thesis has demonstrated that detailed, process-based analysis of model simulations can add this scientific value by placing constraints on extreme model projections and by providing a roadmap for model improvement.

Bibliography

Adebiyi, A. a., and P. Zuidema, 2016: The role of the southern African easterly jet in modifying the southeast Atlantic aerosol and cloud environments. *Q. J. R. Meteorol. Soc.*, **142**, 1574–1589, https://doi.org/10.1002/qj.2765.

Adler, R. F., and Coauthors, 2003: The Version-2 Global Precipitation Climatology Project (GPCP) Monthly Precipitation Analysis (1979–Present). *J. Hydrometeorol.*, **4**, 1147–1167, https://doi.org/10.1175/1525-7541(2003)004<1147:TVGPCP>2.0.CO;2.

Allan, R. P., B. J. Soden, V. O. John, W. Ingram, and P. Good, 2010: Current changes in tropical precipitation. *Environ. Res. Lett.*, **5**, 1–8, https://doi.org/10.1088/1748-9326/5/2/025205.

Allen, M. R., and W. J. Ingram, 2002: Constraints on future changes in climate and the hydrologic cycle. *Nature*, **419**, 224–232, https://doi.org/10.1038/nature01092.

Archer, E., W. Landman, M. Tadross, J. Malherbe, H. Weepener, P. Maluleke, and F. Marumbwa, 2017: Understanding the evolution of the 2014-2016 summer rainfall seasons in southern Africa: Key lessons. *Clim. Risk Manag.*, **16**, 22–28, https://doi.org/10.1016/j.crm.2017.03.006.

Arkin, P. A., and B. N. Meisner, 1987: The Relationship between Large-Scale Convective Rainfall and Cold Cloud over the Western Hemisphere during 1982-84. *Mon. Weather Rev.*, **115**, 51–74, https://doi.org/10.1175/1520-0493(1987)115<0051:TRBLSC>2.0.CO;2.

Awange, J. L., V. G. Ferreira, E. Forootan, Khandu, S. a. Andam-Akorful, N. O. Agutu, and X. F. He, 2015: Uncertainties in remotely sensed precipitation data over Africa. *Int. J. Climatol.*, **36**, 303–323, https://doi.org/10.1002/joc.4346.

Barimalala, R., F. Desbiolles, R. Blamey, and C. J. C. Reason, 2018: Madagascar Influence on the South Indian Ocean Convergence Zone, the Mozambique Channel Trough and Southern African Rainfall. *Geophys. Res. Lett.*, **45**, 11380–11389, https://doi.org/10.1029/2018GL079964.

Baumberger, C., R. Knutti, and G. Hirsch Hadorn, 2017: Building confidence in climate model projections: an analysis of inferences from fit. *Wiley Interdiscip. Rev. Clim. Chang.*, **8**, 1–20, https://doi.org/10.1002/wcc.454.

Behera, S. K., and T. Yamagata, 2001: Subtropical SST dipole events in the southern Indian Ocean. 0–3.

Berckmans, J., T. Woollings, M. E. Demory, P. L. Vidale, and M. Roberts, 2013: Atmospheric blocking in a high resolution climate model: Influences of mean state, orography and eddy forcing. *Atmos. Sci. Lett.*, **14**, 34–40, https://doi.org/10.1002/asl2.412.

Biasutti, M., 2013: Forced Sahel rainfall trends in the CMIP5 archive. *J. Geophys. Res. Atmos.*, **118**, 1613–1623, https://doi.org/10.1002/jgrd.50206.

Biasutti, M., and A. H. Sobel, 2009: Delayed Sahel rainfall and global seasonal cycle in a warmer climate. *Geophys. Res. Lett.*, **36**, https://doi.org/10.1029/2009GL041303.

Biasutti, M., a. H. Sobel, and S. J. Camargo, 2009: The role of the Sahara low in summertime Sahel rainfall variability and change in the CMIP3 models. *J. Clim.*, **22**, 5755–5771, https://doi.org/10.1175/2009JCLI2969.1.

Blamey, R. C., and C. J. C. Reason, 2013: The role of mesoscale convective complexes in southern Africa summer rainfall. *J. Clim.*, **26**, 1654–1668, https://doi.org/10.1175/JCLI-D-12-00239.1.

——, C. Middleton, C. Lennard, and C. J. C. Reason, 2017: A climatology of potential severe convective environments across South Africa. *Clim. Dyn.*, **49**, 2161–2178, https://doi.org/10.1007/s00382-016-3434-7.

Bracegirdle, T. J., E. Shuckburgh, J. B. Sallee, Z. Wang, A. J. S. Meijers, N. Bruneau, T. Phillips, and L. J. Wilcox, 2013: Assessment of surface winds over the atlantic, indian, and pacific ocean sectors of the southern ocean in cmip5 models: Historical bias, forcing response, and state dependence. *J. Geophys. Res. Atmos.*, **118**, 547–562, https://doi.org/10.1002/jgrd.50153.

——, P. Hyder, and C. R. Holmes, 2018: CMIP5 diversity in Southern Westerly jet projections related to historical sea ice area: Strong link to strengthening and weak link to shift. *J. Clim.*, **31**, 195–211, https://doi.org/10.1175/JCLI-D-17-0320.1.

Brown, J. R., A. F. Moise, R. Colman, and H. Zhang, 2016: Will a warmer world mean a wetter or drier Australian monsoon? *J. Clim.*, **29**, 4577–4596, https://doi.org/10.1175/JCLI-D-15-0695.1.

Chadwick, R., I. Boutle, and G. Martin, 2013: Spatial patterns of precipitation change in CMIP5: Why the rich do not get richer in the tropics. *J. Clim.*, **26**, 3803–3822, https://doi.org/10.1175/JCLI-D-12-00543.1.

Chan, S. C., and S. Nigam, 2009: Residual diagnosis of diabatic heating from ERA-40 and NCEP reanalyses: Intercomparisons with TRMM. *J. Clim.*, **22**, 414–428, https://doi.org/10.1175/2008JCLI2417.1.

Chou, C., and J. D. Neelin, 2004: Mechanisms of Global Warming Impacts on Regional Tropical Precipitation*. *J. Clim.*, **17**, 2688–2701, https://doi.org/10.1175/1520-0442(2004)017<2688:MOGWIO>2.0.CO;2.

——, J. Y. Tu, and P. H. Tan, 2007: Asymmetry of tropical precipitation change under global warming. *Geophys. Res. Lett.*, **34**, 1–5, https://doi.org/10.1029/2007GL030327.

——, J. D. Neelin, C. A. Chen, and J. Y. Tu, 2009: Evaluating the "rich-get-richer" mechanism in tropical precipitation change under global warming. *J. Clim.*, **22**, 1982–2005, https://doi.org/10.1175/2008JCLI2471.1.

Christensen, J. H., and Coauthors, 2007: Regional Climate Projections. *Climate Change 2007: The Physical Science Basis. Contribution of Working Group I to the Fourth Assessment Report of the Intergovernmental Panel on Climate Change*, S. Solomon, D. Qin, M. Manning, Z. Chen, M. Marquis, K.B. Averyt, M. Tignor, and H.L. Miller, Eds., Cambridge University Press, Cambridge, United Kingdom and New York, NY, USA.

Collins, M., and Coauthors, 2013: Long-term Climate Change: Projections, Commitments and Irreversibility. *Climate Change 2013: The Physical Science Basis. Contribution of Working Group I to the Fifth Assessment Report of the Intergovernmental Panel on Climate Change*, T. Stocker et al., Eds., Cambridge University Press, Cambridge, United Kingdom and New York, NY, USA.

Compo, G. P., and Coauthors, 2011: The Twentieth Century Reanalysis Project. *Q. J. R. Meteorol. Soc.*, **137**, 1–28, https://doi.org/10.1002/qj.776.

Conway, D., and Coauthors, 2015: Climate and southern Africa's water-energy-food nexus. *Nat. Clim. Chang.*, **5**, 837–846, https://doi.org/10.1038/Nclimate2735.

Cook, B., G. Bonan, and S. Levis, 2006: Soil Moisture Feedbacks to Precipitation in Southern Africa. *J. Clim.*, **19**, 4198–4206.

Cook, C., C. J. C. Reason, and B. C. Hewitson, 2004: Wet and dry spells within particularly wet and dry summers in the South African summer rainfall region. *Clim. Res.*, **26**, 17–31,

https://doi.org/10.3354/cr026017.

Cook, K. H., 2000: The South Indian Convergence Zone and Interannual Rainfall Variability over Southern Africa. *J. Clim.*, **13**, 3789–3804, https://doi.org/10.1175/1520-0442(2000)013<3789:TSICZA>2.0.CO;2.

——, 2001: A Southern Hemisphere Wave Response to ENSO with Implications for Southern Africa Precipitation. *J. Atmos. Sci.*, **58**, 2146–2162, https://doi.org/10.1175/1520-0469(2001)058<2146:ASHWRT>2.0.CO;2.

——, 2003: Reply. *J. Clim.*, **16**, 563–565.

——, and E. K. Vizy, 2013: Projected changes in east african rainy seasons. *J. Clim.*, **26**, 5931–5948, https://doi.org/10.1175/JCLI-D-12-00455.1.

Creese, A., and R. Washington, 2016: Using qflux to constrain modeled Congo Basin rainfall in the CMIP5 ensemble. *J. Geophys. Res. Atmos.*, **121**, 13415–13442, https://doi.org/10.1002/2015JD024524.Received.

Creese, A., and R. Washington, 2018: A process-based assessment of CMIP5 rainfall in the Congo Basin: the September-November rainy season. *J. Clim.*, **31**, 7417–7439, https://doi.org/10.1175/JCLI-D-17-0818.1.

Crétat, J., B. Pohl, Y. Richard, and P. Drobinski, 2012: Uncertainties in simulating regional climate of Southern Africa: Sensitivity to physical parameterizations using WRF. *Clim. Dyn.*, **38**, 613–634, https://doi.org/10.1007/s00382-011-1055-8.

——, ——, B. Dieppois, S. Berthou, and J. Pergaud, 2018: The Angola Low: relationship with southern African rainfall and ENSO. *Clim. Dyn.*, **0**, 1–21, https://doi.org/10.1007/s00382-018-4222-3.

D'Abreton, P. C., and J. A. Lindesay, 1993: Water Vapour Transport Over Southern Africa. *Int. J. Climatol.*, **13**, 151–170.

D'Abreton, P. C., and P. D. Tyson, 1995: Divergent and non-divergent water vapour transport over southern Africa during wet and dry conditions. *Meteorol. Atmos. Phys.*, **55**, 47–59, https://doi.org/10.1007/BF01029601.

Dai, A., 2006: Precipitation characteristics in eighteen coupled climate models. *J. Clim.*, **19**, 4605–4630, https://doi.org/10.1175/JCLI3884.1.

——, I. Y. Fung, A. D. Del Genio, A. Dai, I. Y. Fung, and A. D. Del Genio, 1997: Surface Observed Global Land Precipitation Variations during 1900–88. *J. Clim.*, **10**, 2943–2962, https://doi.org/10.1175/1520-0442(1997)010<2943:SOGLPV>2.0.CO;2.

Dedekind, Z., F. a. Engelbrecht, and J. Van Der Merwe, 2016: Model simulations of rainfall over southern africa and its eastern escarpment. *Water SA*, **42**, 129–143, https://doi.org/10.4314/wsa.v42i1.13.

Dee, D. P., and Coauthors, 2011: The ERA-Interim reanalysis: Configuration and performance of the data assimilation system. *Q. J. R. Meteorol. Soc.*, **137**, 553–597, https://doi.org/10.1002/qj.828.

Dieppois, B., M. Rouault, and M. New, 2015: The impact of ENSO on Southern African rainfall in CMIP5 ocean atmosphere coupled climate models. *Clim. Dyn.*, https://doi.org/10.1007/s00382-015-2480-x.

Dixon, R. D., A. S. Daloz, D. J. Vimont, and M. Biasutti, 2017: Saharan heat low biases in CMIP5 models. *J. Clim.*, **30**, 2867–2884, https://doi.org/10.1175/JCLI-D-16-0134.1.

——, D. J. Vimont, and A. S. Daloz, 2018: The relationship between tropical precipitation

biases and the Saharan heat low bias in CMIP5 models. *Clim. Dyn.*, **50**, 3729–3744, https://doi.org/10.1007/s00382-017-3838-z.

Driver, P., and C. J. C. Reason, 2017: Variability in the Botswana High and its relationships with rainfall and temperature characteristics over southern Africa. *Int. J. Climatol.*, **37**, 570–581, https://doi.org/10.1002/joc.5022.

Dunning, C. M., R. P. Allan, and E. Black, 2017: Identification of deficiencies in seasonal rainfall simulated by CMIP5 climate models. *Environ. Res. Lett.*, **12**, 114001, https://doi.org/10.1088/1748-9326/aa869e.

Dyer, E. L. E., D. B. A. Jones, R. Li, H. Sawaoka, and L. Mudryk, 2017: Sahel precipitation and regional teleconnections with the Indian Ocean. *J. Geophys. Res.*, **122**, 5654–5676, https://doi.org/10.1002/2016JD026014.

Engelbrecht, C. J., F. a. Engelbrecht, and L. L. Dyson, 2013: High-resolution model-projected changes in mid-tropospheric closed-lows and extreme rainfall events over southern Africa. *Int. J. Climatol.*, **33**, 173–187, https://doi.org/10.1002/joc.3420.

Engelbrecht, F., and Coauthors, 2015: Projections of rapidly rising surface temperatures over Africa under low mitigation. *Environ. Res. Lett.*, **10**, https://doi.org/10.1088/1748-9326/10/8/085004.

Engelbrecht, F. A., J. L. McGregor, and C. J. Engelbrecht, 2009: Dynamics of the Conformal-Cubic Atmopsheric Model projected climate-change signal over southern Africa. *Int. J. Climatol.*, **29**, 1013–1033, https://doi.org/10.1002/joc.1742.

Engelstaedter, S., R. Washington, C. Flamant, D. J. Parker, C. J. T. Allen, and M. C. Todd, 2015: The Saharan heat low and moisture transport pathways in the central Sahara - Multiaircraft observations and Africa-LAM evaluation. *J. Geophys. Res. Atmos.*, **120**, 1–26, https://doi.org/10.1002/2015JD023123.Received.

Fauchereau, N., S. Trzaska, Y. Richard, P. Roucou, and P. Camberlin, 2003: Sea-surface temperature co-variability in the southern Atlantic and Indian Oceans and its connections with the atmospheric circulation in the Southern Hemisphere. *Int. J. Climatol.*, **23**, 663–677, https://doi.org/10.1002/joc.905.

Fauchereau, N., and Coauthors, 2009a: Recurrent daily OLR patterns in the Southern Africa/Southwest Indian ocean region, implications for South African rainfall and teleconnections. *Clim. Dyn.*, **32**, 575–591, https://doi.org/10.1007/s00382-008-0426-2.

——, B. Pohl, C. J. C. Reason, M. Rouault, and Y. Richard, 2009b: Recurrent daily OLR patterns in the Southern Africa/Southwest Indian ocean region, implications for South African rainfall and teleconnections. *Clim. Dyn.*, **32**, 575–591, https://doi.org/10.1007/s00382-008-0426-2.

Favre, A., B. Hewitson, C. Lennard, R. Cerezo-Mota, and M. Tadross, 2013: Cut-off Lows in the South Africa region and their contribution to precipitation. *Clim. Dyn.*, **41**, 2331–2351, https://doi.org/10.1007/s00382-012-1579-6.

——, and Coauthors, 2016: Spatial distribution of precipitation annual cycles over South Africa in 10 CORDEX regional climate model present-day simulations. *Clim. Dyn.*, **46**, 1799–1818, https://doi.org/10.1007/s00382-015-2677-z.

Fields, S., 2005: Continental divide: Why Africa's climate change burden is greater. *Environ. Health Perspect.*, **113**, A534–A537.

Findlater, J., 1969: A major low level air current near the Indian ocean during the nothern ummer. *Q. J. R. Meteorol. Soc.*, **95**, 362–380.

Flato, G., and Coauthors, 2013: Evaluation of Climate Models. *Clim. Chang. 2013 Phys. Sci. Basis. Contrib. Work. Gr. I to Fifth Assess. Rep. Intergov. Panel Clim. Chang.*, 741–866, https://doi.org/10.1017/CBO9781107415324.

Friedman, A. R., Y. T. Hwang, J. C. H. Chiang, and D. M. W. Frierson, 2013: Interhemispheric temperature asymmetry over the twentieth century and in future projections. *J. Clim.*, **26**, 5419–5433, https://doi.org/10.1175/JCLI-D-12-00525.1.

Gaetani, M., C. Flamant, S. Bastin, S. Janicot, C. Lavaysse, F. Hourdin, P. Braconnot, and S. Bony, 2017: West African monsoon dynamics and precipitation: the competition between global SST warming and CO2increase in CMIP5 idealized simulations. *Clim. Dyn.*, **48**, 1353–1373, https://doi.org/10.1007/s00382-016-3146-z.

Gates, W. L., 1992: AMIP: The Atmospheric Model Intercomparison Project. *Bull. Amer. Meteor. Soc.*, **73**, 1962–1970.

Giannini, A., 2010: Mechanisms of Climate Change in the Semiarid African Sahel : The Local View. *J. Clim.*, **23**, 743–756, https://doi.org/10.1175/2009JCLI3123.1.

——, B. Lyon, R. Seager, and N. Vigaud, 2018: Dynamic and Thermodynamic Elements of Modeled Climate Change at the East African Margin of Convection. *J. Geophys. Res.*, **45**, 992–1000, https://doi.org/10.1002/2017GL075486.

Giorgi, F., C. Jones, and G. R. Asrar, 2009: Addressing climate information needs at the regional level: The CORDEX framework. *World Meteorol. Organ. Bull.*, **58**, 175–183.

Gleckler, P. J., K. E. Taylor, and C. Doutriaux, 2008: Performance metrics for climate models. *J. Geophys. Res. Atmos.*, **113**, 1–20, https://doi.org/10.1029/2007JD008972.

Goddard, L., and N. E. Graham, 1999: Importance of the Indian Ocean for simulating rainfall anomalies over eastern and southern Africa. *J. Geophys. Res.*, **104**, 19099, https://doi.org/10.1029/1999JD900326.

Gosling, S. N., and N. W. Arnell, 2016: A global assessment of the impact of climate change on water scarcity. *Clim. Change*, **134**, 371–385, https://doi.org/10.1007/s10584-013-0853-x.

Grimm, A. M., J. S. Pal, and F. Giorgi, 2007: Connection between spring conditions and peak summer monsoon rainfall in South America: Role of soil moisture, surface temperature, and topography in eastern Brazil. *J. Clim.*, **20**, 5929–5945, https://doi.org/10.1175/2007JCLI1684.1.

Guilyardi, E., A. Wittenberg, A. Fedorov, M. Collins, C. Wang, A. Capotondi, G. J. van Oldenborgh, and T. Stockdale, 2009: Understanding El Niño in ocean-atmosphere general circulation models: Progress and challenges. *Bull. Am. Meteorol. Soc.*, **90**, 325–340, https://doi.org/10.1175/2008BAMS2387.1.

Hachigonta, S., and C. J. C. Reason, 2006: Interannual variability in dry and wet spell characteristics over Zambia. *Clim. Res.*, **32**, 49–62, https://doi.org/10.3354/cr032049.

Hall, A., and X. Qu, 2006: Using the current seasonal cycle to constrain snow albedo feedback in future climate change. **33**, 1–4, https://doi.org/10.1029/2005GL025127.

Harris, I., P. D. Jones, T. J. Osborn, and D. H. Lister, 2014: Updated high-resolution grids of monthly climatic observations - the CRU TS3.10 Dataset. *Int. J. Climatol.*, **34**, 623–642, https://doi.org/10.1002/joc.3711.

Harrison, M. S. J., 1984: A generalized classification of South African summer rain-bearing synoptic systems. *J. Climatol.*, **4**, 547–560, https://doi.org/10.1002/joc.3370040510.

Hart, N., C. J. C. Reason, and N. Fauchereau, 2010: Tropical-extratropical interactions over Southern Africa: three cases of heavy summer season rainfall. *Monthl*, **138**, 2608–2623,

https://doi.org/10.1175/2010MWR3070.1.

Hart, N. C. G., C. J. C. Reason, and N. Fauchereau, 2012: Building a tropical-extratropical cloud band metbot. *Mon. Weather Rev.*, **140**, 4005–4016, https://doi.org/10.1175/MWR-D-12-00127.1.

Hart, N. C. G., C. J. C. Reason, and N. Fauchereau, 2013: Cloud bands over southern Africa: Seasonality, contribution to rainfall variability and modulation by the MJO. *Clim. Dyn.*, **41**, 1199–1212, https://doi.org/10.1007/s00382-012-1589-4.

Hart, N. C. G., R. Washington, and R. A. Stratton, 2018: Stronger Local Overturning in Convective-Permitting Regional Climate Model Improves Simulation of the Subtropical Annual Cycle. 334–342, https://doi.org/10.1029/2018GL079563.

Hawcroft, M., J. M. Haywood, M. Collins, A. Jones, A. C. Jones, and G. Stephens, 2017: Southern Ocean albedo, inter-hemispheric energy transports and the double ITCZ: global impacts of biases in a coupled model. *Clim. Dyn.*, **48**, 2279–2295, https://doi.org/10.1007/s00382-016-3205-5.

Hawkins, E., and R. Sutton, 2009: The potential to narrow uncertainty in regional climate predictions. *Bull. Am. Meteorol. Soc.*, **90**, 1095–1107, https://doi.org/10.1175/2009BAMS2607.1.

He, J., and B. J. Soden, 2016: A re-examination of the projected subtropical precipitation decline. *Nat. Clim. Chang.*, **7**, 53–57, https://doi.org/10.1038/nclimate3157.

van Heerden, J., and Taljaard, 1998: Africa and surrounding waters. *Meteorology of the Southern Hemisphere, Meteor. Monogr.*, Amer. Meteor. Soc., 141–174.

Held, I. M., 2005: The gap between simulation and understanding in climate modeling. *Bull. Am. Meteorol. Soc.*, **86**, 1609–1614, https://doi.org/10.1175/BAMS-86-11-1609.

Held, I. M., and B. J. Soden, 2006: Robust responses of the hydrologic cycle to global warming. *J. Clim.*, **19**, 5686–5699, https://doi.org/10.1175/JCLI3990.1.

Held, I. M., T. L. Delworth, J. Lu, K. L. Findell, and T. R. Knutson, 2005: Simulation of Sahel drought in the 20th and 21st centuries. *PNAS*, **102**, https://doi.org/10.1073/pnas.0509057102.

Hermes, J. C., and C. J. C. Reason, 2005: Ocean model diagnosis of interannual coevolving SST variability in the South Indian and South Atlantic Oceans. *J. Clim.*, **18**, 2864–2882, https://doi.org/10.1175/JCLI3422.1.

Hermes, J. C., and C. J. C. Reason, 2008: Annual cycle of the South Indian Ocean (Seychelles-Chagos) thermocline ridge in a regional ocean model. *J. Geophys. Res. Ocean.*, **113**, 1–10, https://doi.org/10.1029/2007JC004363.

Hermes, J. C., and C. J. C. Reason, 2009a: Variability in sea-surface temperature and winds in the tropical south-east Atlantic Ocean and regional rainfall relationships. *Int. J. Climatol.*, **29**, 11–21, https://doi.org/10.1002/joc.1711.

Hermes, J. C., and C. J. C. Reason, 2009b: The sensitivity of the seychelles-chagos thermocline ridge to large-scale wind anomalies. *ICES J. Mar. Sci.*, **66**, 1455–1466, https://doi.org/10.1093/icesjms/fsp074.

Hewitson, B. C., and R. G. Crane, 2006: Consensus between GCM climate change projections with empirical downscaling: Precipitation downscaling over South Africa. *Int. J. Climatol.*, **26**, 1315–1337, https://doi.org/10.1002/joc.1314.

Hirons, L., and N. Klingaman, 2016: *El Niño 2015 / 2016 : Impact Analysis*. 1–30 pp.

——, and A. Turner, 2018: The impact of Indian Ocean mean-state biases in climate models on the representation of the East African short rains. *J. Clim.*, **31**, 6611–6631, https://doi.org/10.1175/JCLI-D-17-0804.1.

Howard, E., and R. Washington, 2018: Characterizing the Synoptic Expression of the Angola Low. *J. Clim.*, **31**, 7147–7165, https://doi.org/10.1175/JCLI-D-18-0017.1.

Huang, B., and Coauthors, 2017: Extended reconstructed Sea surface temperature, Version 5 (ERSSTv5): Upgrades, validations, and intercomparisons. *J. Clim.*, **30**, 8179–8205, https://doi.org/10.1175/JCLI-D-16-0836.1.

Huang, P., S. P. Xie, K. Hu, G. Huang, and R. Huang, 2013: Patterns of the seasonal response of tropical rainfall to global warming. *Nat. Geosci.*, **6**, 357–361, https://doi.org/10.1038/ngeo1792.

Hurley, J. V., and W. R. Boos, 2013: Interannual variability of monsoon precipitation and local subcloud equivalent potential temperature. *J. Clim.*, **26**, 9507–9527, https://doi.org/10.1175/JCLI-D-12-00229.1.

Hwang, Y.-T., and D. M. W. Frierson, 2013: Link between the double-Intertropical Convergence Zone problem and cloud biases over the Southern Ocean. *Proc. Natl. Acad. Sci.*, **110**, 4935–4940, https://doi.org/10.1073/pnas.1213302110.

James, R., R. Washington, and R. Jones, 2015: Process-based assessment of an ensemble of climate projections for West Africa. *J. Geophys. Res.*, **120**, 1–18, https://doi.org/10.1002/2014JD022513.Received.

——, and Coauthors, 2017: Evaluating climate models with an African lens. *Bull. Am. Meteorol. Soc.*, BAMS-D-16-0090.1, https://doi.org/10.1175/BAMS-D-16-0090.1.

——, and Coauthors, 2018: Evaluating climate models with an African lens. *Bull. Am. Meteorol. Soc.*, **99**, 313–336, https://doi.org/10.1175/BAMS-D-16-0090.1.

Jiang, J. H., and Coauthors, 2012: Evaluation of cloud and water vapor simulations in CMIP5 climate models Using NASA "A-Train" satellite observations. *J. Geophys. Res. Atmos.*, **117**, https://doi.org/10.1029/2011JD017237.

Joubert, A. M., 1995: Simulations of Southern African Climate by Early Generation General-Circulation Models. *S. Afr. J. Sci.*, **91**, 85–91.

——, and B. C. Hewitson, 1997: Simulating present climates of southern Africa using general circulation models *Prog. Phys. Geogr.*, **21**, 51–78, https://doi.org/10.1177/030913339702100104.

Jury, M. R., 1992: A climatic dipole governing the interannual variability of convection over the SW Indian Ocean and SE Africa region. *Trends Geophys. Res.*, **1**, 165–172.

Jury, M. R., 2016: Summer climate of Madagascar and monsoon pulsing of its vortex. *Meteorol. Atmos. Phys.*, **128**, 117–129, https://doi.org/10.1007/s00703-015-0401-5.

Kalnay, E., and Coauthors, 1996: The NCEP/NCAR 40-Year Reanalysis Project. *Bull. Am. Meteorol. Soc.*, **77**, 437–471, https://doi.org/http://dx.doi.org/10.1175/1520-0477(1996)077<0437:TNYRP>2.0.CO;2.

Kalognomou, E. A., and Coauthors, 2013: A diagnostic evaluation of precipitation in CORDEX models over Southern Africa. *J. Clim.*, **26**, 9477–9506, https://doi.org/10.1175/JCLI-D-12-00703.1.

Kanamitsu, M., W. Ebisuzaki, J. Woollen, S.-K. Yang, J. J. Hnilo, M. Fiorino, and G. L. Potter, 2002: NCEP–DOE AMIP-II Reanalysis (R-2). *Bull. Am. Meteorol. Soc.*, **83**, 1631–1643, https://doi.org/10.1175/BAMS-83-11-1631.

Kennedy, J. J., 2014: A review of uncertainty in in situ measurements and data sets of sea surface temperature. *Rev. Geophys.*, **52**, 1–32, https://doi.org/10.1002/2013RG000434.

Kent, C., R. Chadwick, and D. P. Rowell, 2015: Understanding uncertainties in future projections of seasonal tropical precipitation. *J. Clim.*, **28**, 4390–4413, https://doi.org/10.1175/JCLI-D-14-00613.1.

Kidston, J., and E. P. Gerber, 2010: Intermodel variability of the poleward shift of the austral jet stream in the CMIP3 integrations linked to biases in 20th century climatology. *Geophys. Res. Lett.*, **37**, 1–5, https://doi.org/10.1029/2010GL042873.

Knutti, R., 2010: The end of model democracy? *Clim. Change*, **102**, 395–404, https://doi.org/10.1007/s10584-010-9800-2.

——, and J. Sedláček, 2013: Robustness and uncertainties in the new CMIP5 climate model projections. *Nat. Clim. Chang.*, **3**, 369–373, https://doi.org/10.1038/nclimate1716.

——, R. Furrer, C. Tebaldi, J. Cermak, and G. Meehl, 2010: Challenges in Combining Projections from Multiple Climate Models. *J. Clim.*, **23**, 2739–2758, https://doi.org/10.1175/2009JCLI3361.1.

——, D. Masson, and A. Gettelman, 2013: Climate model genealogy: Generation CMIP5 and how we got there. *Geophys. Res. Lett.*, **40**, 1194–1199, https://doi.org/10.1002/grl.50256.

Kodama, Y. M., T. Sagawa, S. Ishida, and T. Yoshikane, 2012: Roles of the Brazilian plateau in the formation of the SACZ. *J. Clim.*, **25**, 1745–1758, https://doi.org/10.1175/2011JCLI3785.1.

Koseki, S., and T. Demissie, 2018: Does the Drakensberg dehydrate southwestern Africa? *J. Arid Environ.*, **158**, 35–42, https://doi.org/10.1016/j.jaridenv.2018.08.003.

Lavaysse, C., C. Flamant, S. Janicot, D. J. Parker, J. P. Lafore, B. Sultan, and J. Pelon, 2009: Seasonal evolution of the West African heat low: A climatological perspective. *Clim. Dyn.*, **33**, 313–330, https://doi.org/10.1007/s00382-009-0553-4.

Lazenby, M., M. Todd, and Y. Wang, 2016: Climate model simulation of the South Indian Ocean Convergence Zone: mean state and variability. *Clim. Res.*, **68**, 59–71, https://doi.org/10.3354/cr01382.

Lazenby, M. J., M. C. Todd, R. Chadwick, Y. Wang, M. J. Lazenby, M. C. Todd, R. Chadwick, and Y. Wang, 2018: Future precipitation projections over central and southern Africa and the adjacent Indian Ocean: What causes the changes and the uncertainty? *J. Clim.*, JCLI-D-17-0311.1, https://doi.org/10.1175/JCLI-D-17-0311.1.

Lehner, F., C. Coats, T. Stocker, A. Pendergrass, B. Sanderson, C. Raible, and J. Smerdon, 2017: Projected drought risk in 1.5°C and 2°C warmer climates. **44**, 1–10, https://doi.org/10.1002/2017GL074117.

Lenters, J. D., and K. H. Cook, 1997: On the Origin of the Bolivian High and Related Circulation Features of the South American Climate. *J. Atmos. Sci.*, **54**, 656–678, https://doi.org/10.1175/1520-0469(1997)054<0656:OTOOTB>2.0.CO;2.

Leroux, M., 1983: *The Meteorology and Climate of Tropical Africa*. Springer, 548 pp.

Lindesay, J. A., 1988: South African rainfall, the Southern Oscillation and a Southern Hemisphere semi-annual cycle. *J. Climatol.*, **8**, 17–30, https://doi.org/10.1002/joc.3370080103.

Lintner, B. R., D. K. Adams, K. A. Schiro, A. M. Stansfield, A. A. Amorim Rocha, and J. D. Neelin, 2017: Relationships among climatological vertical moisture structure, column water vapor, and precipitation over the central Amazon in observations and CMIP5

models. *Geophys. Res. Lett.*, **44**, 1981–1989, https://doi.org/10.1002/2016GL071923.

Livezey, R. E., and W. Y. Chen, 1983: Statistical Field Significance and its Determination by Monte Carlo Techniques. *Mon. Weather Rev.*, **111**, 46–59, https://doi.org/10.1175/1520-0493(1983)111<0046:SFSAID>2.0.CO;2.

Lott, F., and M. J. Miller, 1997: A new subgrid-scale orographic drag parametrization: Its formulation and testing. *Q. J. R. Meteorol. Soc.*, **123**, 101–127, https://doi.org/10.1002/qj.49712353704.

Ma, J., and S. P. Xie, 2013: Regional Patterns of Sea Surface Temperature Change: A Source of Uncertainty in Future Projections of Precipitation and Atmospheric Circulation. *J. Clim.*, **26**, 2482–2501, https://doi.org/10.1175/JCLI-D-12-00283.1.

——, ——, and Y. Kosaka, 2012: Mechanisms for tropical tropospheric circulation change in response to global warming. *J. Clim.*, **25**, 2979–2994, https://doi.org/10.1175/JCLI-D-11-00048.1.

Macron, C., B. Pohl, Y. Richard, and M. Bessafi, 2014: How do tropical temperate troughs form and develop over Southern Africa? *J. Clim.*, **27**, 1633–1647, https://doi.org/10.1175/JCLI-D-13-00175.1.

Maher, P., G. K. Vallis, S. C. Sherwood, M. J. Webb, and P. G. Sansom, 2018: The Impact of Parameterized Convection on Climatological Precipitation in Atmospheric Global Climate Models. *Geophys. Res. Lett.*, **45**, 3728–3736, https://doi.org/10.1002/2017GL076826.

Maidment, R. I., R. P. Allan, and E. Black, 2015: Recent observed and simulated changes in precipitation over Africa. *Geophys. Res. Lett.*, **42**, 1–10, https://doi.org/10.1002/2015GL065765.Received.

Manabe, S., R. J. Stouffer, M. J. Spelman, and K. Bryan, 1991: Transient responses of a coupled ocean-atmosphere model to gradual changes of atmospheric C02, Part II: Seasonal response. *J. Clim.*, **4**, 785–817, https://doi.org/10.1175/1520-0442(1992)005<0105:TROACO>2.0.CO;2.

Manatsa, D., and C. Reason, 2017: ENSO–Kalahari Desert linkages on southern Africa summer surface air temperature variability. *Int. J. Climatol.*, **37**, 1728–1745, https://doi.org/10.1002/joc.4806.

Marsham, J. H., D. J. Parker, M. C. Todd, J. R. Banks, H. E. Brindley, L. Garcia-Carreras, A. J. Roberts, and C. L. Ryder, 2015: The contrasting roles of water and dust in controlling daily variations in radiative heating of the summertime Saharan Heat Low. *Atmos. Chem. Phys. Discuss.*, **15**, 19447–19476, https://doi.org/10.5194/acpd-15-19447-2015.

Martin, E. R., and C. Thorncroft, 2015: Representation of African easterly waves in CMIP5 models. *J. Clim.*, **28**, 7702–7715, https://doi.org/10.1175/JCLI-D-15-0145.1.

Mason, S. J., 1995: Sea-Surface Temperature - South African Rainfall Associations, 1910-1989. *Int. J. Climatol.*, **15**, 119–135, https://doi.org/https://doi.org/10.1002/joc.3370150202.

Mason, S. J., and A. . Joubert, 1997: Simulated changes in extreme rainfall over southern Africa. *Int. J. Climatol.*, **17**, 291–301, https://doi.org/10.1002/(SICI)1097-0088(19970315)17:3<291::AID-JOC120>3.3.CO;2-T.

Masson, D., and R. Knutti, 2011: Climate model genealogy. *Geophys. Res. Lett.*, **38**, 1–4, https://doi.org/10.1029/2011GL046864.

Massonnet, F., O. Bellprat, V. Guemas, and F. J. Doblas-Reyes, 2016: Using climate models to estimate the quality of global observational data sets. *Science (80-.).*, **354**, 452–455, https://doi.org/10.1126/science.aaf6369.

Matarira, C. H., 1990: Drought Over Zimbabwe in a Regional and Global Context. *Int. J. Climatol.*, **10**, 609–625, https://doi.org/10.1002/joc.3370100605.

McSweeney, C. F., R. G. Jones, and B. B. B. Booth, 2012: Selecting ensemble members to provide regional climate change information. *J. Clim.*, **25**, 7100–7121, https://doi.org/10.1175/JCLI-D-11-00526.1.

Mechoso, C. R., and Coauthors, 1995: The Seasonal Cycle over the Tropical Pacific in Coupled Ocean–Atmosphere General Circulation Models. *Mon. Weather Rev.*, **123**, 2825–2838, https://doi.org/10.1175/1520-0493(1995)123<2825:TSCOTT>2.0.CO;2.

Meehl, G. A., and Coauthors, 2000: Trends in Extreme Weather and Climate Events: Issues Related to Modeling Extremes in Projections of Future Climate Change *. *Bull. Am. Meteorol. Soc.*, **81**, 427–436, https://doi.org/10.1175/1520-0477(2000)081<0427:TIEWAC>2.3.CO;2.

Meehl, G. A., and Coauthors, 2007: Global Climate Projections. *Clim. Chang. 2007 Contrib. Work. Gr. I to Fourth Assess. Rep. Intergov. Panel Clim. Chang.*, 747–846, https://doi.org/10.1080/07341510601092191.

Mehran, A., A. Aghakouchak, and T. . Phillips, 2014: Evaluation of CMIP5 continental preciptiation simulations relative to satellite-based gauge-adjusted observations. *J. geo*, **119**, 1695–1707, https://doi.org/10.1002/2013JD021272.Received.

Midgley, G. F., and W. Thuiller, 2011: Potential responses of terrestrial biodiversity in Southern Africa to anthropogenic climate change. *Reg Env. Chang.*, **11**, 127–135, https://doi.org/10.1007/s10113-010-0191-8.

Moise, a. F., and D. a. Hudson, 2008: Probabilistic predictions of climate change for Australia and southern Africa using the reliability ensemble average of IPCC CMIP3 model simulations. *J. Geophys. Res. Atmos.*, **113**, 1–26, https://doi.org/10.1029/2007JD009250.

Moore, G. W. K., 2013: Impact of the high topography of Madagascar on the structure of the Findlater Jet. *Geophys. Res. Lett.*, **40**, 2367–2372, https://doi.org/10.1002/grl.50399.

Moufouma-Okia, W., and R. Jones, 2014: Resolution dependence in simulating the African hydroclimate with the HadGEM3-RA regional climate model. *Clim. Dyn.*, **44**, 609–632, https://doi.org/10.1007/s00382-014-2322-2.

Mueller, B., and S. I. Seneviratne, 2014: Systematic land climate and evapotranspiration biases in CMIP5 simulations. *Geophys. Res. Lett.*, **41**, 128–134, https://doi.org/10.1002/2013GL058055.

Mulenga, H., 1998: Southern African Climatic Anomalies, Summer Rainfall and the Angola Low. University of Cape Town, 261 pp.

Mullan, A. B., and B. J. McAvaney, 1995: Validation of high latitude tropospheric circulation in the Southern Hemisphere (Subproject 9). *Proceedings of the first AMIP Scientific Conference*, 205–210.

Munday, C., and R. Washington, Systematic climate model rainfall biases over southern Africa : links to moisture circulation and topography. *J. Clim.*, **31**, 1–42, https://doi.org/10.1175/JCLI-D-18-0008.1.

Munday, C., and R. Washington, 2017: Circulation controls on southern African precipitation in coupled models: The role of the Angola Low. *J. Geophys. Res. Atmos.*, **122**, 1–17, https://doi.org/10.1002/2016JD025736.

Mutai, C. C., M. N. Ward, and a W. Colman, 1998: Towards the prediction of the East Africa short rains based on sea-surface temperature-atmosphere coupling. *Int. J. Climatol.*, **18**,

975–997, https://doi.org/10.1002/(SICI)1097-0088(199807)18:9<975::AID-JOC259>3.3.CO;2-L.

Nagel, J. F., 1962: On the Measurement of Dew. *Arch. Met. Geoph Biokl. B.*, **11**, 403–423.

Neelin, J. D., C. Chou, and H. Su, 2003: Tropical drought regions in global warming and El Niño teleconnections. *Geophys. Res. Lett.*, **30**, 1–4, https://doi.org/10.1029/2003GL018625.

New, M., R. Washington, C. Jack, and B. Hewitson, 2003: Sensitivity of southern African climate to soil moisture. *CLIVAR Exch.*, **8**, 45–47.

Nicholson, S., 2003: Comments on "The South Indian convergence zone and interannual rainfall variability over southern Africa" and the question of ENSO's influence on southern Africa. *J. Clim.*, **16**, 555–562, https://doi.org/10.1175/1520-0442(2003)016<0555:COTSIC>2.0.CO;2.

Nicholson, S. E., 2018: The ITCZ and the seasonal cycle over equatorial Africa. *Bull. Am. Meteorol. Soc.*, **99**, 337–348, https://doi.org/10.1175/BAMS-D-16-0287.1.

Nicholson, S. E., and E. Kim, 1997: The relationship of the El Nino Southern oscillation to African rainfall. *Int. J. Climatol.*, **17**, 117–135, https://doi.org/10.1002/(sici)1097-0088(199702)17:2<117::aid-joc84>3.0.co;2-o.

Nicholson, S. E., J. Kim, M. B. Ba, and A. R. Lare, 1997: The mean surface water balance over Africa and its interannual variability. *J. Clim.*, **10**, 2981–3002, https://doi.org/10.1175/1520-0442(1997)010<2981:TMSWBO>2.0.CO;2.

van Niekerk, A., T. G. Shepherd, S. B. Vosper, and S. Webster, 2016: Sensitivity of resolved and parametrized surface drag to changes in resolution and parametrization. *Q. J. R. Meteorol. Soc.*, **142**, 2300–2313, https://doi.org/10.1002/qj.2821.

Nikulin, G., and Coauthors, 2012: Precipitation climatology in an ensemble of CORDEX-Africa regional climate simulations. *J. Clim.*, **25**, 6057–6078, https://doi.org/10.1175/JCLI-D-11-00375.1.

Niznik, M. J., and B. R. Lintner, 2013: Circulation, moisture, and precipitation relationships along the south pacific convergence zone in reanalyses and CMIP5 models. *J. Clim.*, **26**, 10174–10192, https://doi.org/10.1175/JCLI-D-13-00263.1.

Notz, D., 2015: How well must climate models agree with observations ? Subject Areas : Author for correspondence : *Philos. Trans. R. Soc. A Math. Phys. Eng. Sci.*, **373**, 1–16.

Novella, N. S., and W. M. Thiaw, 2013: African rainfall climatology version 2 for famine early warning systems. *J. Appl. Meteorol. Climatol.*, **52**, 588–606, https://doi.org/10.1175/JAMC-D-11-0238.1.

OCHA, 2011: *Southern Africa • Floods and Cyclones*. 1–8 pp.

Overland, J. E., M. Wang, N. A. Bond, J. E. Walsh, V. M. Kattsov, and W. L. Chapman, 2011: Considerations in the selection of global climate models for regional climate projections: The Arctic as a case study. *J. Clim.*, **24**, 1583–1597, https://doi.org/10.1175/2010JCLI3462.1.

Park, J. Y., J. Bader, and D. Matei, 2015: Northern-hemispheric differential warming is the key to understanding the discrepancies in the projected Sahel rainfall. *Nat. Commun.*, **6**, 1–8, https://doi.org/10.1038/ncomms6985.

Parker, W. S., 2011: When Climate Models Agree : The Significance of Robust Model Predictions. *Philos. Sci.*, **78**, 579–600, https://doi.org/http://www.jstor.org/stable/10.1086/661566.

Peyrille, P., J. P. Lafore, and A. Boone, 2016: The annual cycle of the West African monsoon in a two-dimensional model: Mechanisms of the rain-band migration. *Q. J. R. Meteorol. Soc.*, **142**, 1473–1489, https://doi.org/10.1002/qj.2750.

Pinto, I., C. Lennard, M. Tadross, B. Hewitson, A. Dosio, G. Nikulin, H. J. Panitz, and M. E. Shongwe, 2016: Evaluation and projections of extreme precipitation over southern Africa from two CORDEX models. *Clim. Change*, **135**, 655–668, https://doi.org/10.1007/s10584-015-1573-1.

——, C. Jack, and B. Hewitson, 2018: Process-based model evaluation and projections over southern Africa from Coordinated Regional Climate Downscaling Experiment and Coupled Model Intercomparison Project Phase 5 models. *Int. J. Climatol.*, 1–11, https://doi.org/10.1002/joc.5666.

Pithan, F., T. G. Shepherd, G. Zappa, and I. Sandu, 2016: Climate model biases in jet streams, blocking and storm tracks resulting from missing orographic drag. *Geophys. Res. Lett.*, **43**, 7231–7240, https://doi.org/10.1002/2016GL069551.

Pohl, B., C. Macron, and P.-A. Monerie, 2017: Fewer rainy days and more extreme rainfall by the end of the century in Southern Africa. *Sci. Rep.*, **7**, 46466, https://doi.org/10.1038/srep46466.

Pombo, S., R. Proença de Oliveira, and A. Mendes, 2017: Comparative performance analysis of climate re-analysis approaches in Angola. *Hydrol. Sci. J.*, **62**, 698–714, https://doi.org/10.1080/02626667.2016.1257856.

Potter, S. F., E. J. Dawson, and D. M. W. Frierson, 2017: Southern African orography impacts on low clouds and the Atlantic ITCZ in a coupled model. *Geophys. Res. Lett.*, **44**, 1–7, https://doi.org/10.1002/2017GL073098.

Räisänen, J., 2007: How reliable are climate models? *Tellus, Ser. A Dyn. Meteorol. Oceanogr.*, **59**, 2–29, https://doi.org/10.1111/j.1600-0870.2006.00211.x.

Randriamahefasoa, T. S. M., and C. J. C. Reason, 2017: Interannual variability of rainfall characteristics over southwestern Madagascar. *Theor. Appl. Climatol.*, **128**, 421–437, https://doi.org/10.1007/s00704-015-1719-0.

Ratna, S. B., J. V. Ratnam, S. K. Behera, C. J. deW Rautenbach, T. Ndarana, K. Takahashi, and T. Yamagata, 2014: Performance assessment of three convective parameterization schemes in WRF for downscaling summer rainfall over South Africa. *Clim. Dyn.*, **42**, 2931–2953, https://doi.org/10.1007/s00382-013-1918-2.

Ratnam, J. V., S. K. Behera, Y. Masumoto, and T. Yamagata, 2014: Remote effects of El Niño and Modoki events on the austral summer precipitation of Southern Africa. *J. Clim.*, **27**, 3802–3815, https://doi.org/10.1175/JCLI-D-13-00431.1.

Reason, C. J. C., 2001: Subtropical Indian Ocean SST dipole events and southern African rainfall. **28**, 2225–2227.

Reason, C. J. C., 2016: The Bolivian, Botswana, and Bilybara Highs and Southern Hemisphere drought/floods. *Geophys. Res. Lett.*, **2010**, 1280–1286, https://doi.org/10.1002/2015GL067228.

Reason, C. J. C., 2017: Climate of Southern Africa. *Oxford Res. Encycl. Clim. Sci.*, http://climatescience.oxfordre.com/view/10.1093/ac.

Reason, C. J. C., and H. Mulenga, 1999: Relationships between South African rainfall and SST anomalies in the southwest Indian Ocean. *Int. J. Climatol.*, **19**, 1651–1673, https://doi.org/10.1002/(SICI)1097-0088(199912)19:15<1651::AID-JOC439>3.0.CO;2-U.

——, and D. Jagadheesha, 2005: A model investigation of recent ENSO impacts over southern Africa. *Meteorol. Atmos. Phys.*, **89**, 181–205, https://doi.org/10.1007/s00703-005-0128-9.

Reason, C. J. C., a. Keibel, and S. Africa, 2004: Tropical Cyclone Eline and Its Unusual Penetration and Impacts over the Southern African Mainland. *Weather Forecast.*, **19**, 789–805, https://doi.org/10.1175/1520-0434(2004)019<0789:TCEAIU>2.0.CO;2.

Reason, C. J. C., W. Landman, and W. Tennant, 2006: Seasonal to decadal prediction of southern African climate and its links with variability of the Atlantic ocean. *Bull. Am. Meteorol. Soc.*, **87**, 941–955, https://doi.org/10.1175/BAMS-87-7-941.

Reichler, T., and J. Kim, 2008: How Well Do Coupled Models Simulate Today's Climate ? *Bull. Am. Meteorol. Soc.*, **819**, 303–311, https://doi.org/10.1175/BAMS-89-3-303.

Richard, Y., N. Fauchereau, I. Poccard, M. Rouault, and S. Trzaska, 2001: 20th century droughts in southern Africa: Spatial and temporal variability, teleconnections with oceanic and atmospheric conditions. *Int. J. Climatol.*, **21**, 873–885, https://doi.org/10.1002/joc.656.

Rouault, M., S. a. White, C. J. C. Reason, J. R. E. Lutjeharms, and I. Jobard, 2002: Ocean–Atmosphere Interaction in the Agulhas Current Region and a South African Extreme Weather Event. *Weather Forecast.*, **17**, 655–669, https://doi.org/10.1175/1520-0434(2002)017<0655:OAIITA>2.0.CO;2.

Rouault, M., P. Florenchie, N. Fauchereau, and C. J. C. Reason, 2003: South East tropical Atlantic warm events and southern African rainfall. *Geophys. Res. Lett.*, **30**, 1–4, https://doi.org/10.1029/2002GL014840.

Rowell, D. P., and R. Chadwick, 2018: Causes of the Uncertainty in Projections of Tropical Terrestrial Rainfall Change: East Africa. *J. Clim.*, **31**, JCLI-D-17-0830.1, https://doi.org/10.1175/JCLI-D-17-0830.1.

Rowell, D. P., C. A. Senior, M. Vellinga, and R. J. Graham, 2016: Can climate projection uncertainty be constrained over Africa using metrics of contemporary performance? *Clim. Change*, **134**, 621–633, https://doi.org/10.1007/s10584-015-1554-4.

Rudolf, B., and U. Schneider, 2005: Caculation of gridded precipitation data for the global land-surface using in-situ gauge observation. *2nd Work. Int. Precip. Work. Gr. IPWG*, 231–247.

Sanderson, B. M., and R. Knutti, 2012: On the interpretation of constrained climate model ensembles. *Geophys. Res. Lett.*, **39**, 1–6, https://doi.org/10.1029/2012GL052665.

Schaller, N., I. Mahlstein, J. Cermak, and R. Knutti, 2011: Analyzing precipitation projections: A comparison of different approaches to climate model evaluation. *J. Geophys. Res. Atmos.*, **116**, 1–14, https://doi.org/10.1029/2010JD014963.

Schlenker, W., and D. B. Lobell, 2010: Robust negative impacts of climate change on African agriculture. *Environ. Res. Lett.*, **5**, https://doi.org/10.1088/1748-9326/5/1/014010.

Schmidt, G. A., and S. Sherwood, 2015: A practical philosophy of complex climate modelling. *Eur. J. Philos. Sci.*, **5**, 149–169, https://doi.org/10.1007/s13194-014-0102-9.

Schwendike, J., P. Govekar, M. J. Reeder, R. Wardle, G. J. Berry, and C. Jakob, 2014: Local partitioning of the overturning circulation in the tropics and the connection to the Hadley and Walker circulations. *J. Geophys. Res. Atmos.*, **119**, 1322–1339, https://doi.org/10.1002/2013JD020742.

Seager, R., N. Naik, and G. A. Vecchi, 2010: Thermodynamic and dynamic mechanisms for large-scale changes in the hydrological cycle in response to global warming. *J. Clim.*, **23**, 4651–4668, https://doi.org/10.1175/2010JCLI3655.1.

Serdeczny, O., S. Adams, F. Baarsch, D. Coumou, and J. Reinhardt, 2017: Climate change

impacts in Sub-Saharan Africa : from physical changes to their social repercussions. *Reg Env. Chang.*, 1585–1600, https://doi.org/10.1007/s10113-015-0910-2.

Seth, A., S. A. Rauscher, M. Rojas, A. Giannini, and S. J. Camargo, 2011: Enhanced spring convective barrier for monsoons in a warmer world? *Clim. Change*, **104**, 403–414, https://doi.org/10.1007/s10584-010-9973-8.

——, ——, M. Biasutti, A. Giannini, S. J. Camargo, and M. Rojas, 2013: CMIP5 projected changes in the annual cycle of precipitation in monsoon regions. *J. Clim.*, **26**, 7328–7351, https://doi.org/10.1175/JCLI-D-12-00726.1.

Shekhar, R., and W. R. Boos, 2017: Weakening and shifting of the Saharan shallow meridional circulation during wet years of the West African monsoon. *J. Clim.*, **30**, 7399–7422, https://doi.org/10.1175/JCLI-D-16-0696.1.

Shongwe, M. E., G. J. van Oldenborgh, B. J. J. M. van den Hurk, B. de Boer, C. A. S. Coelho, and M. K. van Aalst, 2009: Projected Changes in Mean and Extreme Precipitation in Africa under Global Warming. Part I: Southern Africa. *J. Clim.*, **22**, 3819–3837, https://doi.org/10.1175/2009JCLI2317.1.

Siderius, C., K. E. Gannon, M. Ndiyoi, A. Opere, N. Batisani, D. Olago, J. Pardoe, and D. Conway, 2018: Hydrological Response and Complex Impact Pathways of the 2015/2016 El Niño in Eastern and Southern Africa. *Earth's Futur.*, **6**, 2–22, https://doi.org/10.1002/eft2.268.

Singleton, A. T., and C. J. C. Reason, 2007: A Numerical Model Study of an Intense Cutoff Low Pressure System over. *Mon. Weather Rev.*, **135**, 1128–1150, https://doi.org/10.1175/MWR3311.1.

Slingo, J., H. Spencer, B. Hoskins, P. Berrisford, and E. Black, 2005: The meteorology of the Western Indian Ocean, and the influence of the East African Highlands. *Philos. Trans. A. Math. Phys. Eng. Sci.*, **363**, 25–42, https://doi.org/10.1098/rsta.2004.1473.

Stouffer, R. J., S. Manabe, and K. Bryan, 1989: Climatic Response to a Gradual Increase of Atmospheric Carbon Dioxide. *Nature*, **342**, 660–662, https://doi.org/10.1016/B978-0-444-88351-3.50016-7.

Streten, N. A., 1973: Some Characteristics of Satellite-Observed Bands Of Persistent Cloudiness Over the Southern Hemisphere. *Mon. Weather Rev.*, **101**, 486–495, https://doi.org/10.1175/1520-0493(1973)101<0486:SCOSBO>2.3.CO;2.

Sylla, M. B., F. Giorgi, E. Coppola, and L. Mariotti, 2013: Uncertainties in daily rainfall over Africa: Assessment of gridded observation products and evaluation of a regional climate model simulation. *Int. J. Climatol.*, **33**, 1805–1817, https://doi.org/10.1002/joc.3551.

Tadross, M. A., W. J. Gutowski, B. C. Hewitson, C. Jack, and M. New, 2006: MM5 simulations of interannual change and the diurnal cycle of southern African regional climate. *Theor. Appl. Climatol.*, **86**, 63–80, https://doi.org/10.1007/s00704-005-0208-2.

Taljaard, J. J., 1972: Synoptic Meteorology of the Southern Hemisphere. *Meteorology of the Southern Hemisphere, Meteor. Monogr.*, Vol. 49 of, Amer. Meteor. Soc., 139–213.

——, 1986: Change of rainfall distribution and circulation patterns over southern Africa in summer\r. *J. Climatol.*, **6**, 579–593.

Taylor, C. M., C. E. Birch, D. J. Parker, N. Dixon, F. Guichard, G. Nikulin, and G. M. S. Lister, 2013: Modeling soil moisture-precipitation feedback in the Sahel: Importance of spatial scale versus convective parameterization. *Geophys. Res. Lett.*, **40**, 6213–6218, https://doi.org/10.1002/2013GL058511.

Taylor, K. E., R. J. Stouffer, and G. a. Meehl, 2012: An overview of CMIP5 and the experiment design. *Bull. Am. Meteorol. Soc.*, **93**, 485–498, https://doi.org/10.1175/BAMS-D-11-00094.1.

Tennant, W., 2003: An Assessment of Intraseasonal Variability from 13-Yr GCM Simulations. *Mon. Weather Rev.*, **131**, 1975–1991, https://doi.org/10.1175/1520-0493(2003)131<1975:AAOIVF>2.0.CO;2.

Thibeault, J. M., and A. Seth, 2014: A framework for evaluating model credibility for warm-season precipitation in northeastern north america: A case study of CMIP5 simulations and projections. *J. Clim.*, **27**, 493–510, https://doi.org/10.1175/JCLI-D-12-00846.1.

Thomas, D. S., M. Knight, and G. F. Wiggs, 2005: Remobilization of southern African desert dune systems by twenty-first century global warming. *Nature*, **435**, 1218–1221, https://doi.org/10.1038/nature03717.

Todd, M., and R. Washington, 1998: Extreme daily rainfall in southern African and Southwest Indian Ocean tropical-temperate links. *S. Afr. J. Sci.*, **94**, 64–70.

Tozuka, T., B. J. Abiodun, and F. a. Engelbrecht, 2014: Impacts of convection schemes on simulating tropical-temperate troughs over southern Africa. *Clim. Dyn.*, **42**, 433–451, https://doi.org/10.1007/s00382-013-1738-4.

Tseng, Y. heng, Y. heng Lin, M. hui Lo, and S. chih Yang, 2016: Diagnosing the possible dynamics controlling Sahel precipitation in the short-range ensemble community atmospheric model hindcasts. *Clim. Dyn.*, **47**, 2747–2764, https://doi.org/10.1007/s00382-016-2995-9.

Tyson, P. D., and S. J. Crimp, 1998: the Climate of the Kalahari Transect. *Trans. R. Soc. South Africa*, **53**, 93–112, https://doi.org/10.1080/00359199809520380.

——, and R. A. Preston-Whyte, 2000: *The Weather and Climate of Southern Africa*. 2nd ed. Oxford University Press,.

Unganai, L. S., and S. J. Mason, 2002: Long-range predictability of Zimbabwe summer rainfall. *Int. J. Climatol.*, **22**, 1091–1103, https://doi.org/10.1002/joc.786.

Vecchi, G. A., B. J. Soden, A. T. Wittenberg, I. M. Held, A. Leetmaa, and M. J. Harrison, 2006: Weakening of tropical Pacific atmospheric circulation due to anthropogenic forcing. *Nature*, **441**, 73–76, https://doi.org/10.1038/nature04744.

Vigaud, N., Y. Richard, M. Rouault, and N. Fauchereau, 2007: Water vapour transport from the tropical Atlantic and summer rainfall in tropical southern Africa. *Clim. Dyn.*, **28**, 113–123, https://doi.org/10.1007/s00382-006-0186-9.

Vigaud, N., Y. Richard, M. Rouault, and N. Fauchereau, 2009: Moisture transport between the South Atlantic Ocean and southern Africa: Relationships with summer rainfall and associated dynamics. *Clim. Dyn.*, **32**, 113–123, https://doi.org/10.1007/s00382-008-0377-7.

Vizy, E. K., K. H. Cook, J. Crétat, and N. Neupane, 2013: Projections of a wetter sahel in the twenty-first century from global and regional models. *J. Clim.*, **26**, 4664–4687, https://doi.org/10.1175/JCLI-D-12-00533.1.

van Vuuren, D. P., and Coauthors, 2011: The representative concentration pathways: An overview. *Clim. Change*, **109**, 5–31, https://doi.org/10.1007/s10584-011-0148-z.

Walker, N. D., 1990: Links between South African summer rainfall and temperature variability of the Agulhas and Benguela Current systems. *J. Geophys. Res.*, **95**, 3297, https://doi.org/10.1029/JC095iC03p03297.

Walker, N. D., and R. D. Mey, 1988: Ocean/atmosphere heat fluxes within the Agulhas Retroflection region. *J. Geophys. Res. Ocean.*, **93**, 15473–15483, https://doi.org/10.1029/JC093iC12p15473.

Wang, C., L. Zhang, and S. Lee, 2014: A global perspective on CMIP5 climate model biases. *Nat. Clim. Chang.*, **4**, 201–205, https://doi.org/10.1038/NCLIMATE2118.

Washington, R., and A. Preston, 2006: Extreme wet years over southern Africa: Role of Indian Ocean sea surface temperatures. *J. Geophys. Res.*, **111**, 1–15, https://doi.org/10.1029/2005JD006724.

——, and Coauthors, 2006: African climate change: Taking the shorter route. *Bull. Am. Meteorol. Soc.*, **87**, 1355–1366, https://doi.org/10.1175/BAMS-87-10-1355.

——, R. James, H. Pearce, W. M. Pokam, and W. Moufouma-Okia, 2013: Congo Basin rainfall climatology: can we believe the climate models? *Philos. Trans. R. Soc. Lond. B. Biol. Sci.*, **368**, 20120296, https://doi.org/10.1098/rstb.2012.0296.

Watterson, I. G., J. Bathols, and C. Heady, 2014: What influences the skill of climate models over the continents? *Bull. Am. Meteorol. Soc.*, **95**, 689–700, https://doi.org/10.1175/BAMS-D-12-00136.1.

Weber, T., A. Haensler, and D. Jacob, 2017: Sensitivity of the atmospheric water cycle to corrections of the sea surface temperature bias over southern Africa in a regional climate model. *Clim. Dyn.*, **0**, 1–15, https://doi.org/10.1007/s00382-017-4052-8.

Wilk, J., D. Kniveton, L. Andersson, R. Layberry, M. C. Todd, D. Hughes, S. Ringrose, and C. Vanderpost, 2006: Estimating rainfall and water balance over the Okavango River Basin for hydrological applications. *J. Hydrol.*, **331**, 18–29, https://doi.org/10.1016/j.jhydrol.2006.04.049.

Wilks, D., 2016: the Stippling Shows Statistically Significant Grid Points. *Bull. Am. Meteorol. Soc.*, **97**, 2263–2274, https://doi.org/10.1175/BAMS-D-15-00267.1.

Williams, C. J. R., and D. R. Kniveton, 2012: Atmosphere-land surface interactions and their influence on extreme rainfall and potential abrupt climate change over southern Africa. *Clim. Change*, **112**, 981–996, https://doi.org/10.1007/s10584-011-0266-7.

World Bank, 2014: *World Development Indicators 2014*.

Xie, P., and P. a. Arkin, 1997: Global Precipitation: A 17-Year Monthly Analysis Based on Gauge Observations, Satellite Estimates, and Numerical Model Outputs. *Bull. Am. Meteorol. Soc.*, **78**, 2539–2558, https://doi.org/10.1175/1520-0477(1997)078<2539:GPAYMA>2.0.CO;2.

Xie, S. P., C. Deser, G. A. Vecchi, J. Ma, H. Teng, and A. T. Wittenberg, 2010: Global warming pattern formation: Sea surface temperature and rainfall. *J. Clim.*, **23**, 966–986, https://doi.org/10.1175/2009JCLI3329.1.

Yang, W., R. Seager, M. A. Cane, and B. Lyon, 2015: The rainfall annual cycle bias over East Africa in CMIP5 coupled climate models. *J. Clim.*, **28**, 9789–9802, https://doi.org/10.1175/JCLI-D-15-0323.1.

Zhang, Q., H. Körnich, and K. Holmgren, 2013: How well do reanalyses represent the southern African precipitation? *Clim. Dyn.*, **40**, 951–962, https://doi.org/10.1007/s00382-012-1423-z.

Zunckel, M., Y. Hong, K. Brassel, and S. O. Beirne, 1996: Characteristics of the nocturnal boundary layer: Okaukuejo, Namibia, during SAFARI-92. **101**, 757–766.